First Stars and Galaxies, ***Austin, Texas***

March 8-11, 2010

The end of the Cosmic Dark Ages

* *Standard model of physics*
* *Initial conditions from inflation*
* *Weakly-interacting Cold Dark Matter*

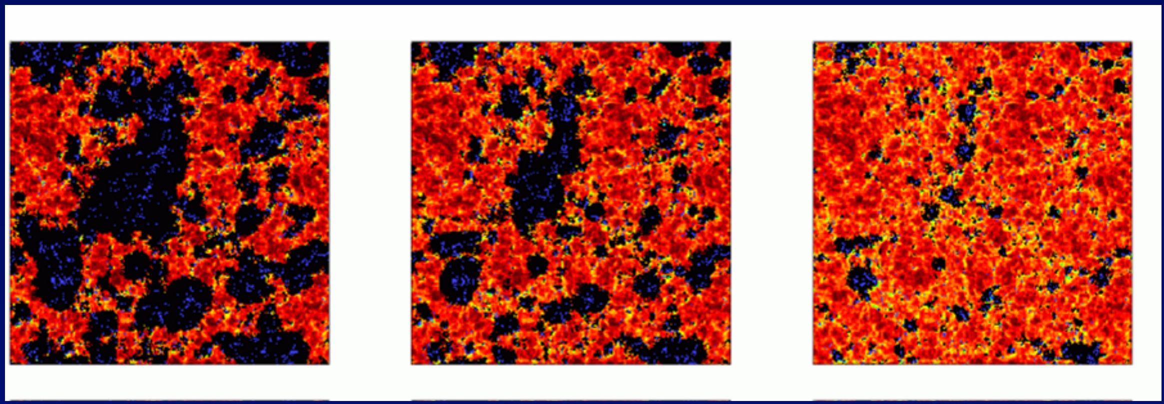

Surprises may signal new physics

How Did the First Stars and Galaxies Form?

Abraham Loeb

PRINCETON UNIVERSITY PRESS
PRINCETON AND OXFORD

Contents

WMAP Cosmological Parameters Model: lcdm Data: all		
$10^2\Omega_b h^2$	=	$2.19^{+0.06}_{-0.08}$
A	=	$0.67^{+0.04}_{-0.05}$
$A_{0.002}$	=	$0.81^{+0.04}_{-0.05}$
$\Delta^2_{\mathcal{R}}$	=	$(20 \times 10^{-10} \pm 1 \times 10^{-10}) \times 10^{-10}$
$\Delta^2_{\mathcal{R}}(k = 0.002/Mpc)$	=	$(24 \times 10^{-10}{}^{+1\times 10^{-10}}_{-2\times 10^{-10}}) \times 10^{-10}$
h	=	$0.71^{+0.01}_{-0.02}$
H_0	=	71^{+1}_{-2} km/s/Mpc
ℓ_A	=	$303.0^{+0.9}_{-1.3}$
n_s	=	$0.938^{+0.013}_{-0.018}$
$n_s(0.002)$	=	$0.938^{+0.012}_{-0.023}$
Ω_b	=	$0.044^{+0.002}_{-0.003}$
$\Omega_b h^2$	=	$0.0220^{+0.0006}_{-0.0008}$
Ω_c	=	$0.22^{+0.01}_{-0.02}$
Ω_Λ	=	0.74 ± 0.02
Ω_m	=	$0.26^{+0.01}_{-0.03}$
$\Omega_m h^2$	=	$0.131^{+0.004}_{-0.010}$
r_s	=	148^{+1}_{-2} Mpc
b_{SDSS}	=	$0.95^{+0.05}_{-0.06}$
σ_8	=	$0.75^{+0.03}_{-0.04}$
$\sigma_8\Omega_m^{0.6}$	=	$0.34^{+0.02}_{-0.03}$
A_{SZ}	=	$0.78^{+0.23}_{-0.78}$
t_0	=	$13.8^{+0.1}_{-0.2}$ Gyr
τ	=	$0.069^{+0.026}_{-0.029}$
θ_A	=	0.594 ± 0.002 °
z_{eq}	=	3135^{+85}_{-159}
z_r	=	$9.3^{+2.8}_{-2.0}$

The initial conditions of the Universe can be summarized on a single sheet of paper, yet thousands of books cannot fully describe the complex structures we see today…

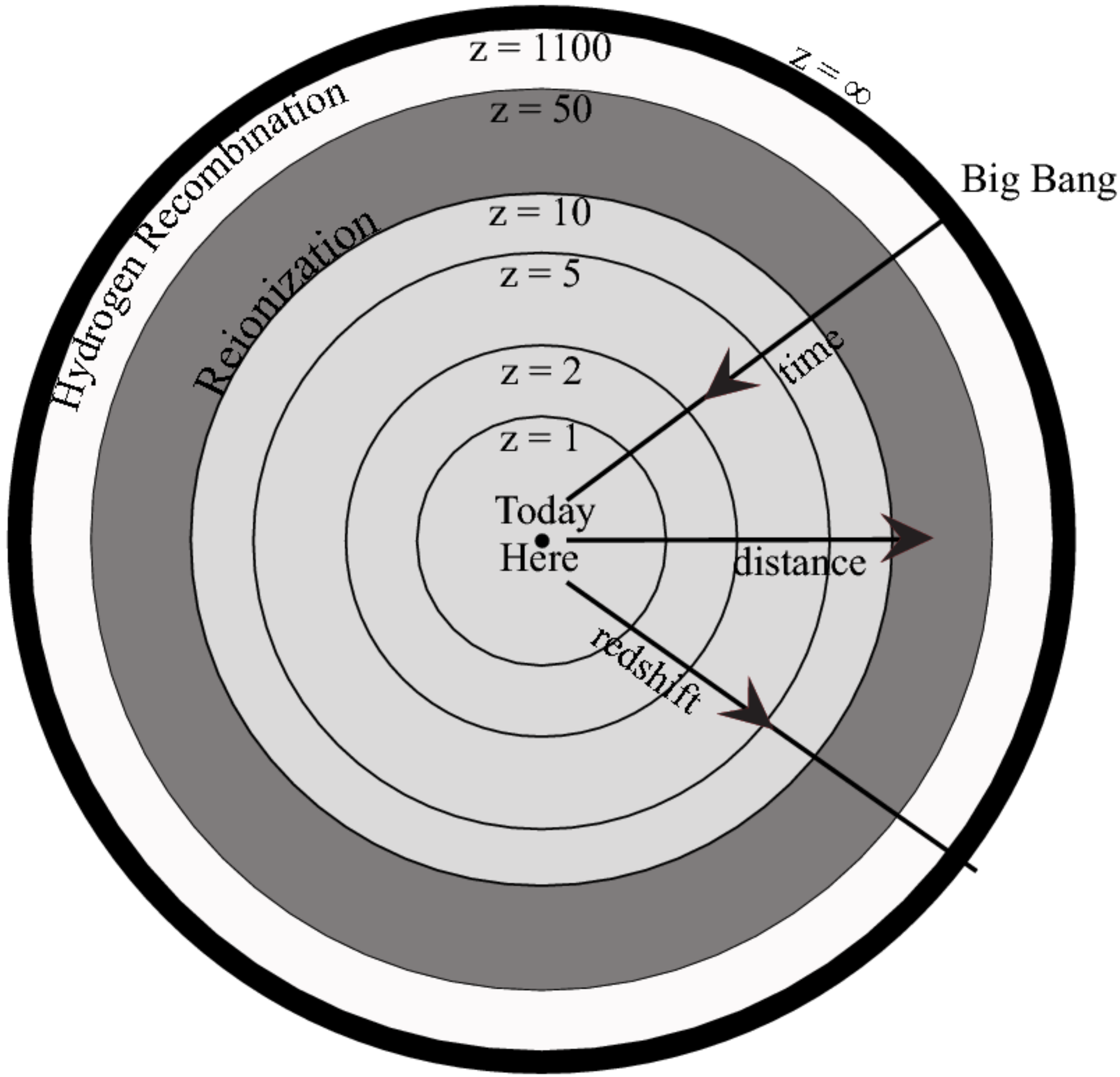
z = 1100
z = ∞
Big Bang
z = 50
Hydrogen Recombination
Reionization
z = 10
z = 5
time
z = 2
z = 1
Today
Here
distance
redshift

THE DARK AGES of the Universe

Astronomers are trying to fill in the blank pages in our photo album of the infant universe

By Abraham Loeb

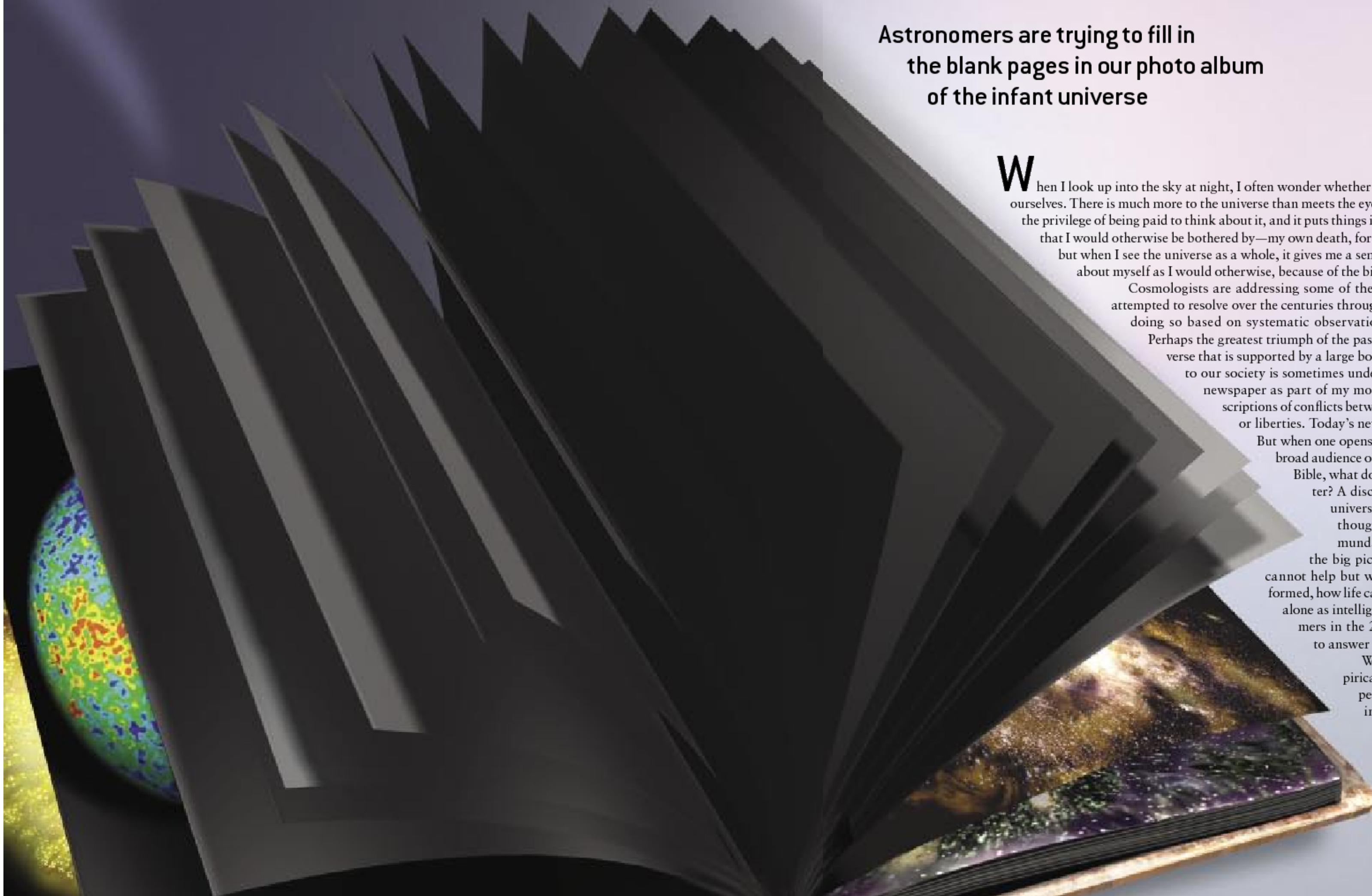

When I look up into the sky at night, I often wonder whether we humans are too preoccupied with ourselves. There is much more to the universe than meets the eye on earth. As an astrophysicist I have the privilege of being paid to think about it, and it puts things in perspective for me. There are things that I would otherwise be bothered by—my own death, for example. Everyone will die sometime, but when I see the universe as a whole, it gives me a sense of longevity. I do not care so much about myself as I would otherwise, because of the big picture.

Cosmologists are addressing some of the fundamental questions that people attempted to resolve over the centuries through philosophical thinking, but we are doing so based on systematic observation and a quantitative methodology. Perhaps the greatest triumph of the past century has been a model of the universe that is supported by a large body of data. The value of such a model to our society is sometimes underappreciated. When I open the daily newspaper as part of my morning routine, I often see lengthy descriptions of conflicts between people about borders, possessions or liberties. Today's news is often forgotten a few days later. But when one opens ancient texts that have appealed to a broad audience over a longer period of time, such as the Bible, what does one often find in the opening chapter? A discussion of how the constituents of the universe—light, stars, life—were created. Although humans are often caught up with mundane problems, they are curious about the big picture. As citizens of the universe we cannot help but wonder how the first sources of light formed, how life came into existence and whether we are alone as intelligent beings in this vast space. Astronomers in the 21st century are uniquely positioned to answer these big questions.

What makes modern cosmology an empirical science is that we are literally able to peer into the past. When you look at your image reflected off a mirror one meter

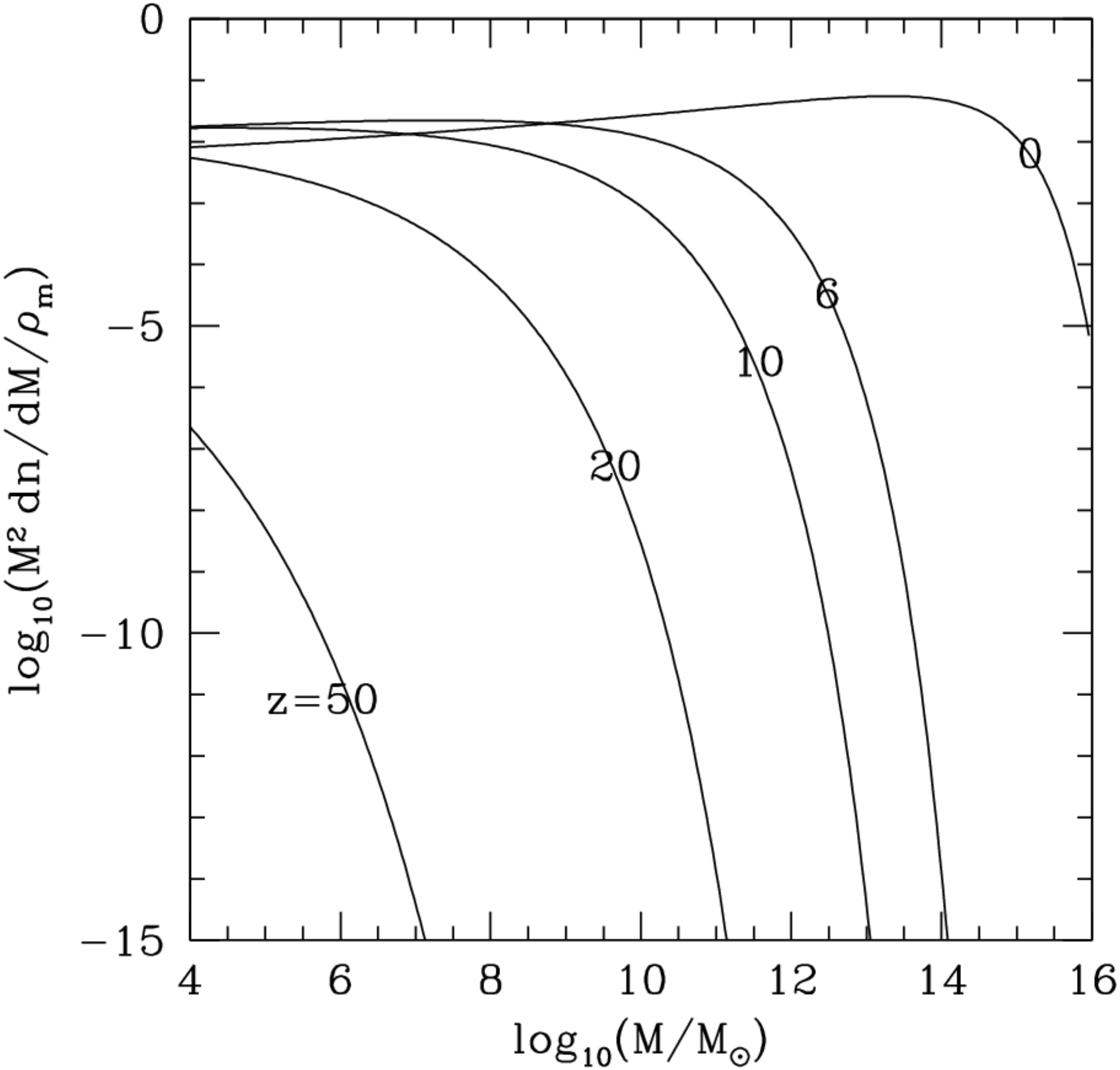

0
−5
−10
−15
4
6
8
10
12
14
16
$\log_{10}(M^2\,dn/dM/\rho_m)$
$\log_{10}(M/M_\odot)$
z=50
20
10
6
0

The First Dwarf Galaxies Form at z~30

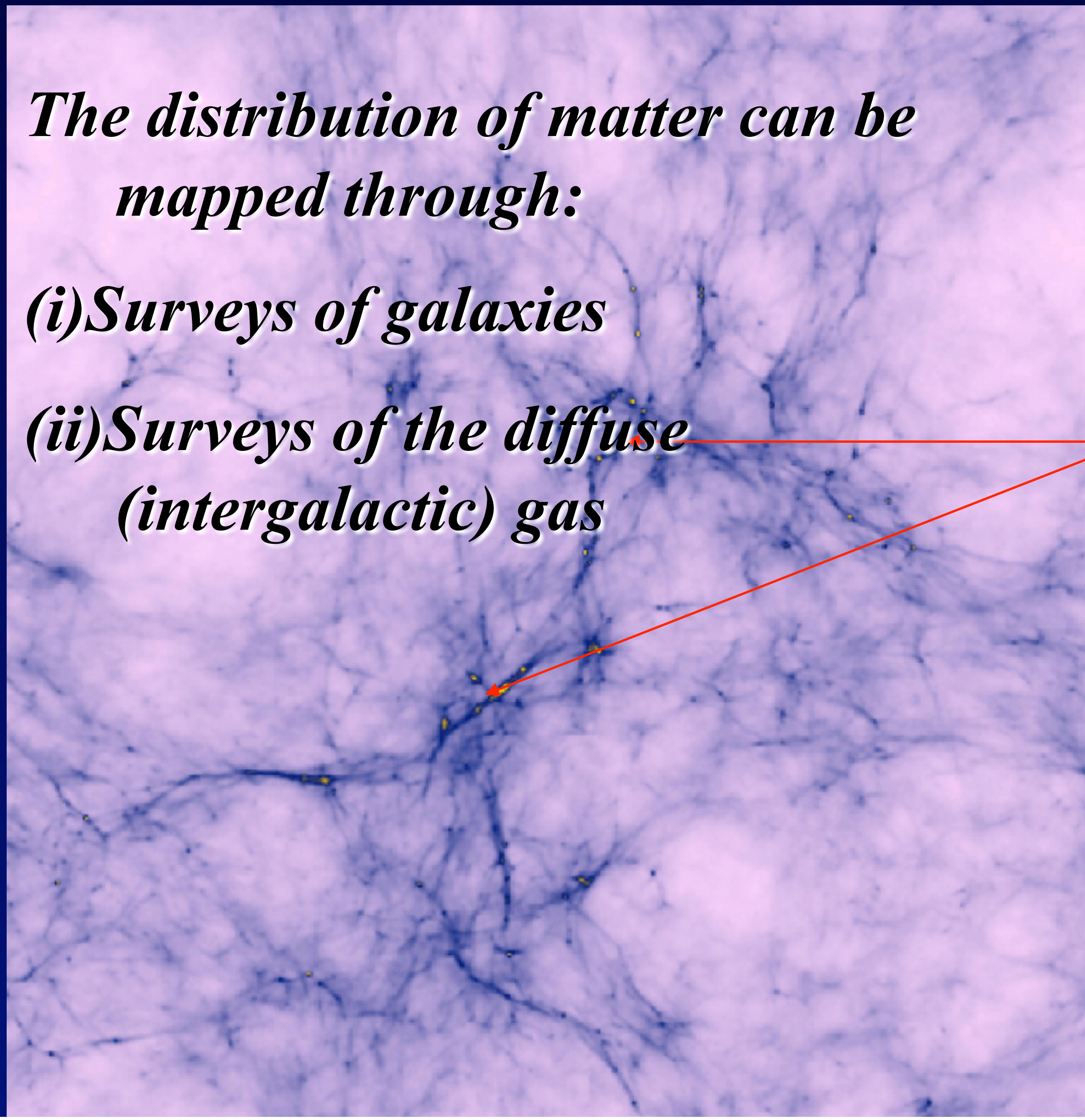

The distribution of matter can be mapped through:

(i)Surveys of galaxies

(ii)Surveys of the diffuse (intergalactic) gas

molecular hydrogen in Jeans mass objects

(ø 10^5Mì)

Yoshida et al. 2003

Observing the Stars

Observed Growth of Stellar Mass Budget

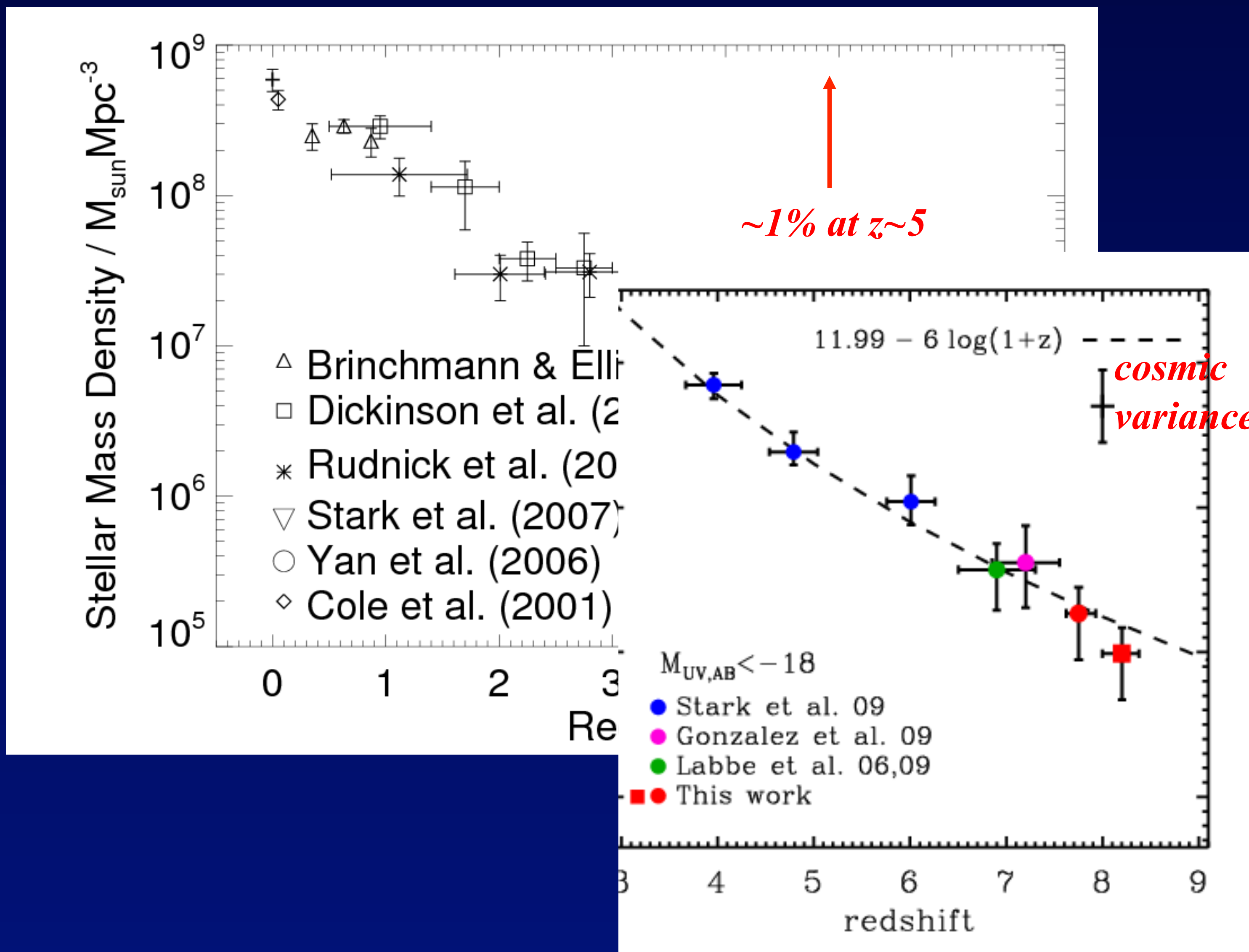

Redshift Record of Observed Galaxies

(Bouwens et al., arXiv:0912.4263)

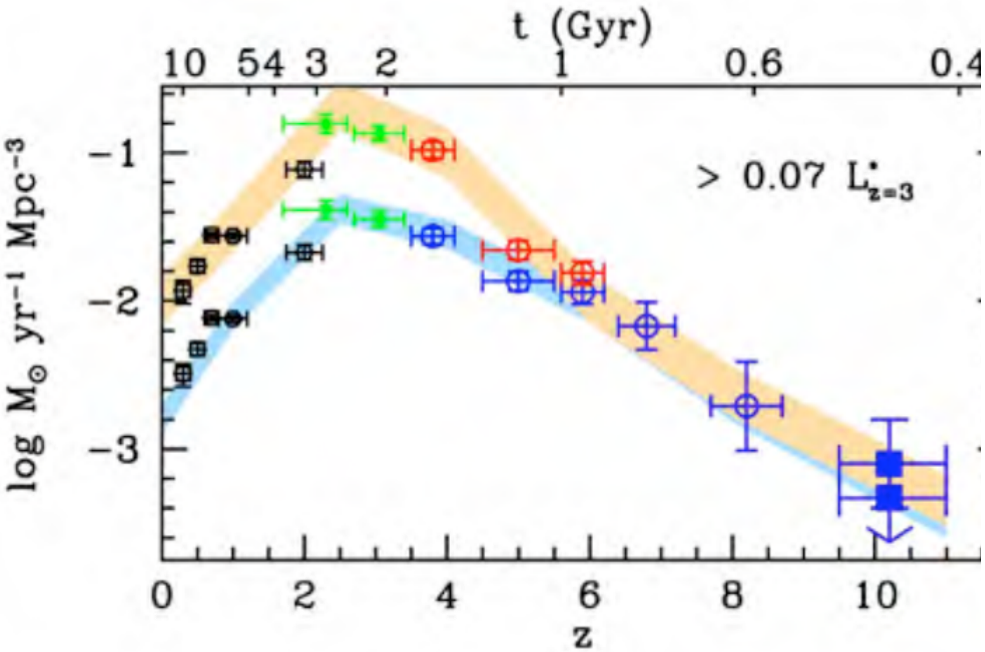

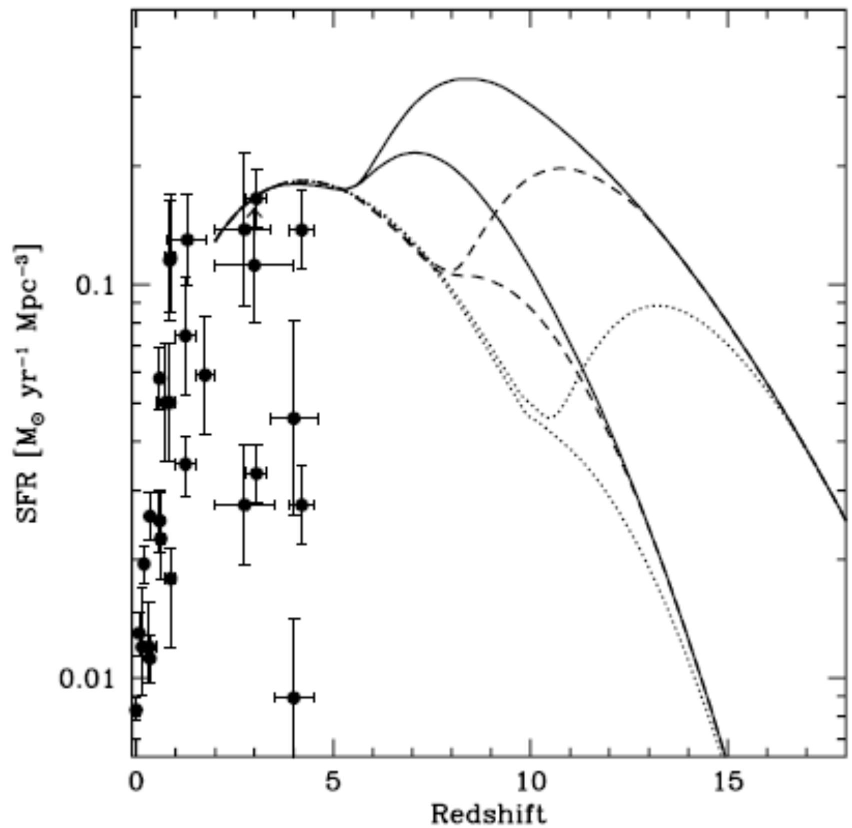

Prediction from Barkana & Loeb (2000):

Most SFR at z>10 is in galaxies fainter than 0.25nJy!

(AB>31.4 at 0.6-3.5 micron, an order of magnitude fainter than WFC3/IR sensitivity)

James Webb Space Telescope: Searching for the First Light

Mirror diameter: 6.5 meter

Material: beryllium

18 segments

Wavelength coverage: 0.6-28 micron

L2 orbit

Launch date: 2014

Extremely Large Telescopes (24-42 meters)

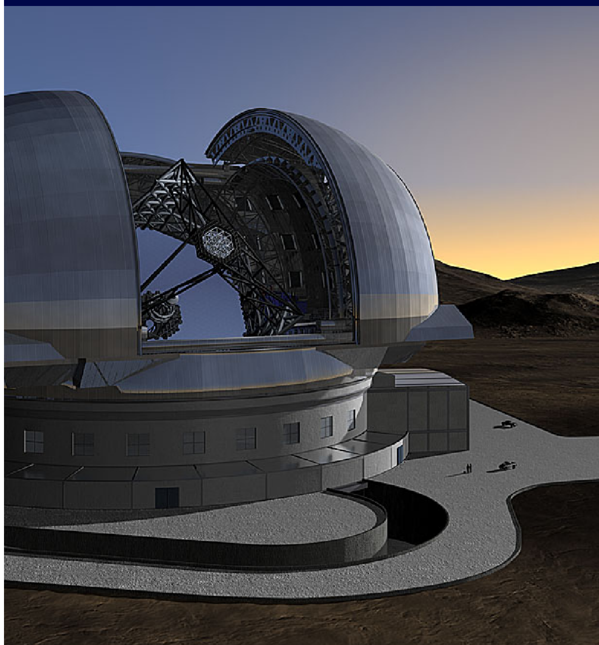

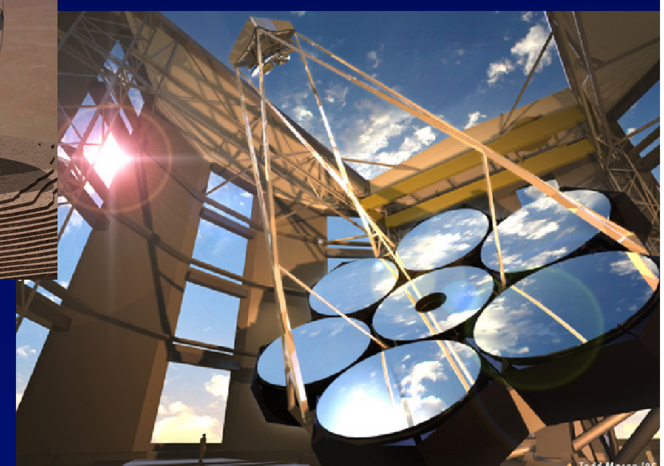

- GMT=Seven mirrors, each 8.4m in diameter
- TMT, EELT – segmented 20-40m aperture

Theoretical Simulations of the First Stars

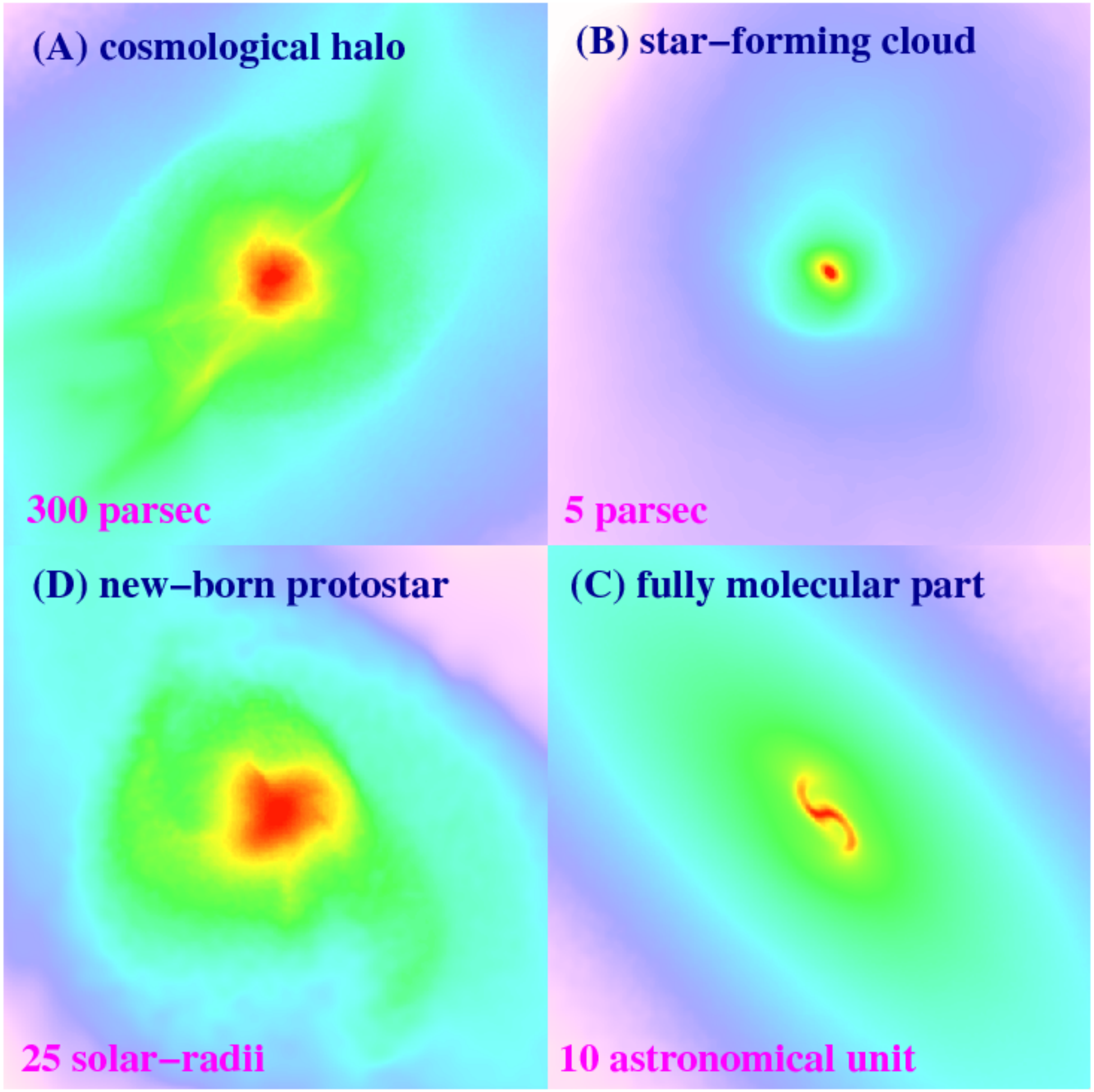

Bromm, Yoshida, Hernquist, & McKee (2009)

Population III Binaries

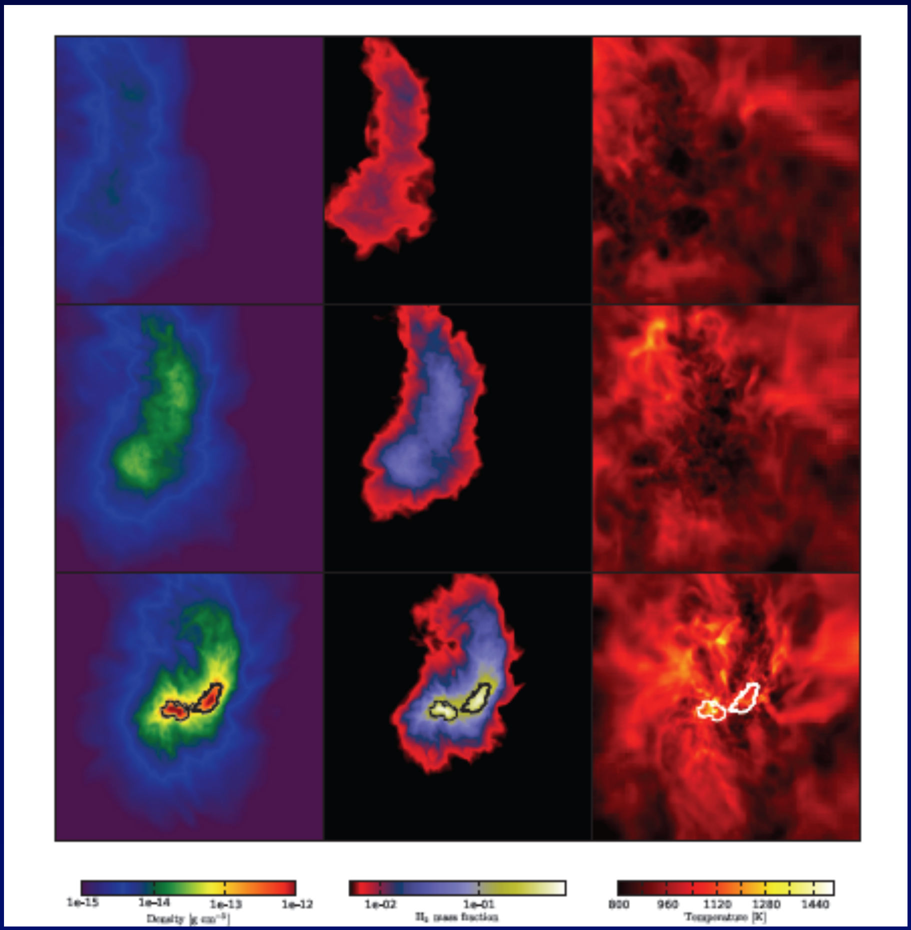

Turk, Abel, & O'Shea 2009

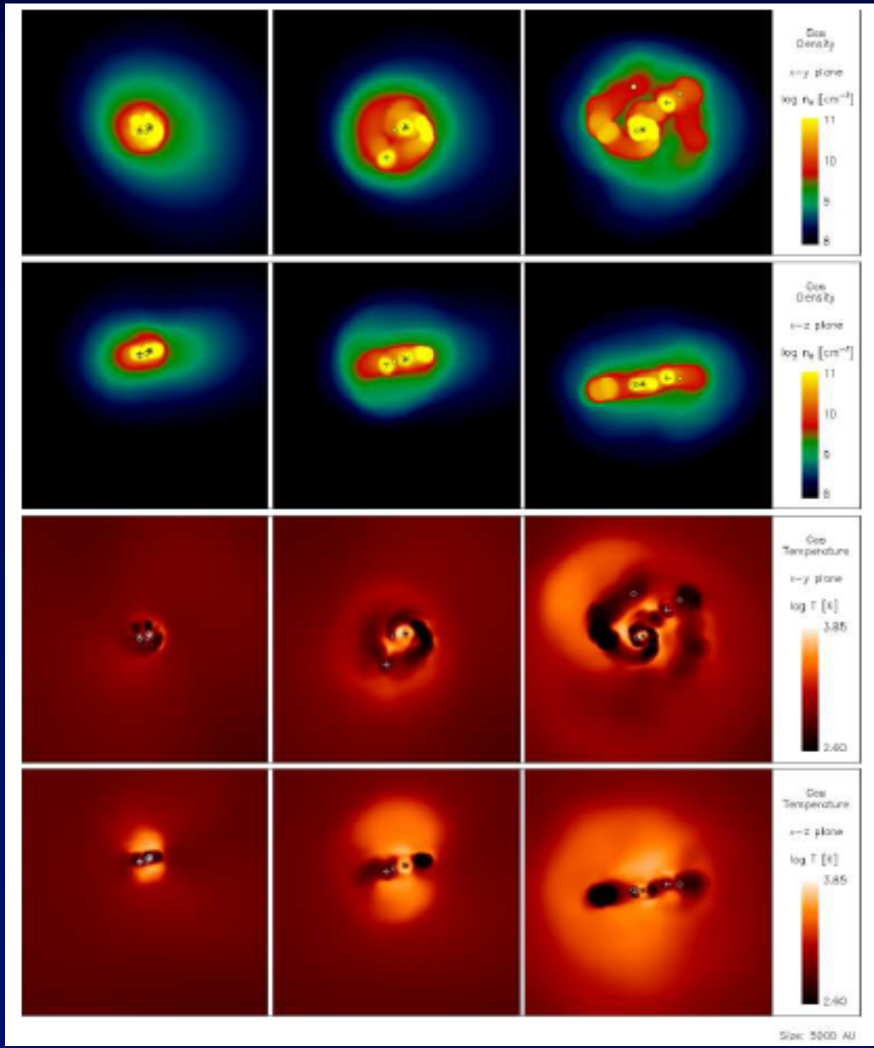

Stacy, Greif, & Bromm 2009

The Initial Mass Function of Stars Populations I/II

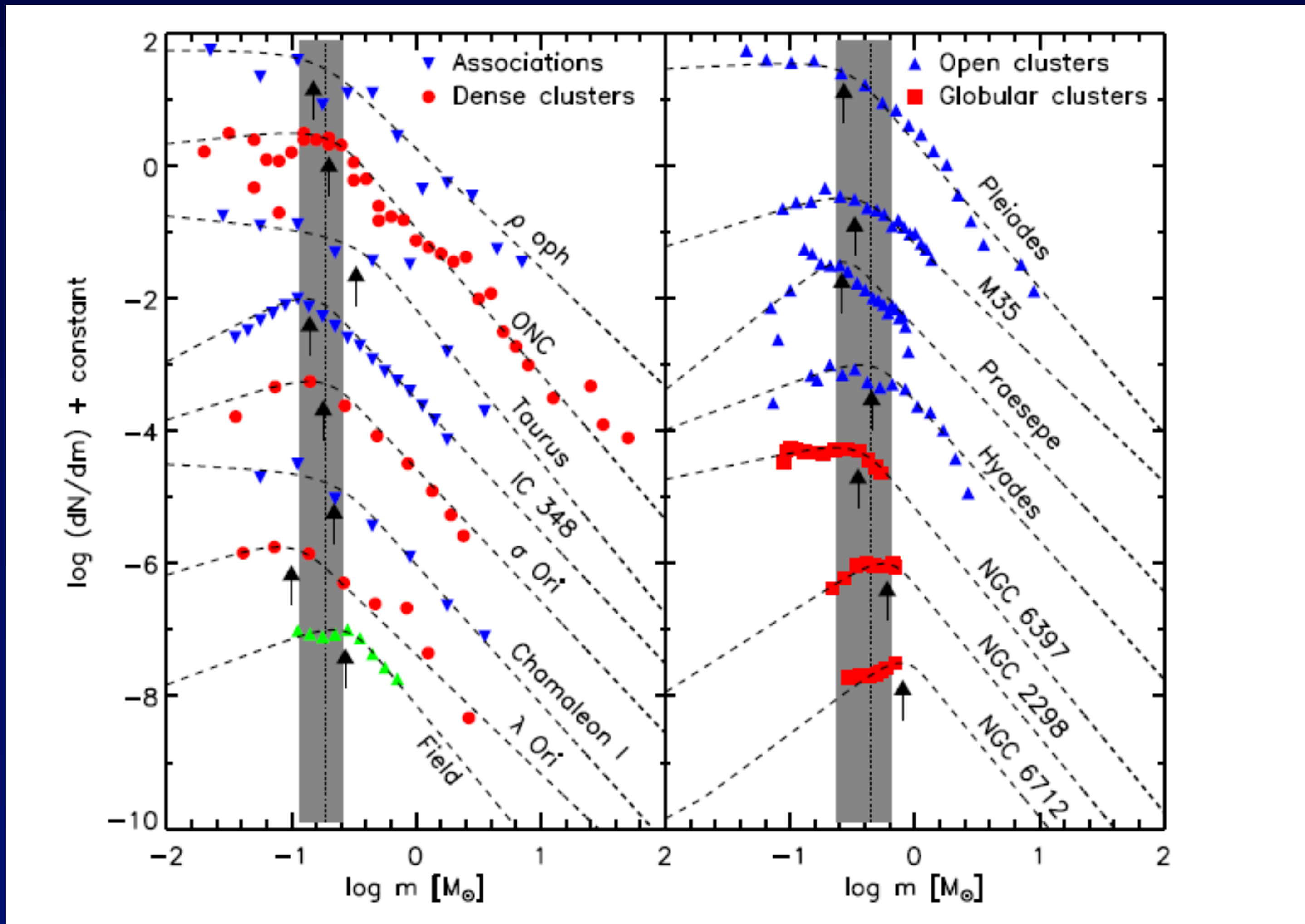

Bestian et al. (2010)

Populations III: $M_c \propto c_s^3/G$ ***with CMB temperature floor***

SN 2007bi – *a Pair Instability Supernova in a Nearby Metal-Poor Dwarf Galaxy*

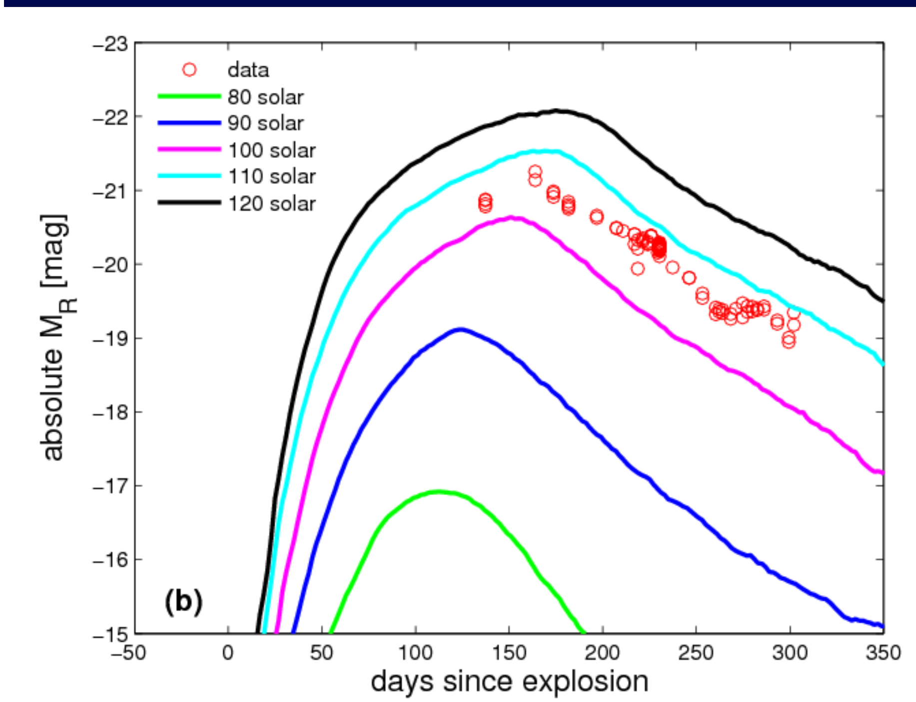

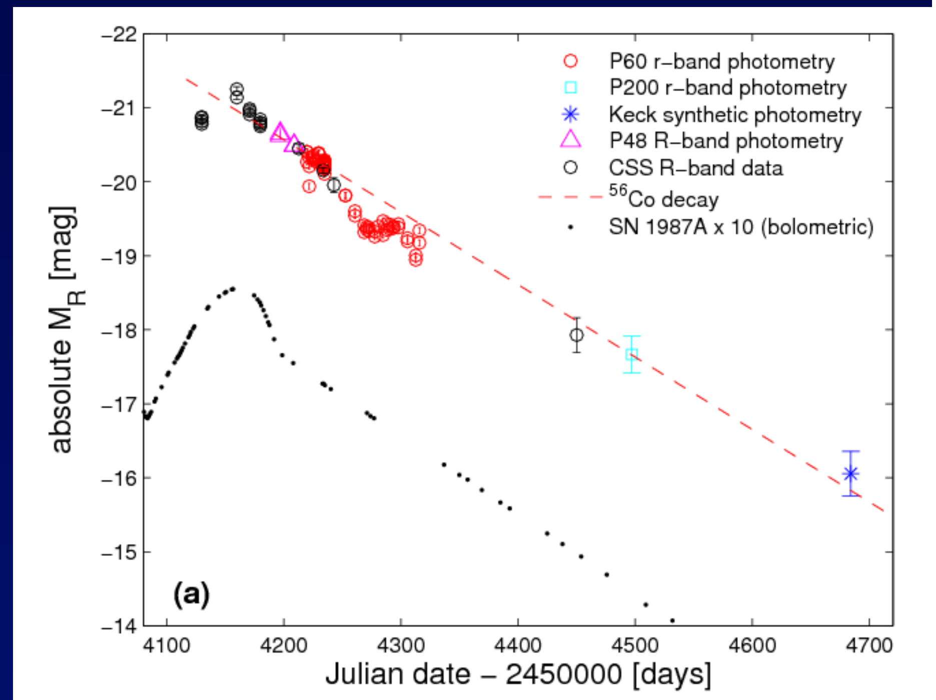

- Nickel mass of ~4-7M ì (ejecta mass of 100 M ì) ; kinetic energy of ø 10^{53}ergs
- Dwarf galaxy at z=0.128 with M_B=-16.3 mag, and 12+[O/H]=8.25

Gal-Yam et al., Nature (arXiv:1001.1156)

Number of ionizing photons (>13.6eV) per baryon incorporated into stars:

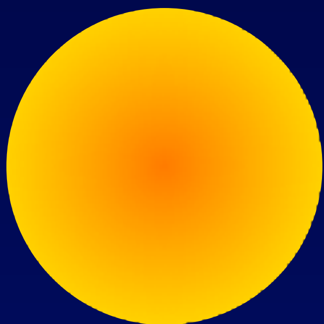

$T_{eff} \approx 10^5 K$
$L = L_E \propto M$

Massive, metal free stars

$M > 300 M_\odot$	$\approx 100,000$
$M > 100 M_\odot$	$\approx 40,000$

Gain by up to a factor of ~30!

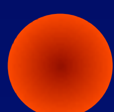

Salpeter mass function

Metal free	$\approx 7,000$
$Z = 0.01 Z_\odot$	$\approx 3,500$

Bromm, Kudritzki, & Loeb 2001, ApJ, 552, 464

Spectral signature of Pop-III stars:

strong UV continuum, helium recombination lines – such as 1640A*(1+z), low metal abundance

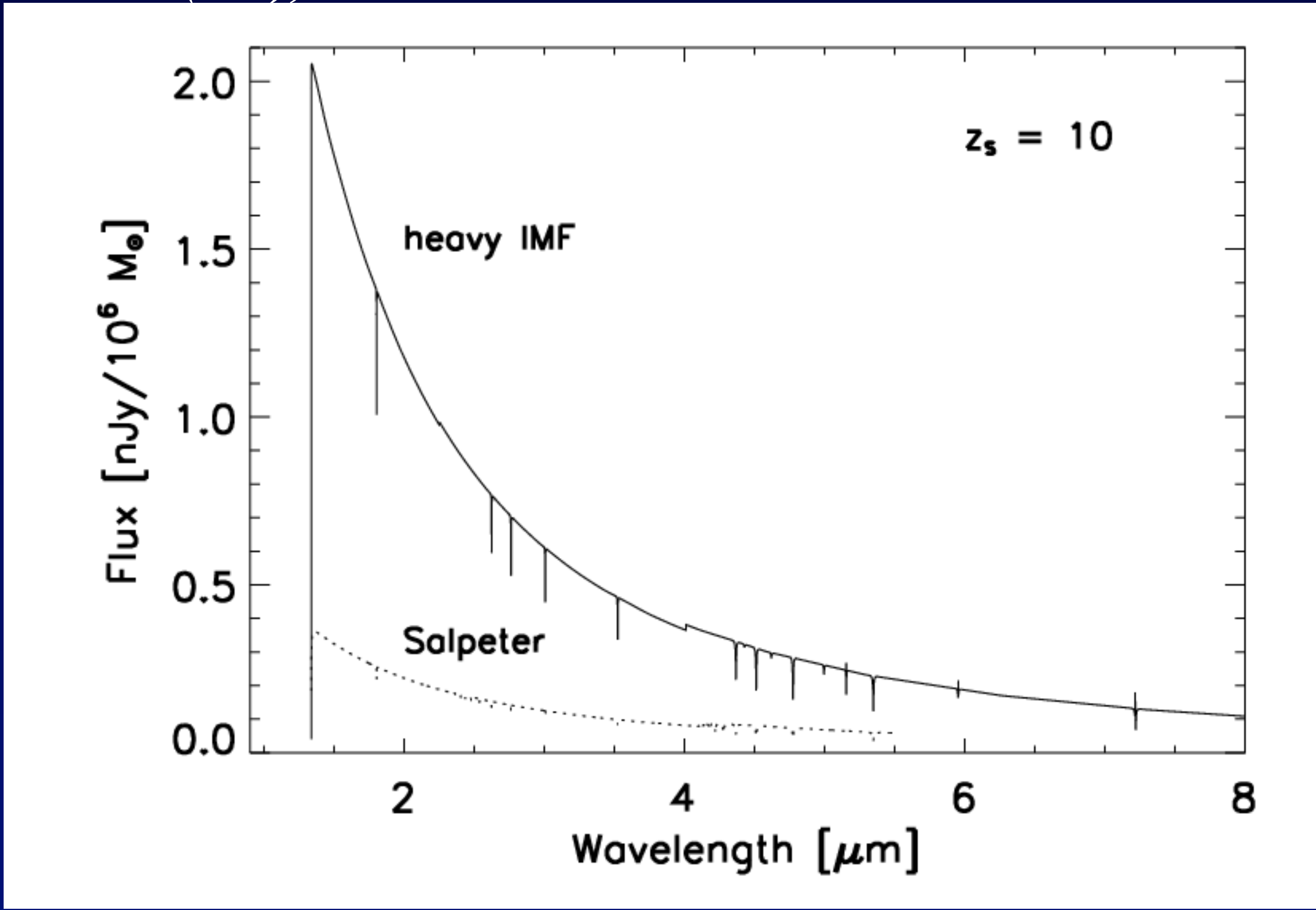

Bromm, Kudritzki, & Loeb (2001)

Outflows Driven by Lya Radiation Pressure

- IGM around the mini-halos hosting the first stars

$$M_{?} = 100 M_{ì}$$

$$M_{halo} = 10^{6} M_{ì}$$

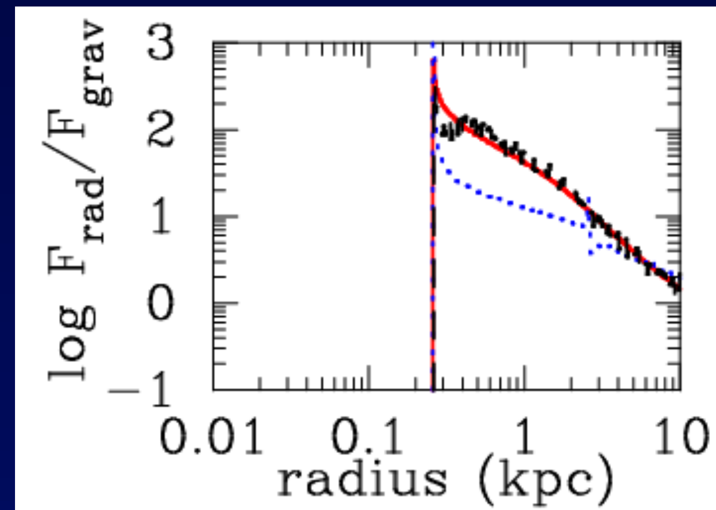

- Supershells around starburst galaxies

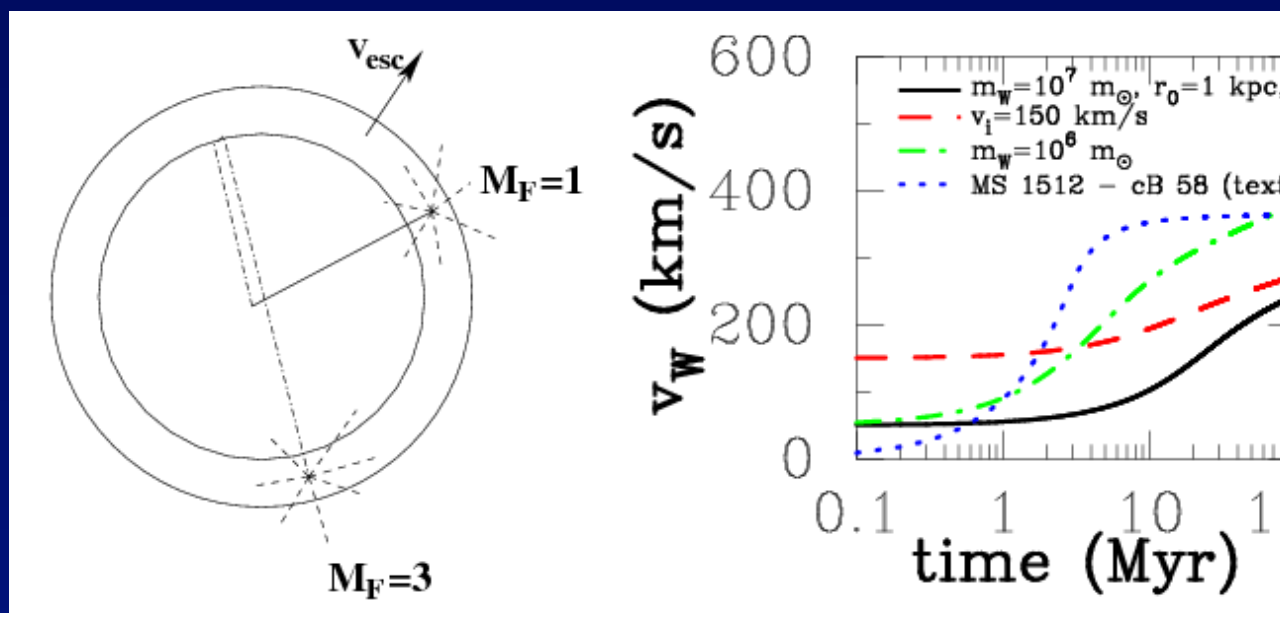

Dijkstra & Loeb 2008

Threshold Metallicity

High mass
(Pop-III) stars

Low mass
(Pop-I/II) stars

Z

Z_{th}

Atomic cooling (CII, OI) → $Z_{th} \approx 10^{-3} Z_\odot$

Dust, molecules (CO) → $Z_{th} < 10^{-5} Z_\odot$

Milky-Way halo metal-poor stars: $Z_{Fe} \approx 10^{-5} Z_\odot$

but: $Z_{C,O} > 10^{-3} Z_\odot$

First Galaxies Were Strongly Clustered on Scales of up to ~100 comoving Mpc

z=20

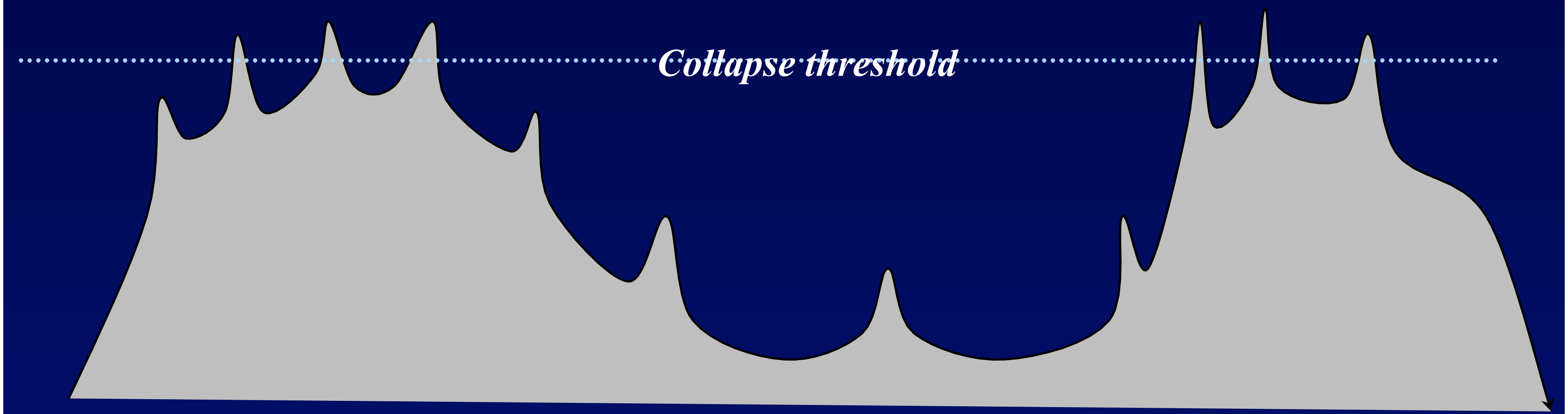

100 Mpc *structure in the simulated distribution of* $10^{10} M_{\odot}$ *galaxies at z=6*

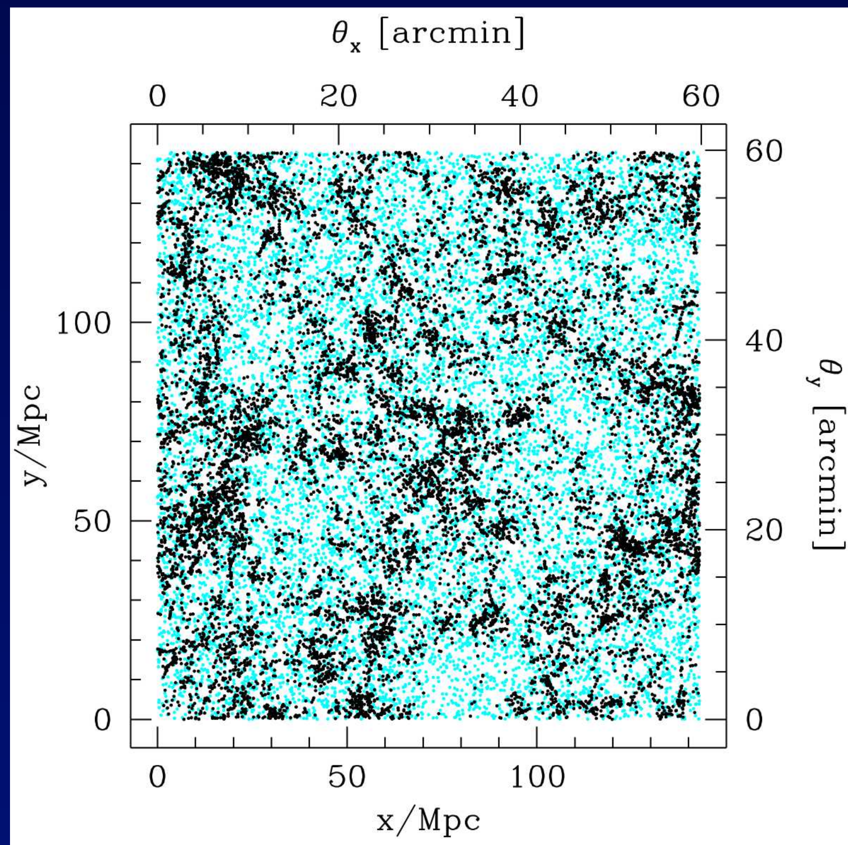

Munoz, Trac, & Loeb 2009

First Galaxies Were Strongly Clustered on Scales of up to ~100 comoving Mpc

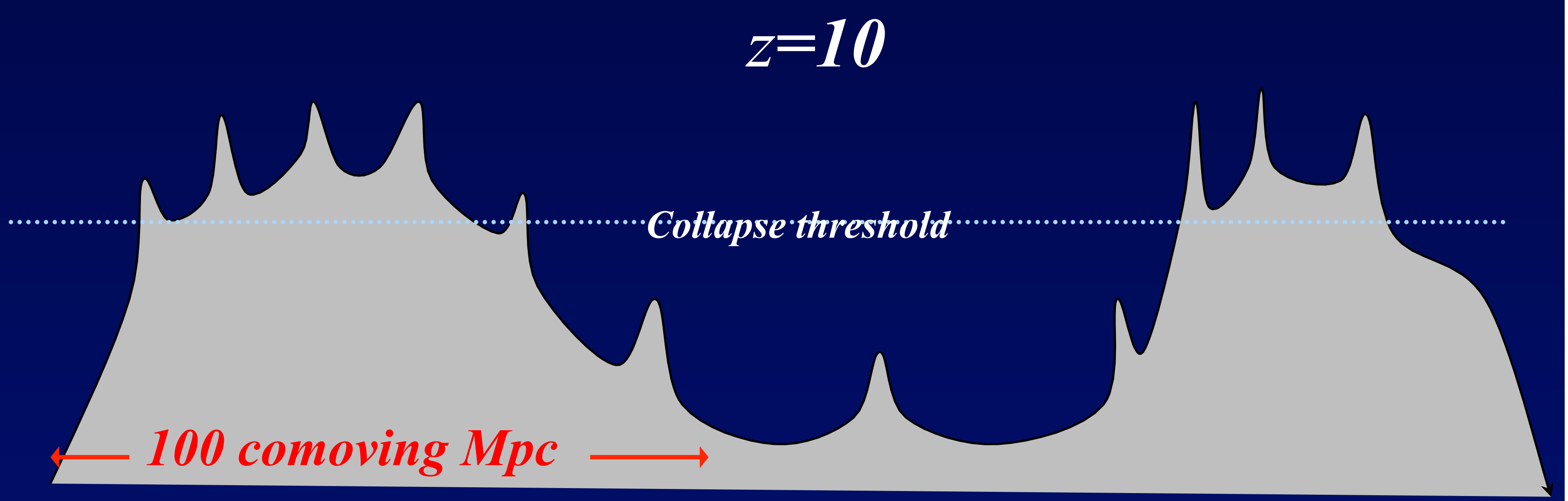

Challenges for numerical simulations of reionization:

**Resolving dwarf galaxies as sources of ionizing photons*

**Simulation box >100 comoving Mpc on a side*

**Following gravity, hydrodynamics, radiative transfer and their interaction*

→Enrichment of Primordial Gas with Heavy Elements was Highly Inhomogeneous

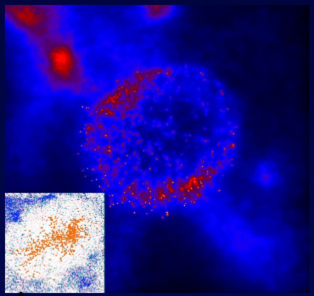

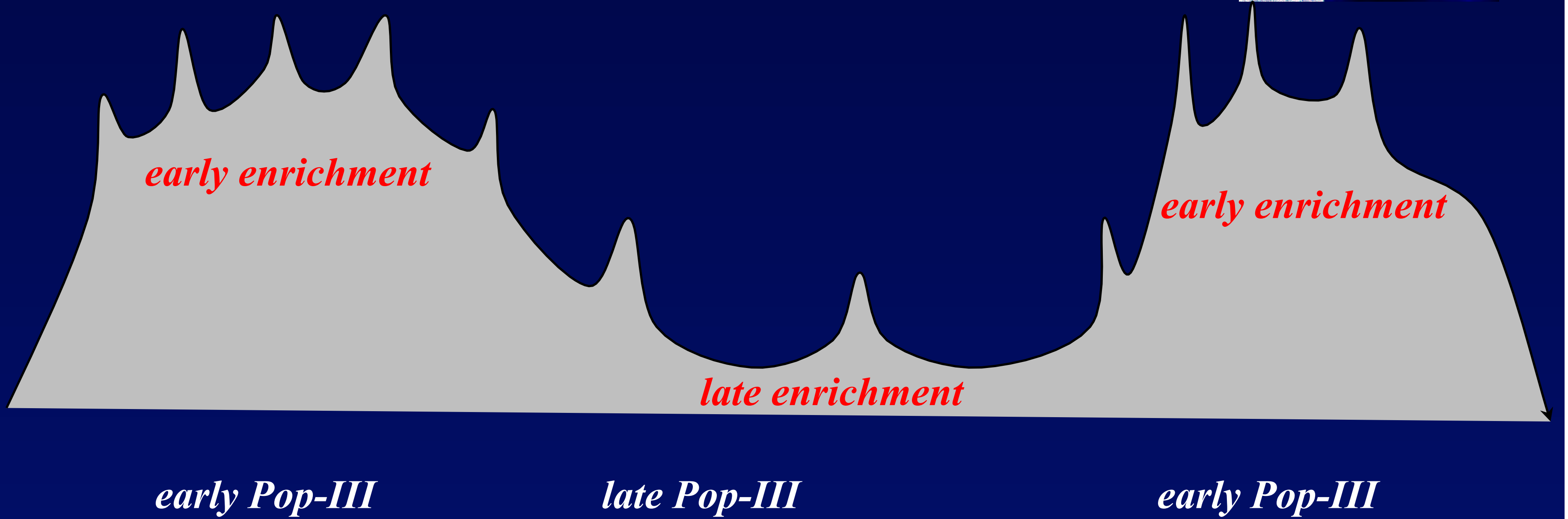

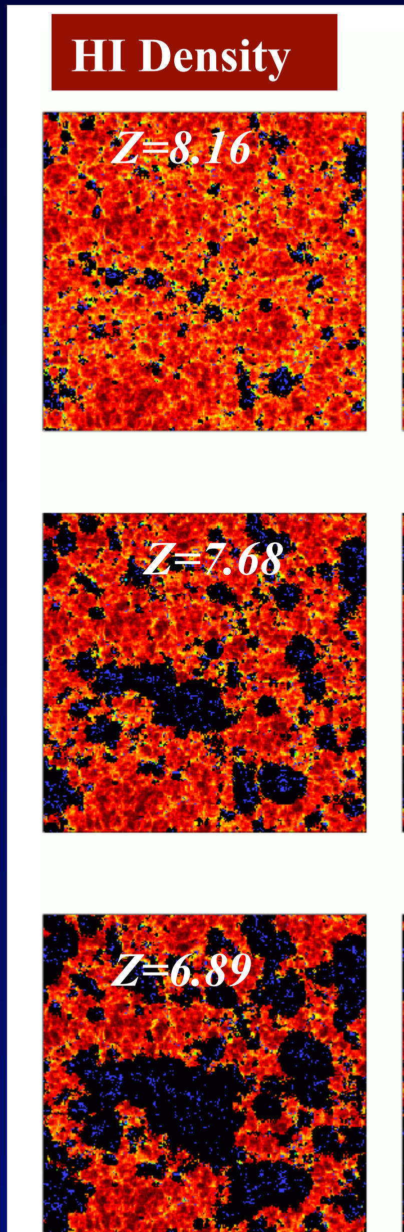

Zahn et al. 2006

Reionization

x_HI(z)

T(z)

PopII/Pop III

Trac, Cen, & Loeb 2008

Imprints of inhomogeneous reionization:

- The minimum virial temperature of galaxies was increased up to ~100,000K inside ionized regions
- Change in the clustering of galaxies (Babich & Loeb 2006; Wyithe & Loeb 2007) and the star formation rate density (Barkana & Loeb 2000)

The Race Between Stars and Quasars in Reionizing Cosmic Hydrogen

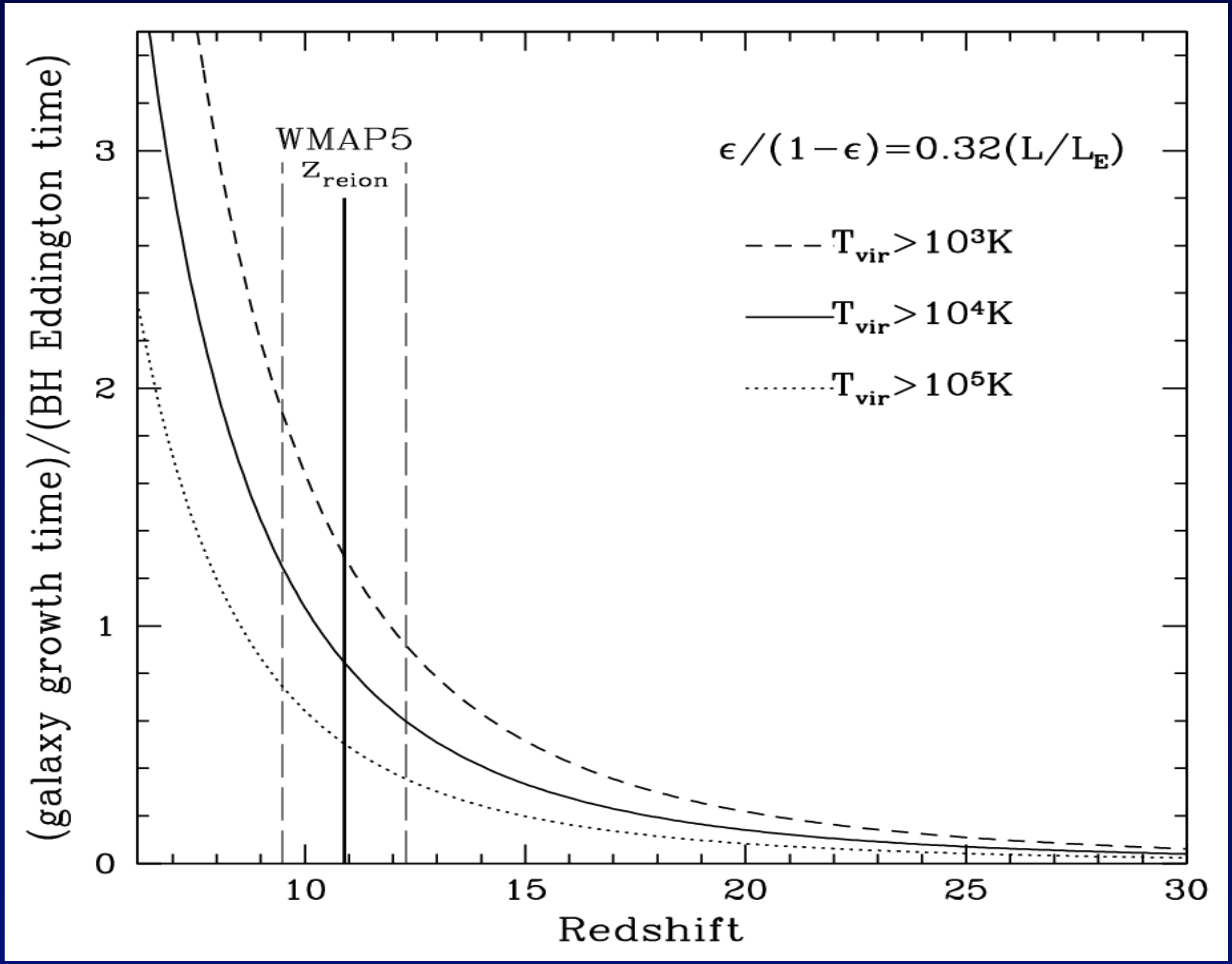

Loeb, arXiv:0811.2222, 2008

Nuclear Black Holes

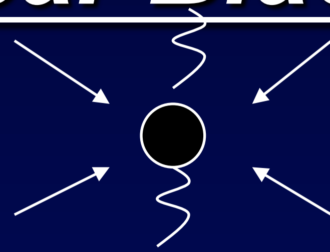

$$L = \epsilon \dot{M} c^2 \qquad t_E = M/\dot{M} = 4 \times 10^7 \frac{(\epsilon/10\%)}{(L/L_E)} \text{years}$$

$$M \propto \exp\{t/t_E\}$$

Stellar mass seed requires ~billion years to grow to an SDSS quasar ($10^9 M_\odot$)

…But a billion year is the Hubble time at z~6, and feedback from star formation and quasar activity as well as BH kicks are likely to suppress continuous accretion…

Gravitational Wave Recoil

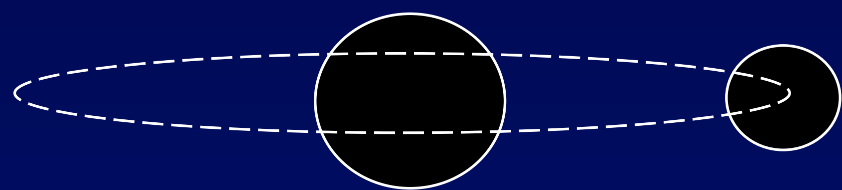

Gravitational Wave Recoil

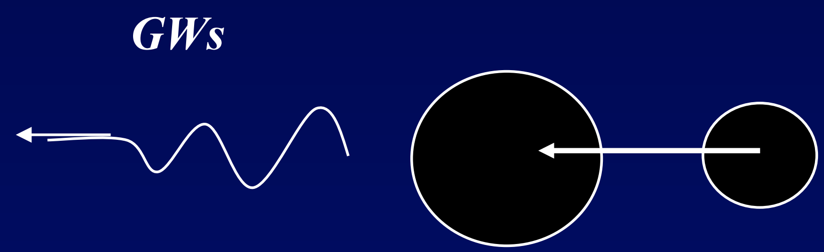

Anisotropic emission of gravitational waves → momentum recoil

Gravitational Wave Recoil

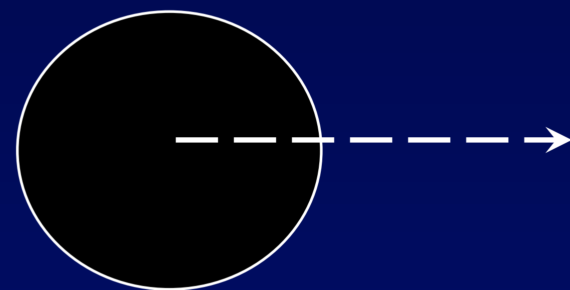

Recoil speed (~tens-4000 km/s) is independent of remnant black hole mass → *low-mass halos may easily lose their low-mass seeds after several mergers*

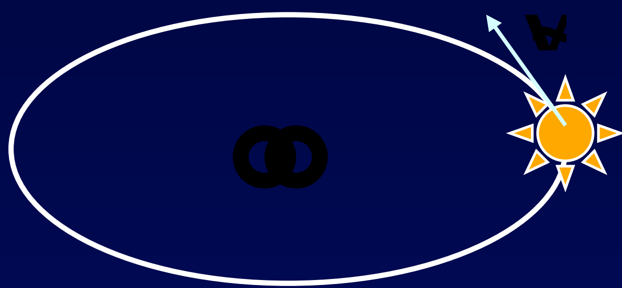

$$E = \frac{1}{2}v^2 \text{ à } \frac{GM}{r} = \text{à } \frac{1}{2}v^2$$

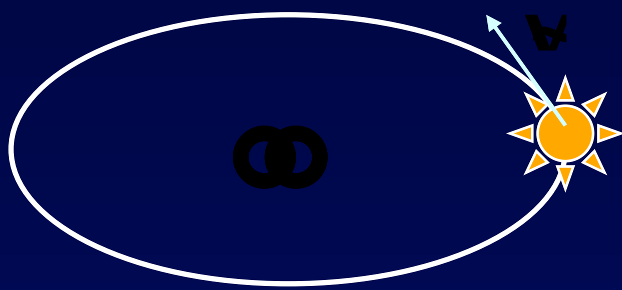

$$E = \frac{1}{2}v^2 - \frac{GM}{r} = -\frac{1}{2}v^2$$

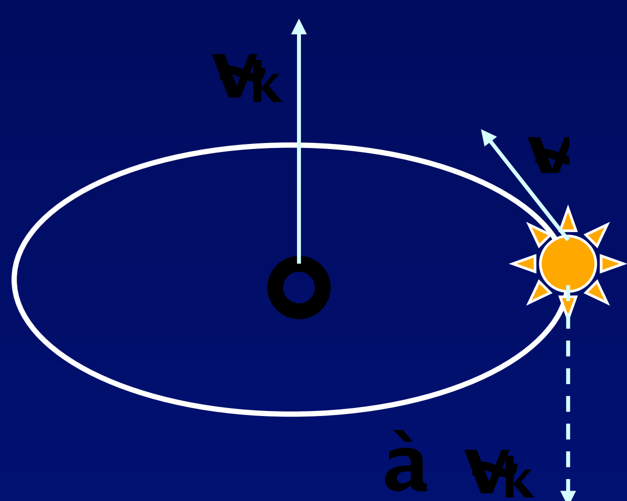

$$E = \frac{1}{2}(\vec{v} - \vec{v}_k)^2 - \frac{GM}{r}$$

$$= \vec{v}\cdot\vec{v}_k + \frac{1}{2}(v_k^2 - v^2)$$

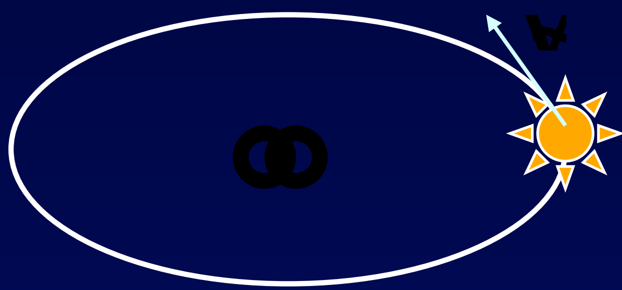

$$E = \frac{1}{2}v^2 - \frac{GM}{r} = -\frac{1}{2}v^2$$

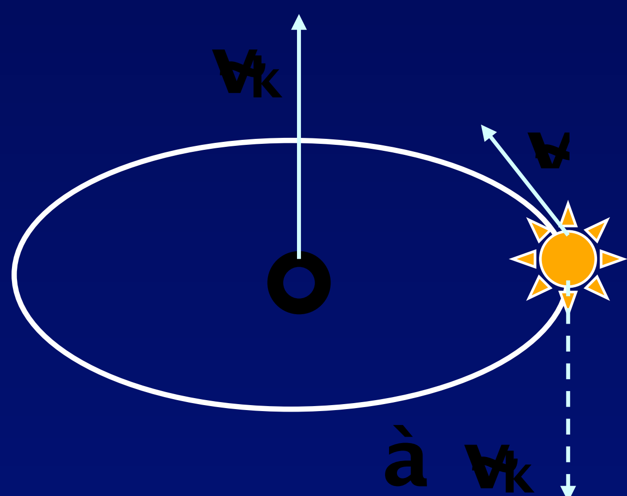

$$E = \frac{1}{2}(\vec{v} - \vec{v}_k)^2 - \frac{GM}{r}$$

$$= -\vec{v}\cdot\vec{v}_k + \frac{1}{2}(v_k^2 - v^2)$$

→ ***test particles with*** $v \gtrsim v_k$ ***remain bound***

Star Clusters Around Recoiled Black Holes in the Milky Way Halo

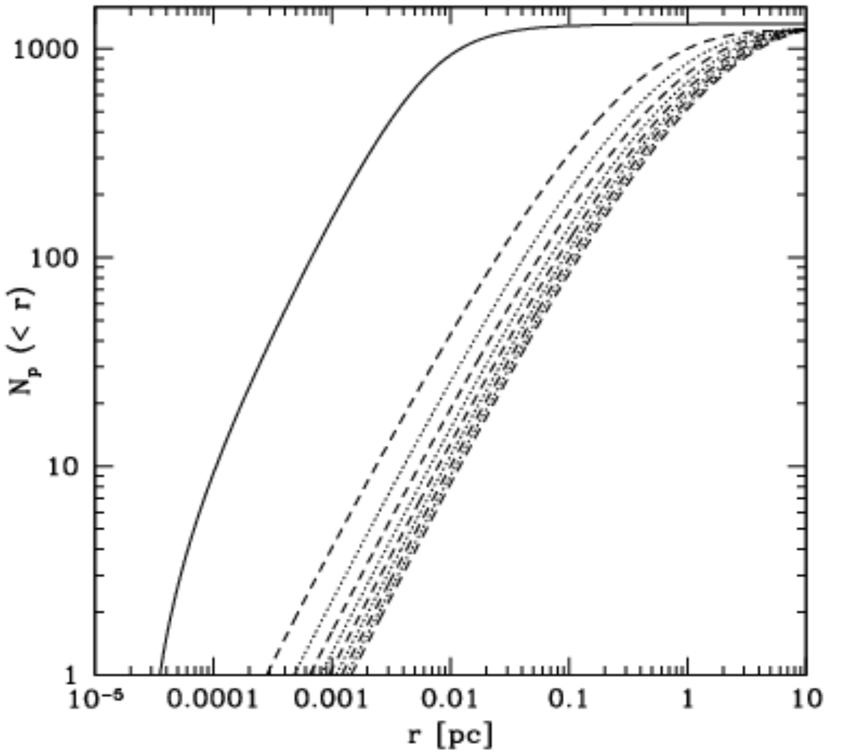

Figure 2. The total number of projected stars interior to r, $N_p(< r)$, for $M_\bullet = 10^5 \mathrm{M}_\odot$ and $\alpha = 1.75$. The solid line corresponds to the cluster immediately after being ejected from its parent galaxy with $v_k = 5.8\sigma_*$. The alternating dashed and dotted lines correspond to the projected number of stars after every $10t_r \approx 650\,\mathrm{Myr}$. Immediately after ejection, the cluster rapidly expands until its relaxation time becomes comparable to the age of the Universe, with very little mass loss. In the case of $\alpha = 1$, the cluster evolves similarly, but only with ~ 100 stars in the cluster. For a $10^5\,\mathrm{M}_\odot$ BH, the circular velocity of the stars is $\approx 66\,\mathrm{km\,s^{-1}}(r/0.1\,\mathrm{pc})^{-1/2}$.

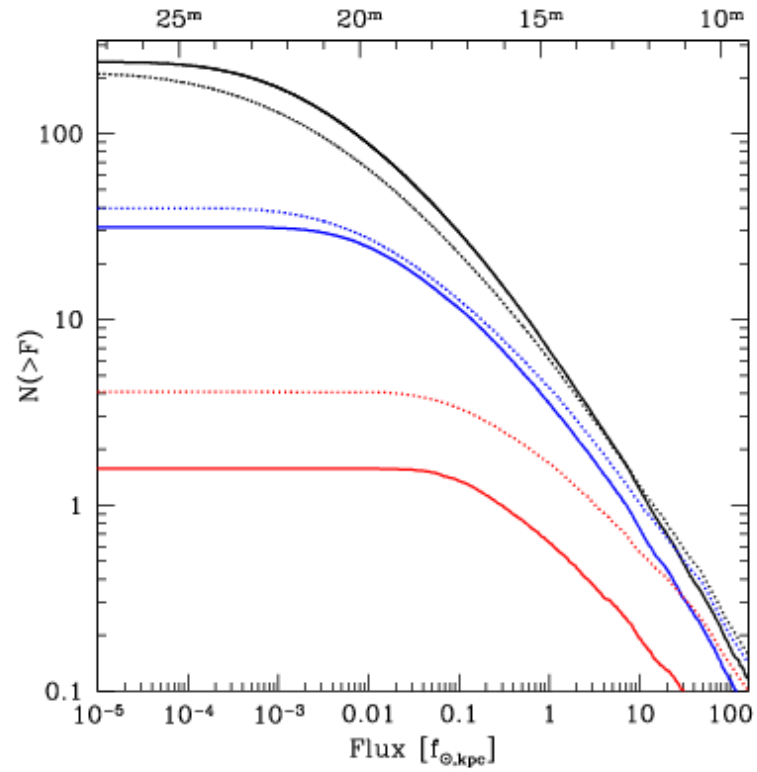

Figure 1. The cumulative distribution of ejected star clusters in the MW Halo. Plotted is the flux distribution associated with BHs masses greater than $10^3\,\mathrm{M}_\odot$ (black), $10^4\,\mathrm{M}_\odot$ (blue), and $10^5\,\mathrm{M}_\odot$ (red), in our models with BH spin $a = 0.9$ (solid) and $a = 0.1$ (dashed) lines, plotted in units of the flux of the Sun at a distance of 1 kpc ($f_{\odot,\mathrm{kpc}}$). The top axis is labeled with the apparent bolometric magnitude of the clusters. Nearly all BHs with $M_\bullet \gtrsim 2\times10^3\,\mathrm{M}_\odot$ have apparent magnitudes greater than 21, the rough magnitude limit of SDSS. The mass distribution of the ejected BHs has approximately equal mass per $\log M_\bullet$ interval, with $\mathrm{d}N_{\mathrm{BH}}/\mathrm{d}M_\bullet \propto M_\bullet^{-1}$.

Massive Black Hole Seeds: *Suppressed Fragmentation in Galaxies Just Above the Atomic Cooling Threshold*

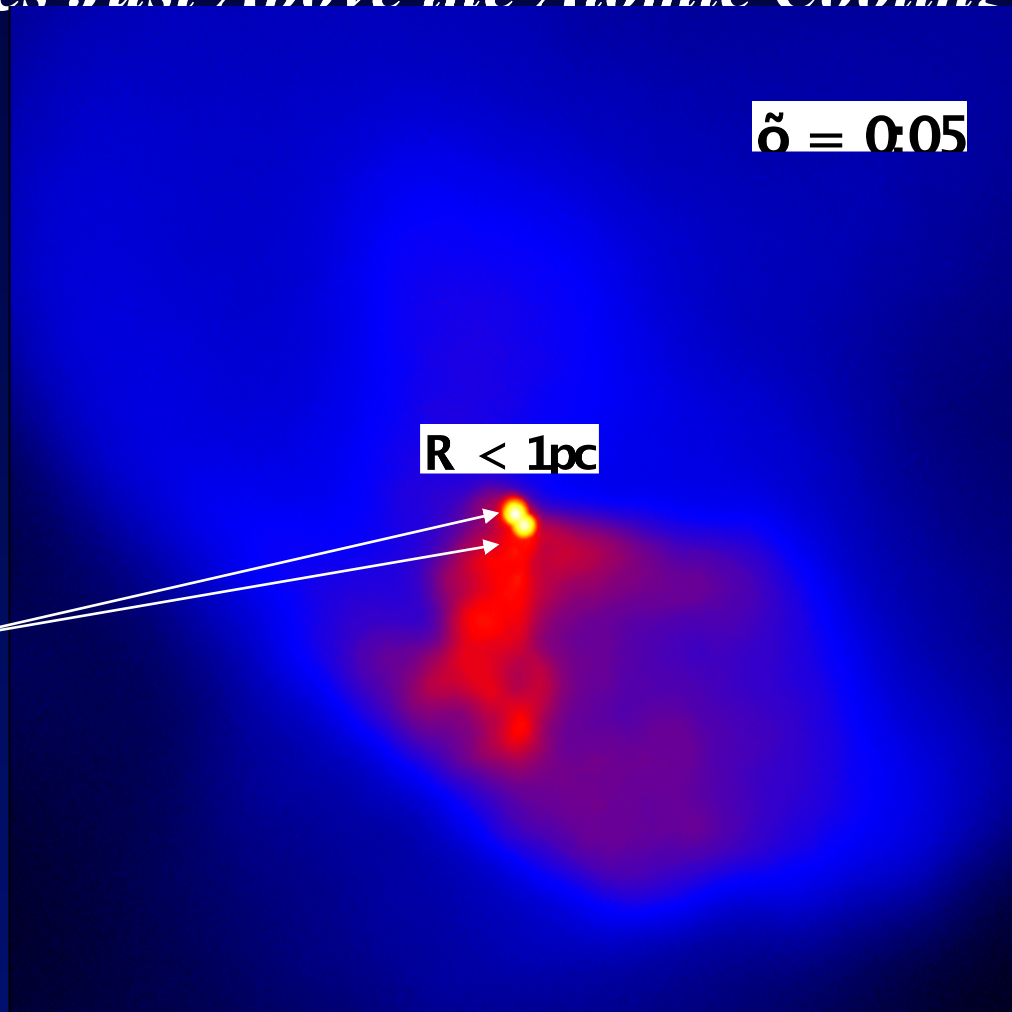

M 1 ø 2:2 â 10^{6}M ì
M 2 ø 3:1 â 10^{6}M ì

Unusual environments: H_2 suppressed *; binary black holes may form –LISA sources*

Numerical simulations: Bromm & Loeb 2002

Recent work: Dijkstra et al. 2008; Regan & Haehnelt 2009

Long Gamma-Ray Bursts: Observing One Star at a Time

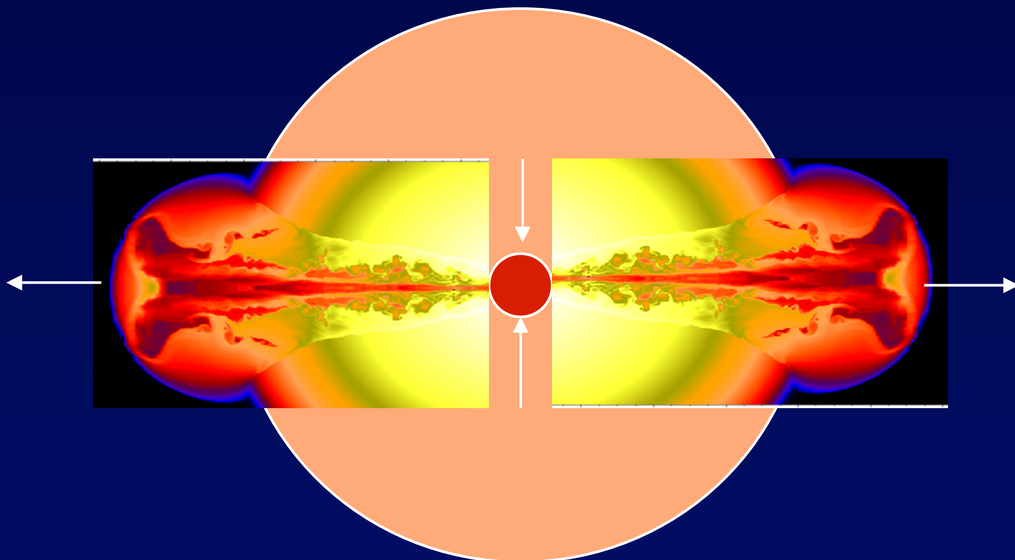

Collapse of a Massive Star

(accompanied by a supernova)

High-Redshift Gamma-Ray Bursts

Existing finder: ***Swift;*** **Proposed:** ***EXIST***

- **Key observational question:** ***how to efficiently identify high-z GRBs ?***
- **Key theoretical question:** ***Pop-III progenitors?***
- **Requirements:** ***sufficient angular momentum to make a disk around the central black hole & loss of progenitor's envelope, so that central engine would still be active upon jet exit. Related issues: binarity, winds.***

A Bright Explosion 620 Million Years after the Big Bang

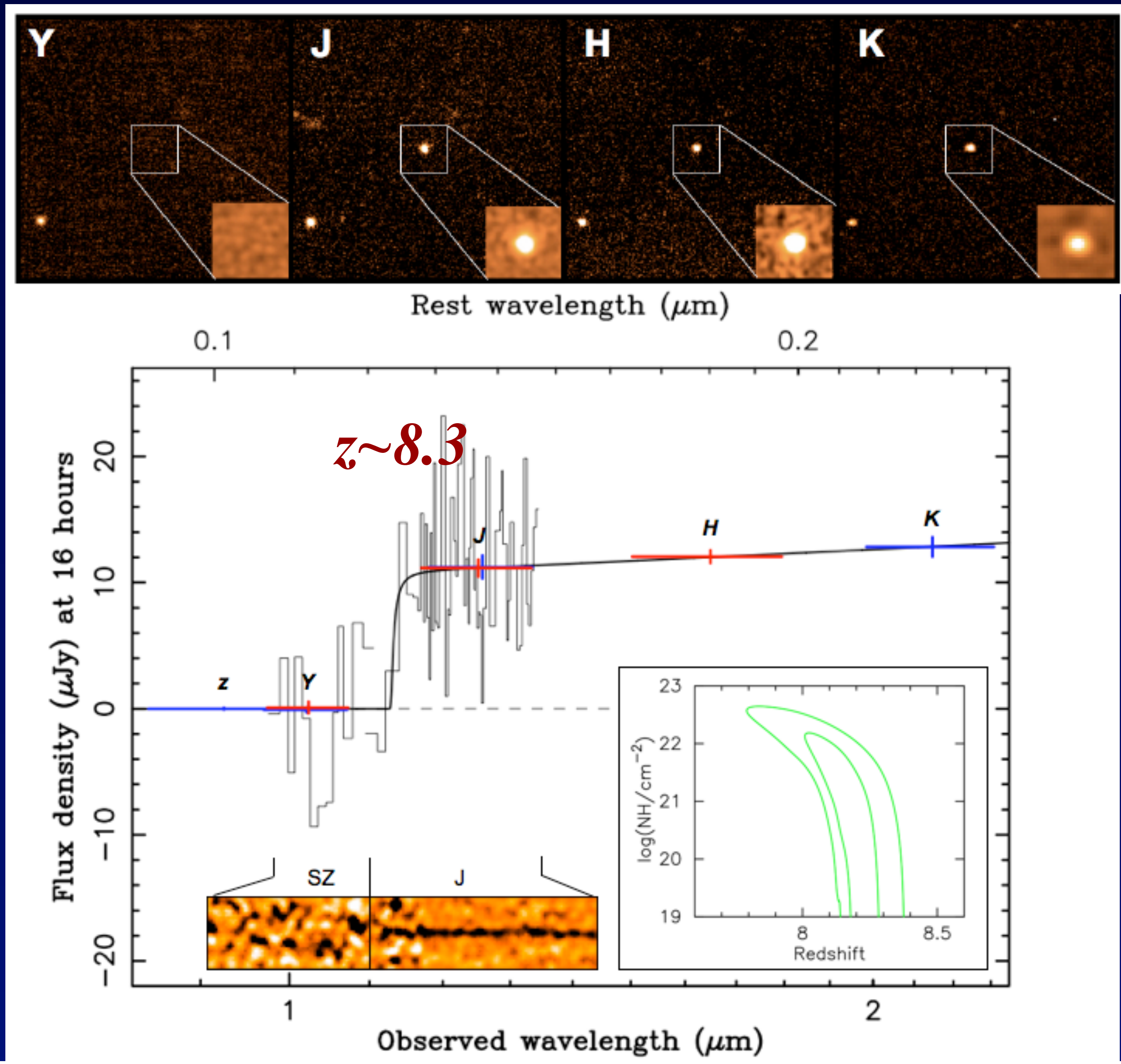

Detectability of Afterglow Emission Near the Lya Wavelength

Photometric redshift identification: based on the Lya trough

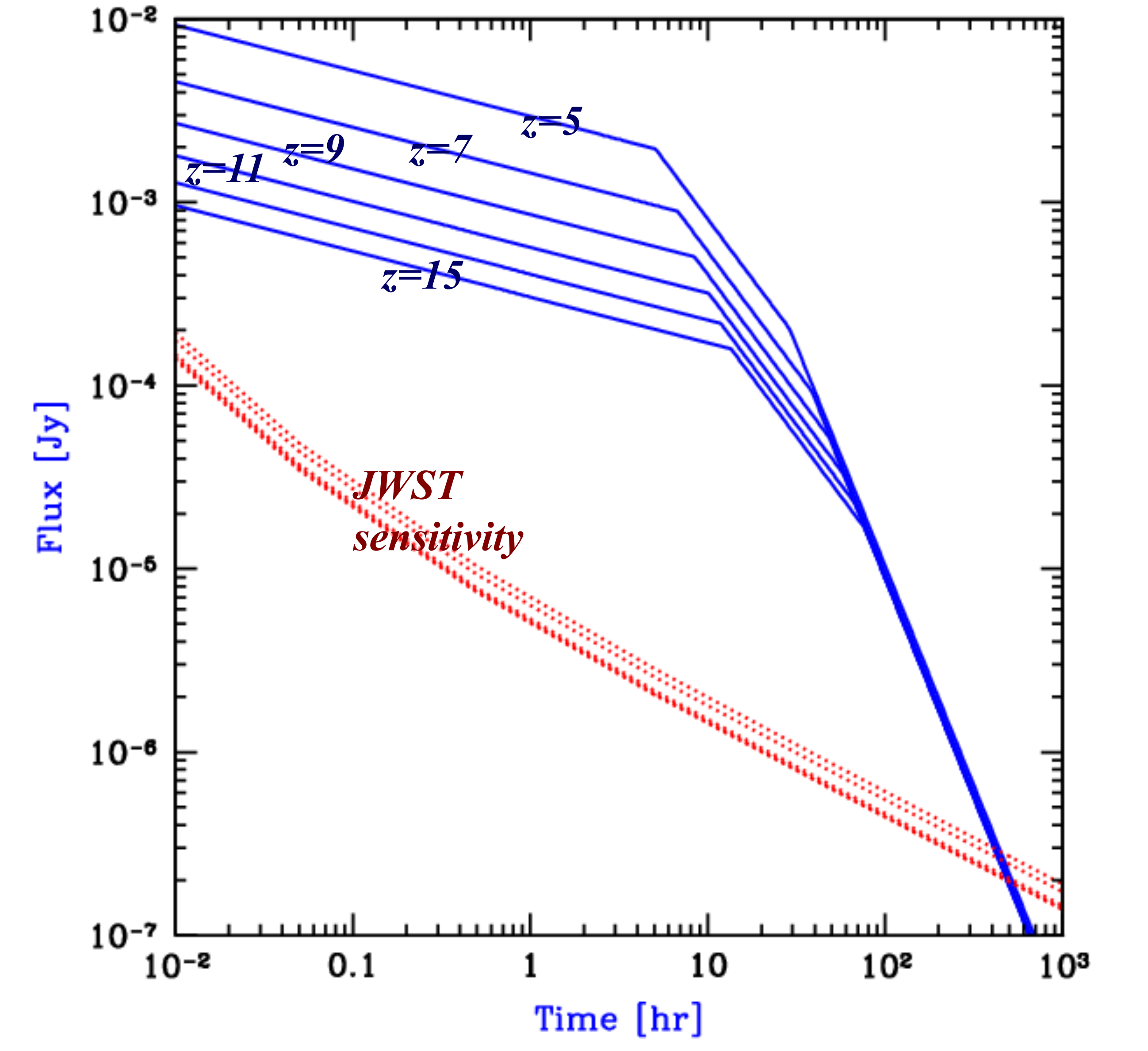

Barkana & Loeb 2003

astro-ph/0305470

Implications for the Cosmic Reionization from the Optical Afterglow Spectrum of the Gamma-Ray Burst 050904 at $z = 6.3$*

Tomonori TOTANI[1], Nobuyuki KAWAI[2], George KOSUGI[3], Kentaro AOKI[4], Toru YAMADA[3] Masanori IYE[3], Kouji OHTA[1], and Takashi HATTORI[4]

But associated DLAs hide Lya absorption from the IGM…

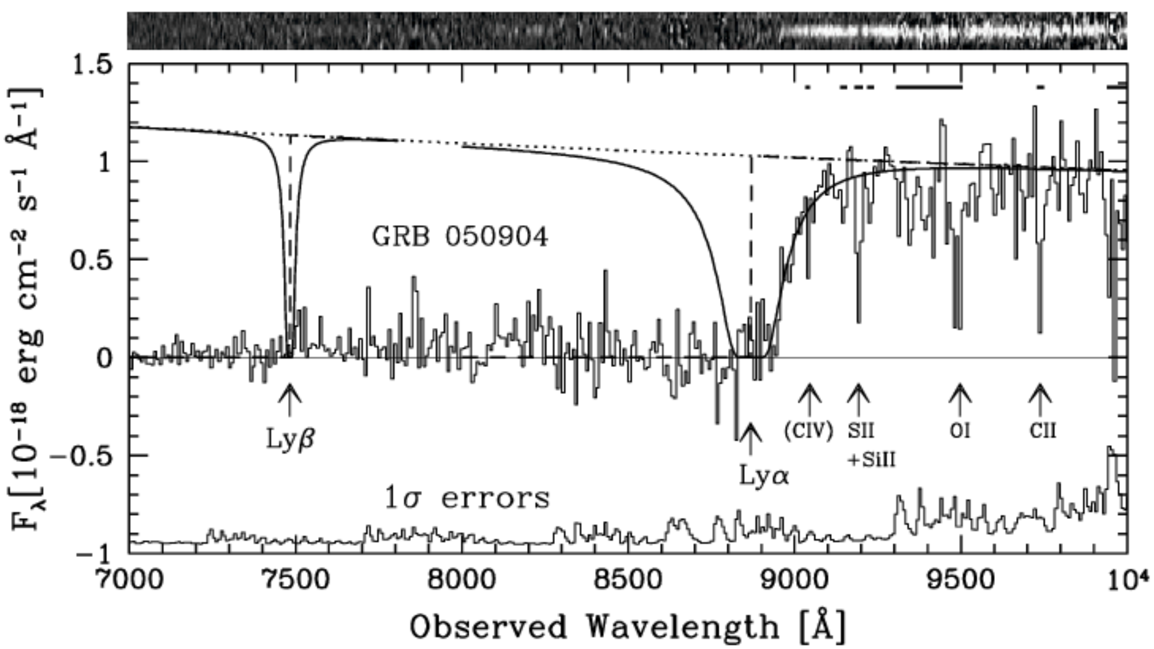

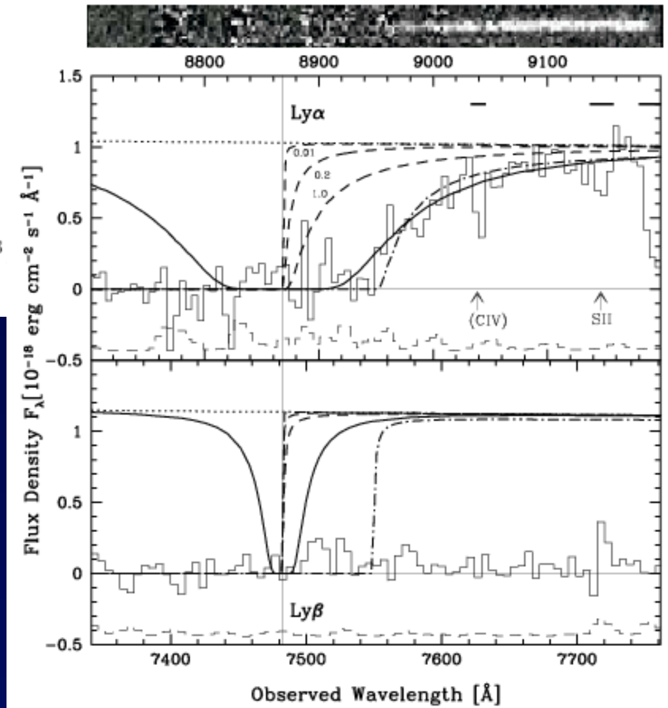

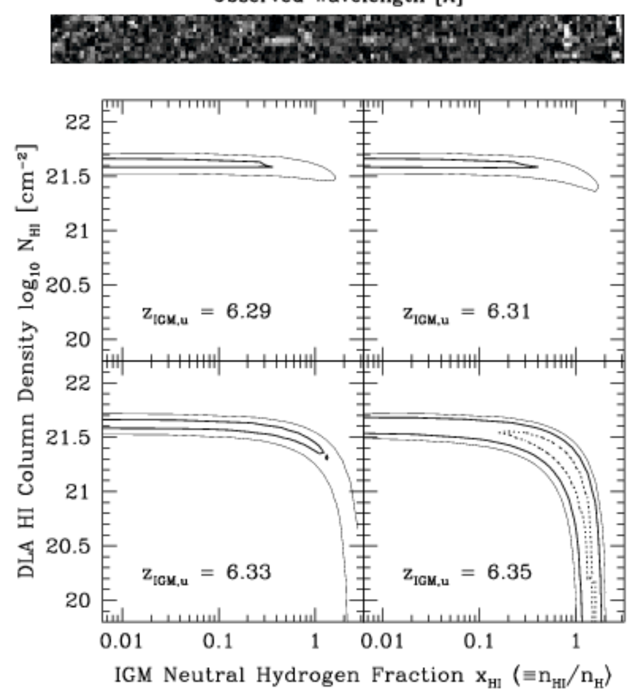

Searches for high-z Galaxies:

- Lyman-break
- Lyë
- Other lines (Hë , CO, CII, OI, He)

A future frontier: ***polarized*** Lyë ***halos***

Collapsing gas cloud

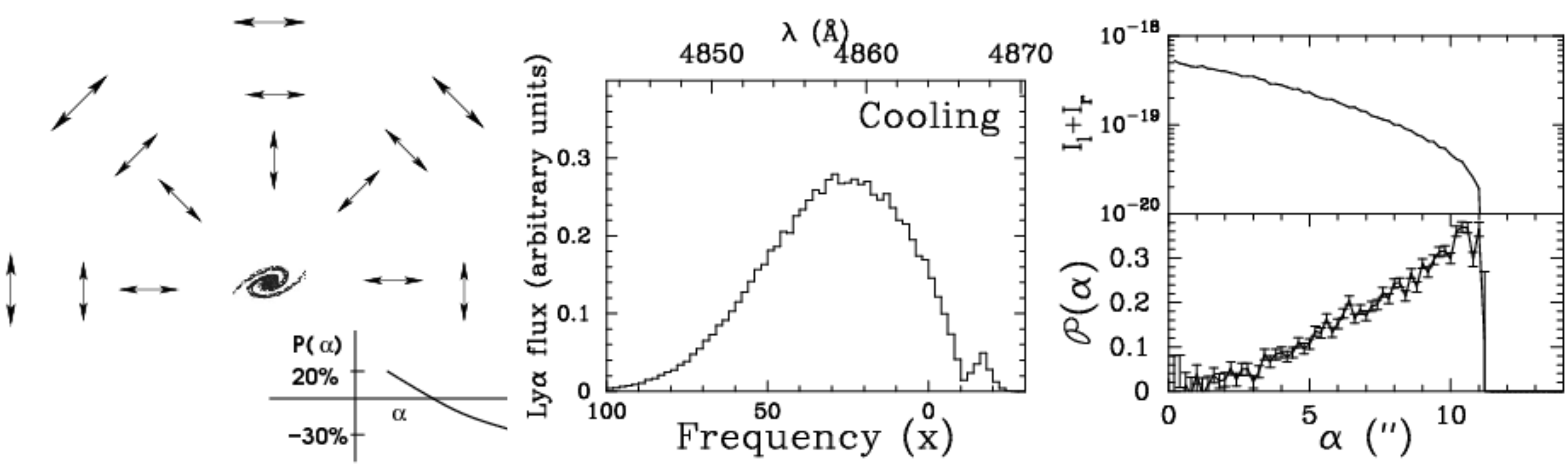

Rybicki & Loeb 1999; Dijkstra & Loeb arxiv:0711.2312

Observing the Diffuse Gas

21cm Mapping of Cosmic History

LIGHTING UP THE COSMOS

In the beginning of the Dark Ages, electrically neutral hydrogen gas filled the universe. As stars formed, they ionized the regions immediately around them, creating bubbles here and there. Eventually these bubbles merged together, and intergalactic gas became entirely ionized.

Time:	210 million years	290 million years	370 million years	460 million years	540 million years	620 million years	710 million years
Width of frame:	2.4 million light-years	3.0 million light-years	3.6 million light-years	4.1 million light-years	4.6 million light-years	5.0 million light-years	5.5 million light-years
Observed wavelength:	4.1 meters	3.3 meters	2.8 meters	2.4 meters	2.1 meters	2.0 meters	1.8 meters
	All the gas is neutral. The white areas are the densest and will give rise to the first stars and quasars.	Faint red patches show that the stars and quasars have begun to ionize the gas around them.	These bubbles of ionized gas grow.	New stars and quasars form and create their own bubbles.	The bubbles are beginning to interconnect.	The bubbles have merged and nearly taken over all of space.	The only remaining neutral hydrogen is concentrated in galaxies.

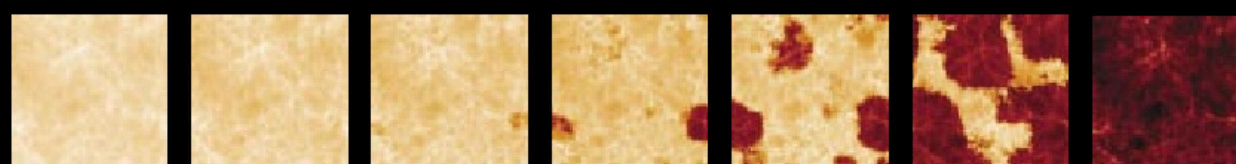

Simulated images of 21-centimeter radiation show how hydrogen gas turns into a galaxy cluster. The amount of radiation (*white is highest; orange and red are intermediate; black is least*) reflects both the density of the gas and its degree of ionization: dense, electrically neutral gas appears white; dense, ionized gas appears black. The images have been rescaled to remove the effect of cosmic expansion and thus highlight the cluster-forming processes. Because of expansion, the 21-centimeter radiation is actually observed at a longer wavelength; the earlier the image, the longer the wavelength.

Mapping the Cosmic Distribution of

Hydrogen

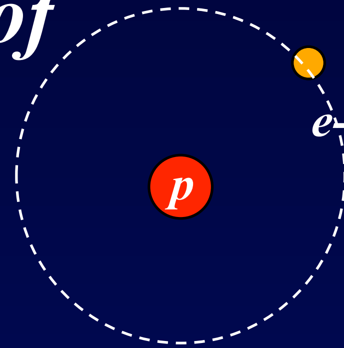

Ground level

excitation rate= (atomic collisions)+(radiative coupling to CMB)

Couple T_s *to* T_k *Couples* T_s *to* T_γ

$$\lambda_{21cm} = (1.4\,\mathrm{GHz})^{-1}$$

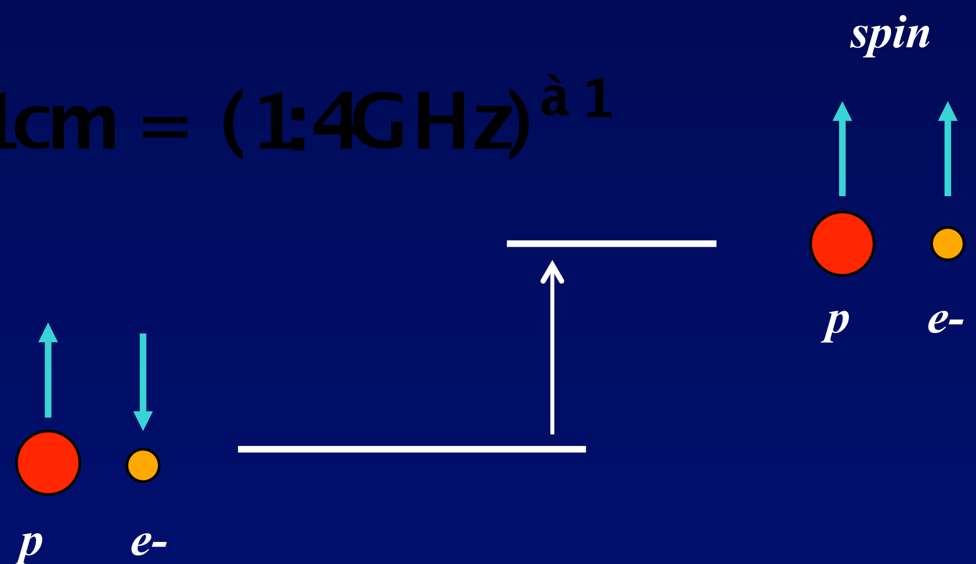

$^1S_{1/2}$

$^0S_{1/2}$

Spin Temperature $$\frac{n_1}{n_0} = \frac{g_1}{g_0}\exp\left\{-\frac{0.068K}{T_s}\right\} \qquad (g_1/g_0) = 3$$

***Predicted** by Van de Hulst in 1944; **Observed** by Ewen &Purcell in 1951 at Harvard*

21cm Tomography of Ionized Bubbles During Reionization is like

Slicing Swiss Cheese

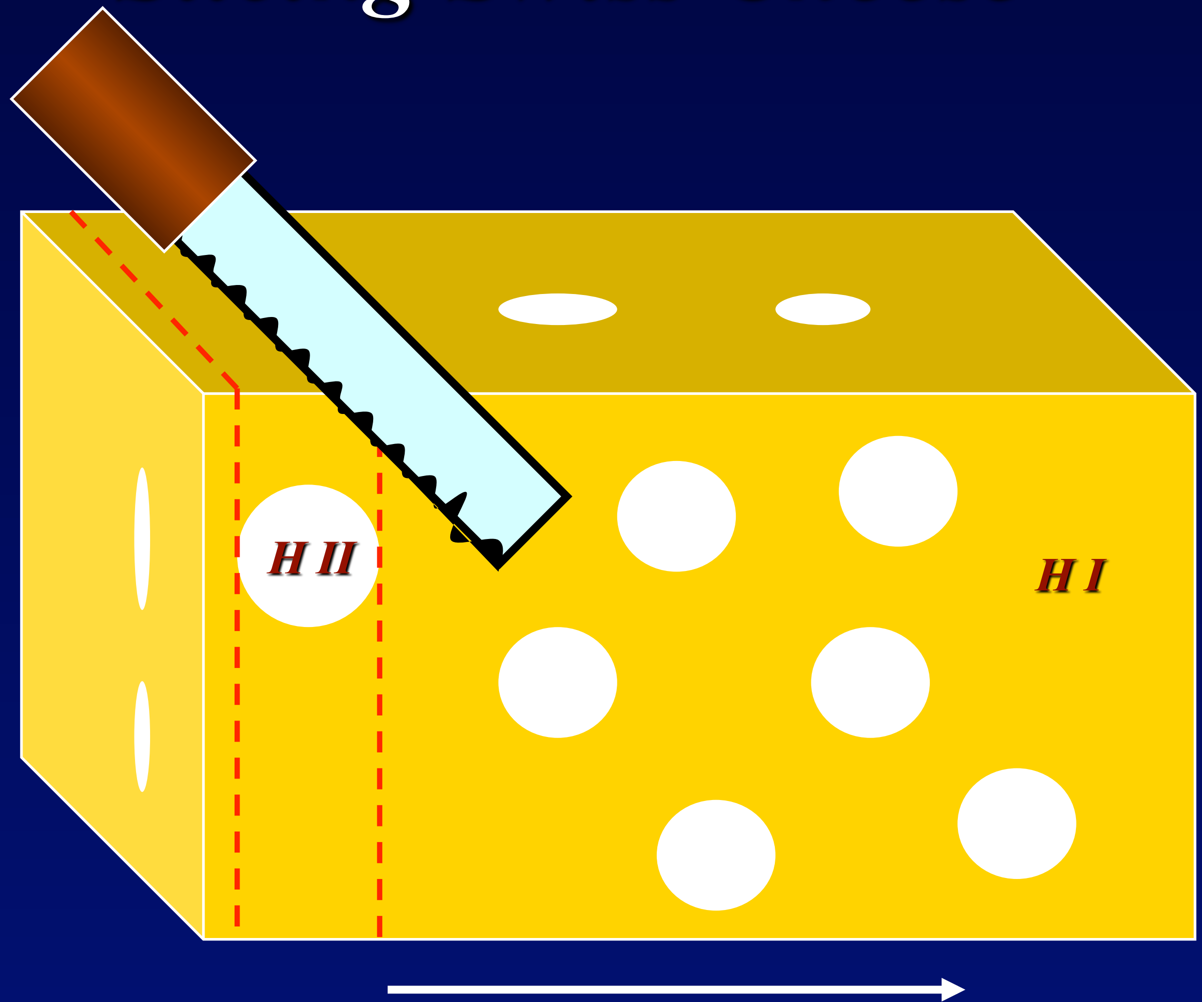

Observed wavelength ⇔ distance

21cm â (1 + z)

Separating the Physics from the Astrophysics

Physics: *initial conditions from inflation; nature of dark matter and dark energy*

Astrophysics: *consequences of star formation*

Three epochs:

- ***Before the first galaxies (z>25):*** mapping of density fluctuations through 21cm absorption
- ***During reionization:*** anisotropy of the 21cm power spectrum due to peculiar velocities
- ***After reionization (z<6):*** dense pockets of residual hydrogen (DLAs) trace large scale structure

Testing gravity: measuring the gravitational growth of perturbations on small scales (not probed so far) which are still in the linear regime at high redshifts ($1<z<15$)

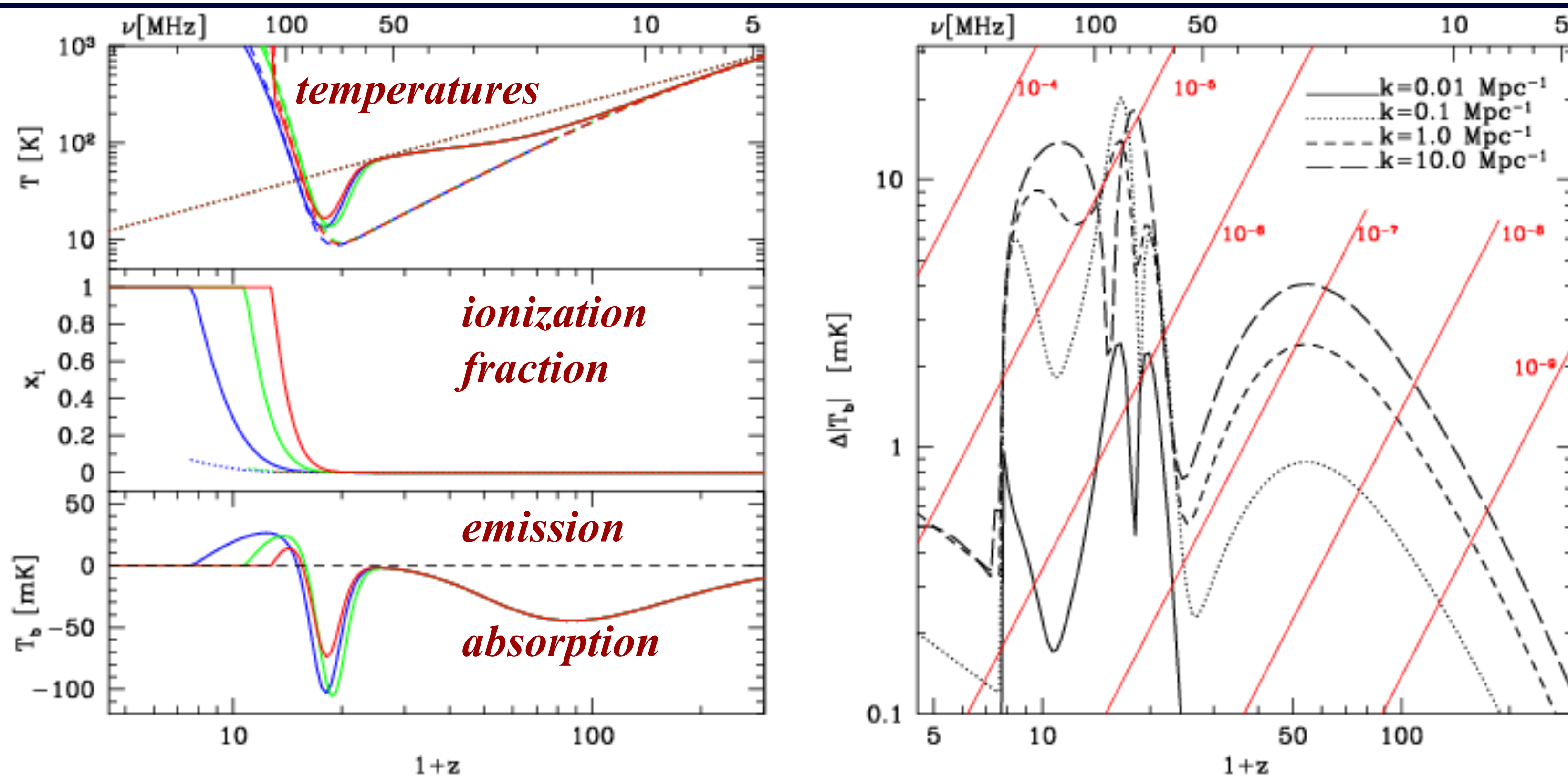

Left: *Top panel:* Evolution of the mean CMB (dotted curve), intergalactic medium (IGM, dashed curve), and spin (solid curve) temperatures. *Middle panel:* Evolution of the filling fraction of ionized bubbles (solid curve) and electron fraction outside the bubbles (dotted curve). *Bottom panel:* Evolution of mean 21cm brightness temperature. Three different astrophysical models are plotted, corresponding to the -1σ (red curve), best-fit (green curve), and $+1\sigma$ (blue curve) optical depth values derived from WMAP [, *Right:* Redshift evolution of the angle-averaged 21cm power spectrum $\bar{\Delta}_{T_b}$ in the -1σ model for wave-numbers $k = 0.01$ (solid curve), 0.1 (dotted curve), 1.0 (short dashed curve), and 10.0 Mpc^{-1} (long dashed curve). Diagonal lines indicate the foreground brightness of the sky $T_{\rm sky}(\nu)$ times a factor r ranging from 10^{-4} to 10^{-9}, indicative of the level of foreground subtraction required .

(Pritchard & Loeb 2008)

Experiments

***MWA (Murchison Wide-Field Array)**

MIT/U.Melbourne,ATNF,ANU/CfA/Raman I.

***LOFAR (Low-frequency Array)**

Netherlands

***21CMA (formerly known as PAST)**

China

***PAPER**

UCB/NRAO

***GMRT (Giant Meterwave Radio Telescope)**

India/CITA/Pittsburg

***SKA (Square Kilometer Array)**

International

Observatory Parameters

experiment	site	type	ν range MHz	Area m^2	date	goal
Mark I[a]	Australia	spiral	100-200	few	2007	All Sky
EDGES[b]	Australia	four-point	100-200	few	2007	All Sky
GMRT[c]	India	parabola array	150-165	4e4	2007	CSS[d]
PAPER[e]	Australia	dipole array	110-190	1e3	2007	PS/CSS/Abs
21CMA[f]	China	dipole array	70-200	1e4	2007	PS
MWAd[g]	Australia	aperture array	80-300	1e4	2008	PS/CSS/Abs
LOFAR[h]	Netherlands	aperture array	115-240	1e5	2008	PS/CSS/Abs
SKA[i]	TBD	aperture array	100-200	1e6	2015	Imaging

Status: analogous to CMB research prior to COBE

Murchison Wide-Field Array: *21cm emission from diffuse hydrogen at z=6.5-15*

- 4mx4m tiles of 16 dipole antennae, 80-300MHz
- 500 antenna tiles with total collecting area 8000 sq.m. at 150MHz across a 1.5km area; few arcmin resolution

When Was the Universe Ionized?

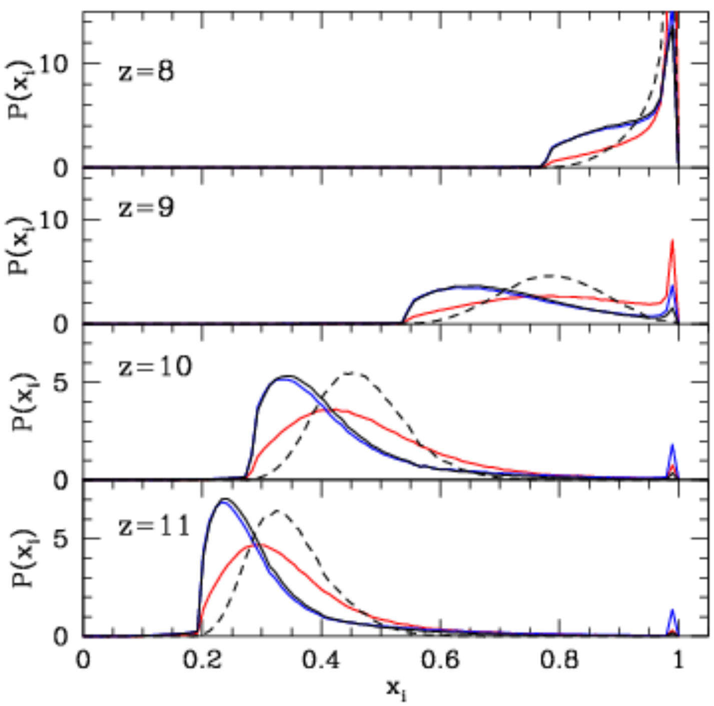

Figure 5. Distribution of x_i at redshifts $z = 8$, 9, 10, and 11 for the ζ parametrization. Same curve styles as for Figure 4.

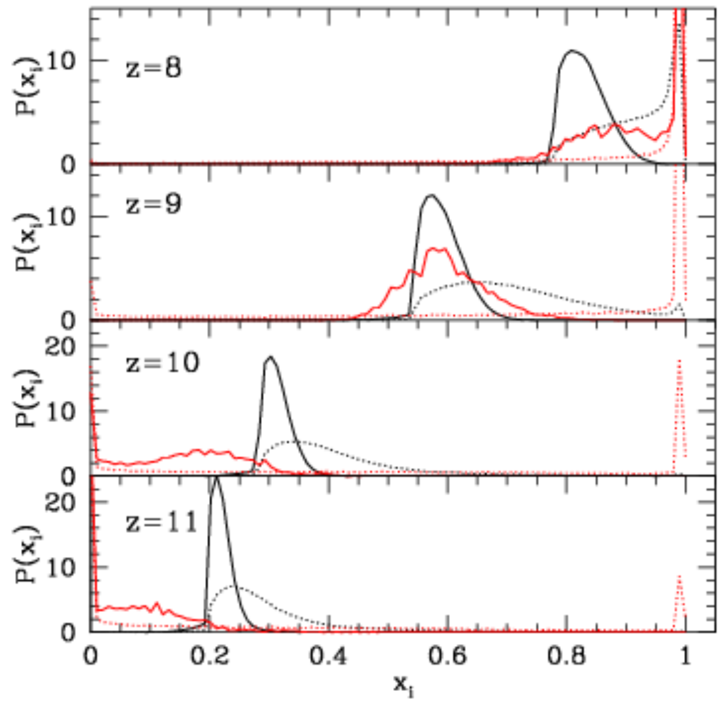

Figure 14. Distribution of x_i at redshifts $z = 8$, 9, 10, and 11 when 21 cm measurements are included. In each panel, we plot the distribution of the ζ (black) and $\dot{N}_{\rm ion}$ (red) parametrizations with (solid curves) and without (dotted curves) a 21 cm measurement of $x_i(z = 9.5) = 0.5 \pm 0.05$.

- Based on Lya forest at z<6 and CMB data

Pritchard, Loeb, & Wyithe, arXiv:0908.3891

The Next Decade Will be Exciting!

- ***Large-aperture infrared telescopes and radio arrays will image the galaxies as well as the diffuse cosmic gas during the epoch of reionization over the coming decade. (21cm brightness fluctuations are expected to be anti-correlated with infrared galaxies during reionization).***
- ***Adequate simulations of reionization will describe large (>100Mpc) boxes with high resolution for source identification.***

On small scales the universe is clumpy

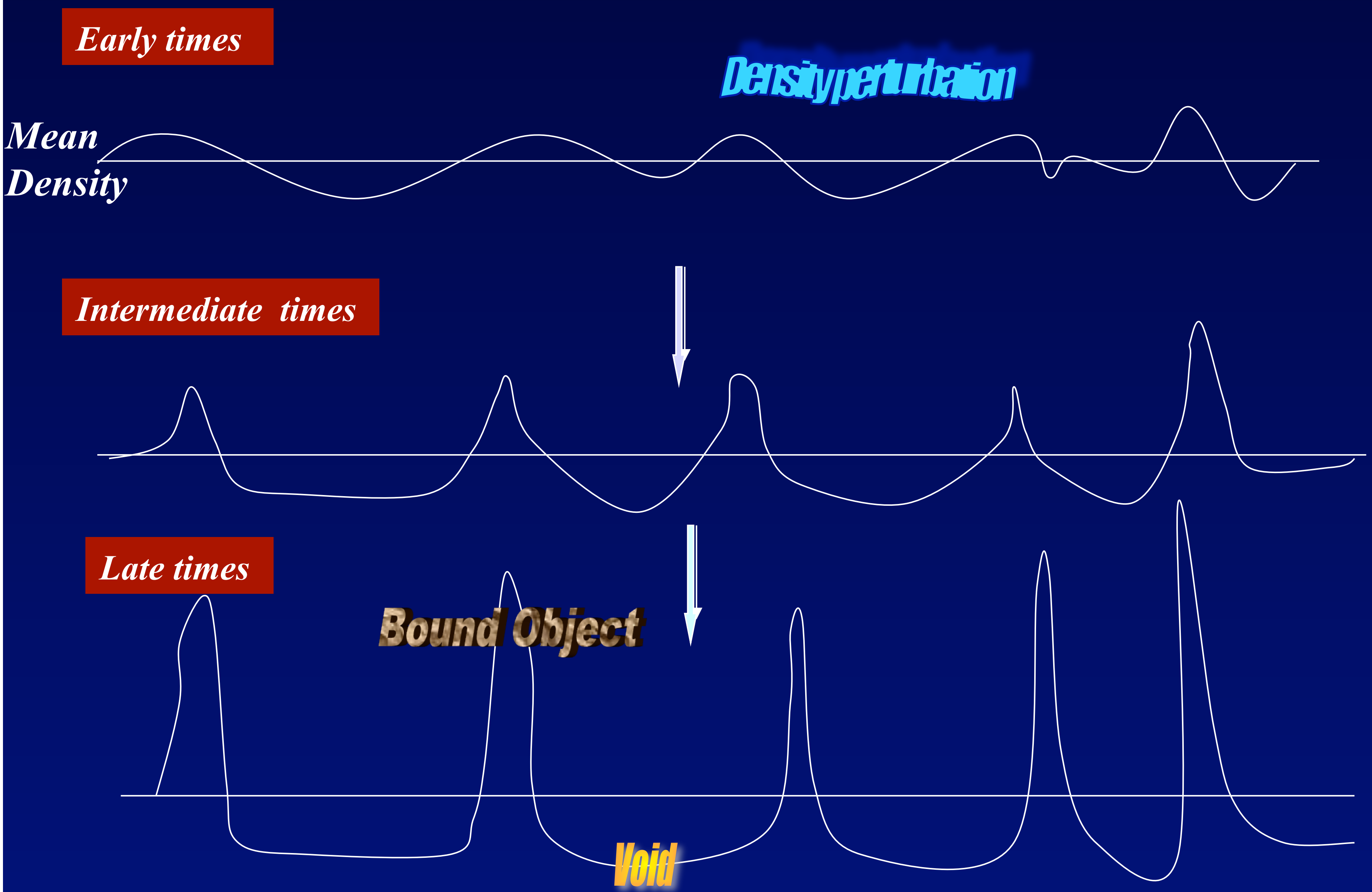

Long Gamma-Ray Bursts: Observing One Star at a Time

GRB080319B –Visible to the naked eye at the edge of the Universe

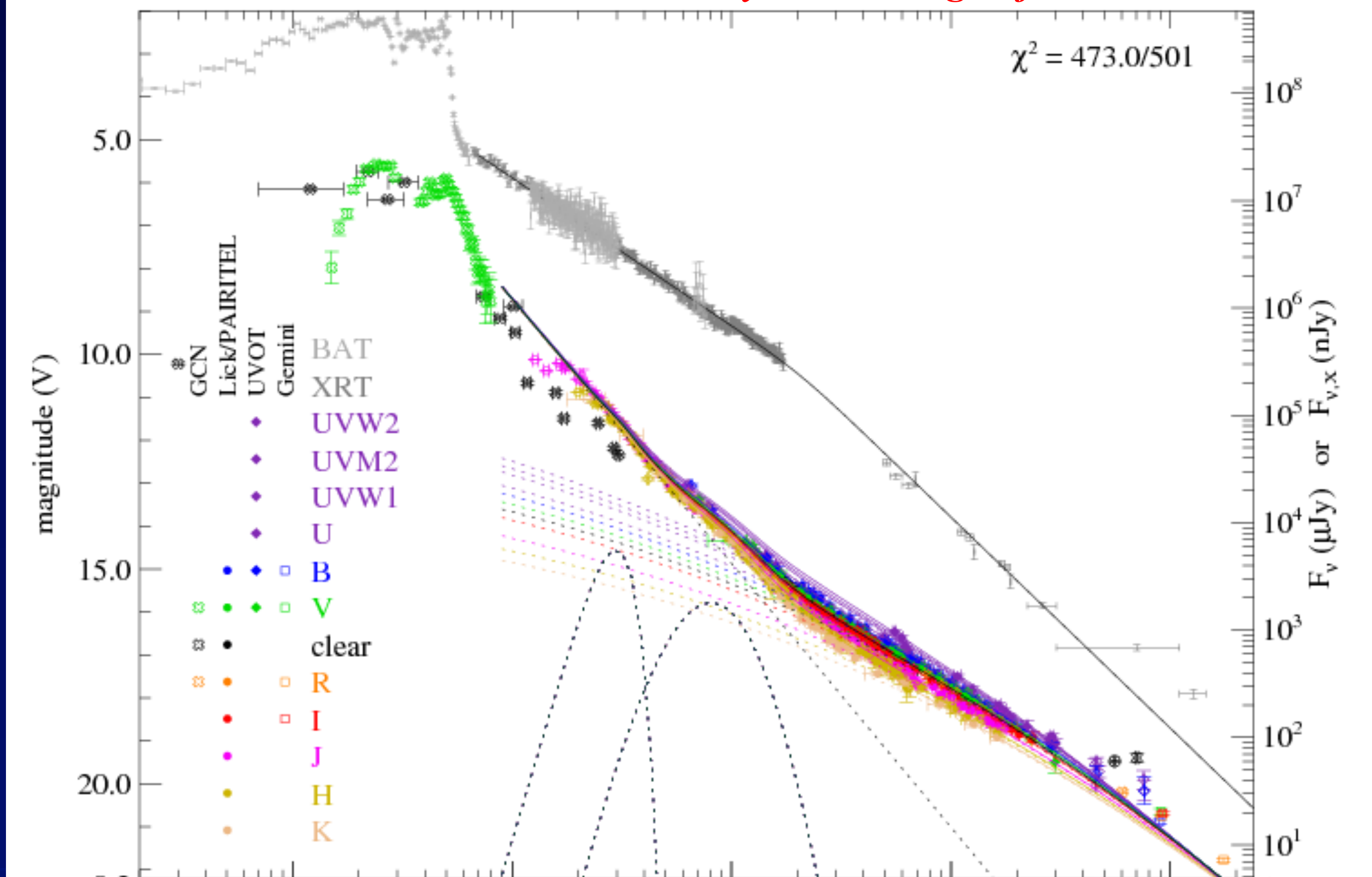

Existing finder: *Swift;*   Proposed: *EXIST (high-z GRBs)*

Key questions: Pop-III progenitors? (binarity, metal-free wind)

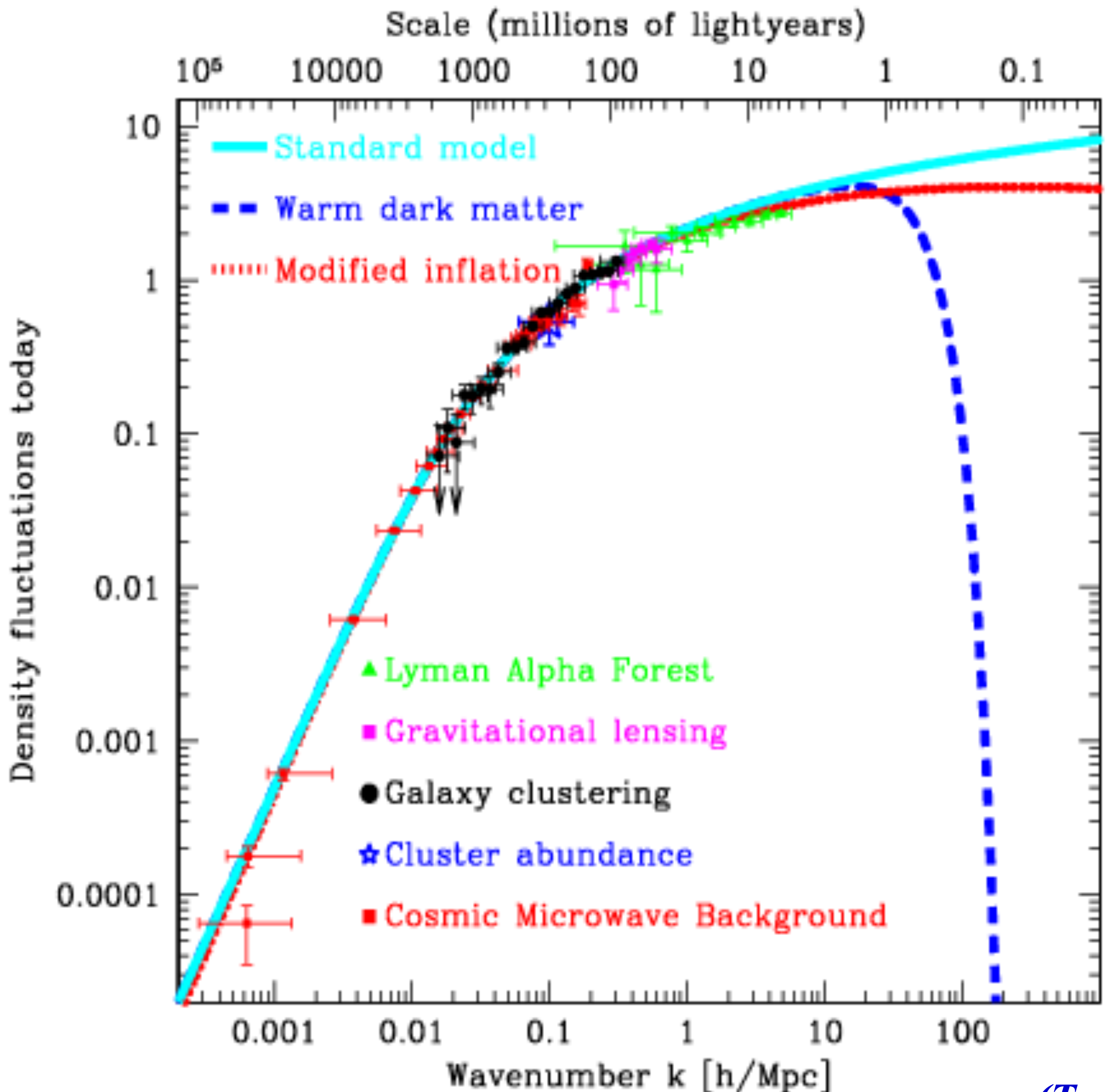

(Tegmark 2008)

Power-Spectrum Sensitivity

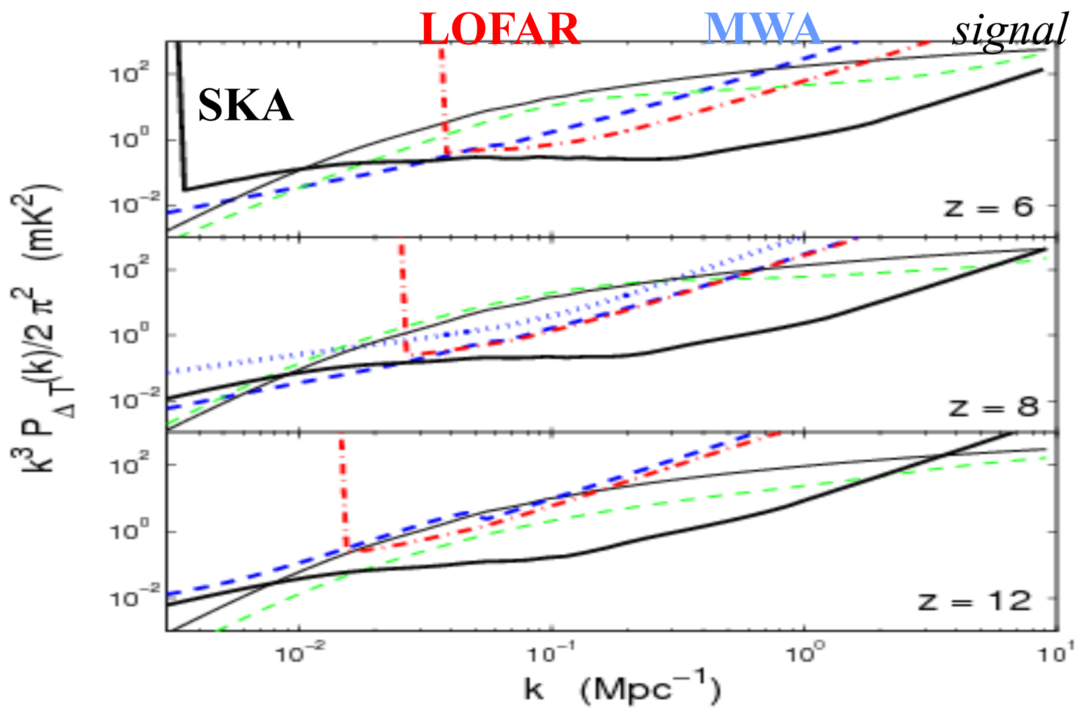

Isotropic power spectrum sensitivity, in logarithmic bins with $\Delta k = k/2$, for several experimental configurations. In each panel, the thin solid and dashed curves show estimates of the signal with and without reionization. The thick solid, dashed, and dot-dashed curves show error estimates for 1000 hour observations over 6 MHz with the SKA, MWA, and LOFAR, respectively. Each assumes perfect foreground removal. The dotted curve in the middle panel assumes a flat antenna distribution for the MWA. From ***McQuinn et al. 2006***

$$T_{\rm sky} \sim 180 \left(\frac{\nu}{180\ {\rm MHz}}\right)^{-2.6} {\rm K}$$

$$\Delta T^N|_{\rm int} \sim 2\ {\rm mK} \left(\frac{A_{\rm tot}}{10^5\ {\rm m}^2}\right)^{-1} \left(\frac{10'}{\Delta\theta}\right)^2 \left(\frac{1+z}{10}\right)^{4.6} \left(\frac{\rm MHz}{\Delta\nu}\,\frac{100\ {\rm hr}}{t_{\rm int}}\right)^{1/2}.$$

Cooling Rate of Primordial Gas

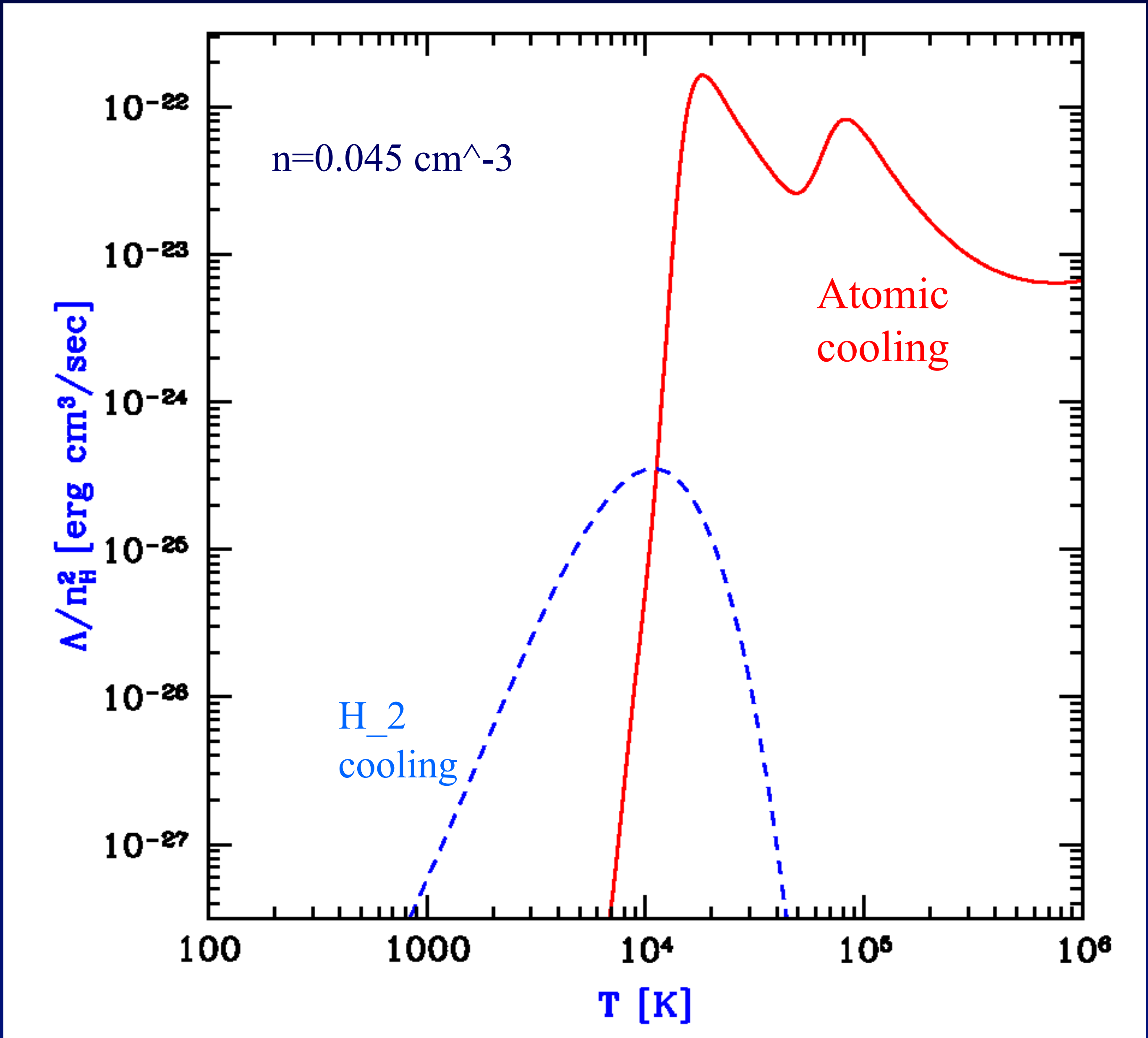

Massive Accretion by Pop-III Proto-Stars

Bromm & Loeb, astro-ph/0312456

Resolving accretion flow down to ~0.03 pc

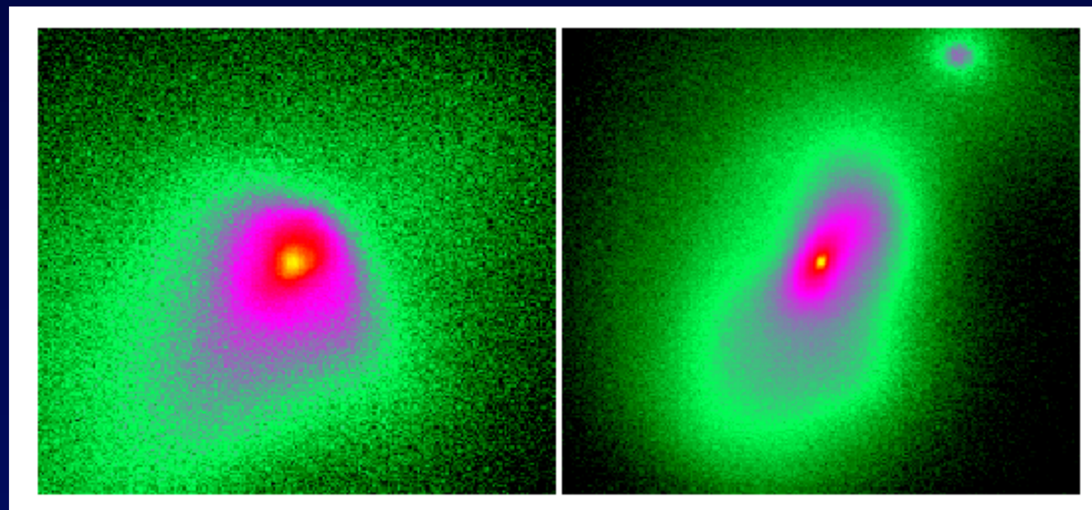

23.5pc *0.5pc*

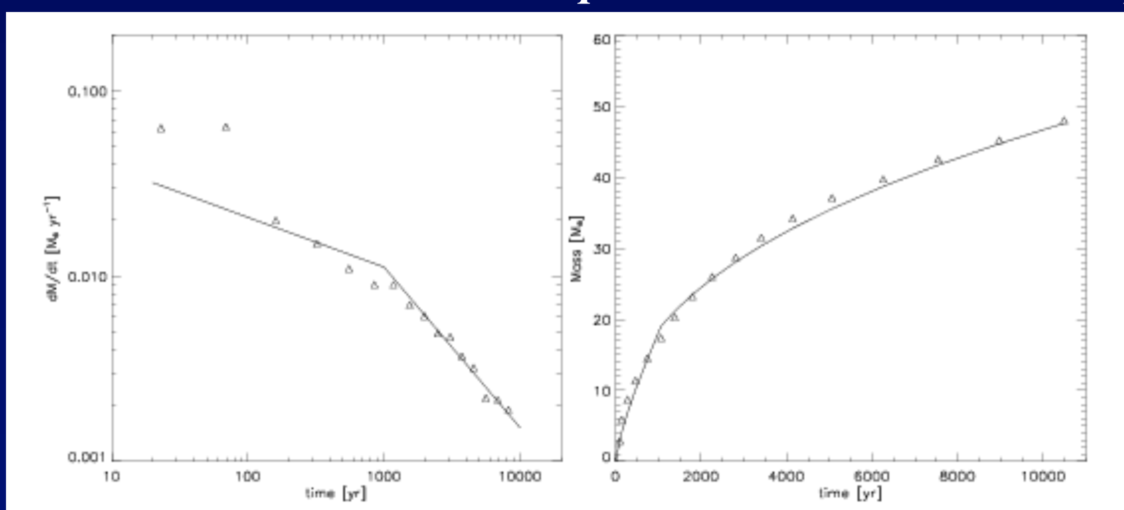

$$\dot{M} \propto c_s^3/G$$

$$T_{min} \propto 200K$$

for : $H_2 \rightarrow$ cooling

Final stellar mass is feedback limited (radiation, wind)

Probing Reionization with MW Satellites

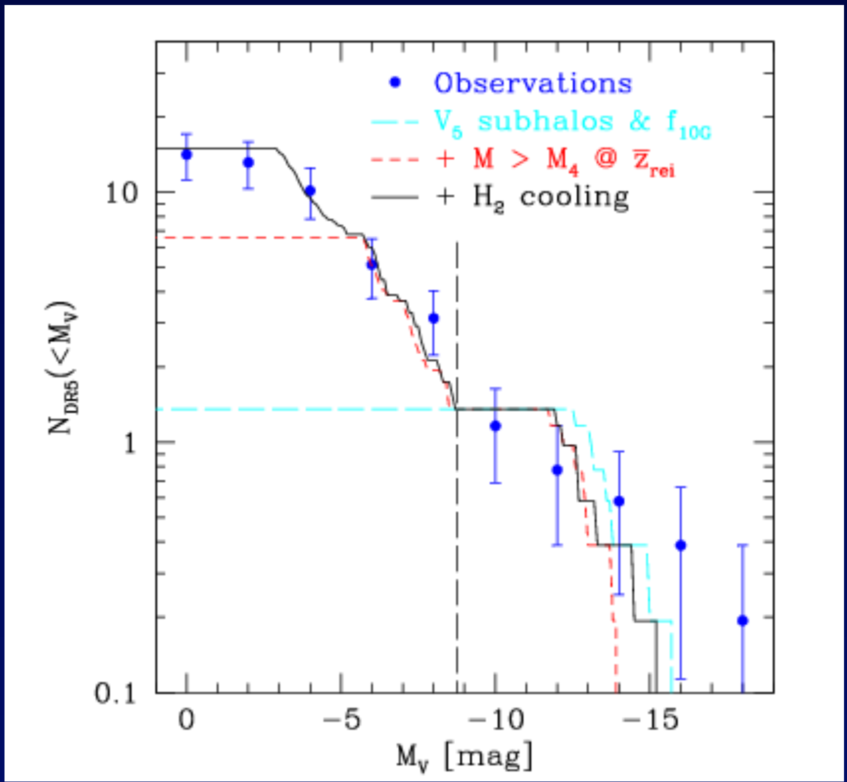

Figure 1. The luminosity function (LF) of MW satellites in the SDSS footprint with the DR5 selection threshold. The observed function is shown by the blue points with the non-SDSS objects each contributing a fractional amount $f_{DR5} = 0.194$ to the total. The curves show the theoretical predictions including successively more elaborate models. The model given by the long-dashed, cyan curve illuminates only those VLII subhalos with maximum circular velocities that exceed V_5 at some point in their histories and continue to form stars after reionization via atomic hydrogen cooling (with an efficiency of $f_5 = 0.02$) and metal cooling in the last 10 Gyr ($f_{10G} \neq 0$). The short-dashed, red curve includes star formation in subhalo progenitors more massive than M_4 at $\bar{z}_{rei} = 11.2$ assuming a single redshift of reionization for the entire MWgfr and $f_{\mathrm{H\,I,ex}} = 0.02$. The solid, black curve fitting the faint end of the observed LF additionally takes into account molecular hydrogen cooling, prior to suppression at $z_{\mathrm{H_2}} = 23.1$, in progenitors more massive than $M_{\mathrm{H_2}} = 10^5\,M_\odot$ with $f_{\mathrm{H_2}} = 0.4$. The long-dashed vertical line demarcates the luminosities at which pre- vs. post-SDSS satellites are observed.

- ***Via-Lactae II:*** dark matter simulation of the MW halo merger tree
- ***Resolution to "missing satellite problem":*** photo-ionization heating and molecular hydrogen suppression

Munoz, Madau, Loeb & Diemand 2009

Effect of Recoil on BH Growth and Feedback

440 km/s ***740 km/s***

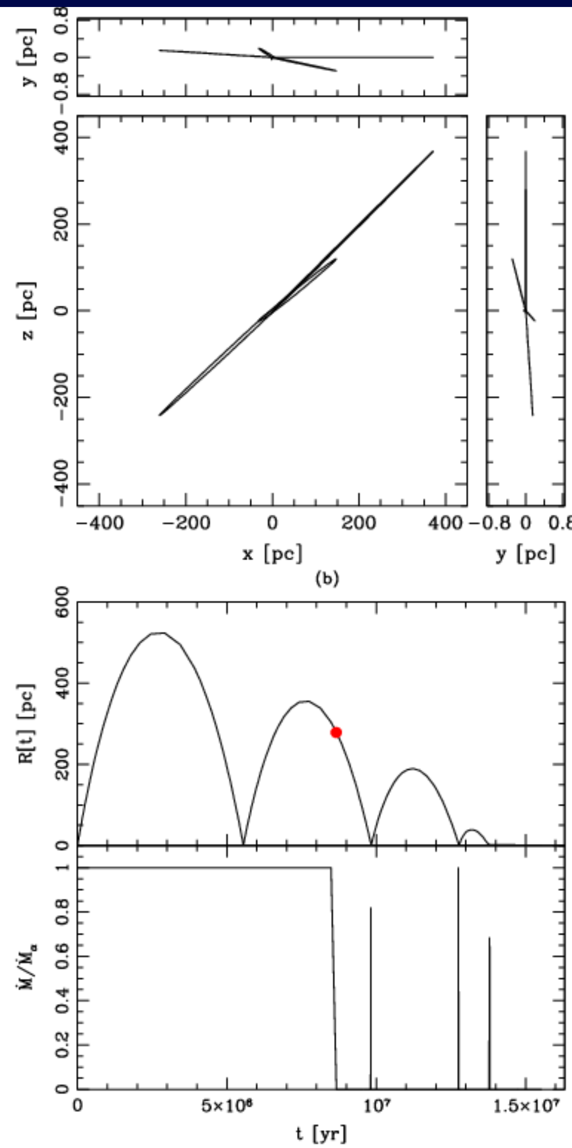

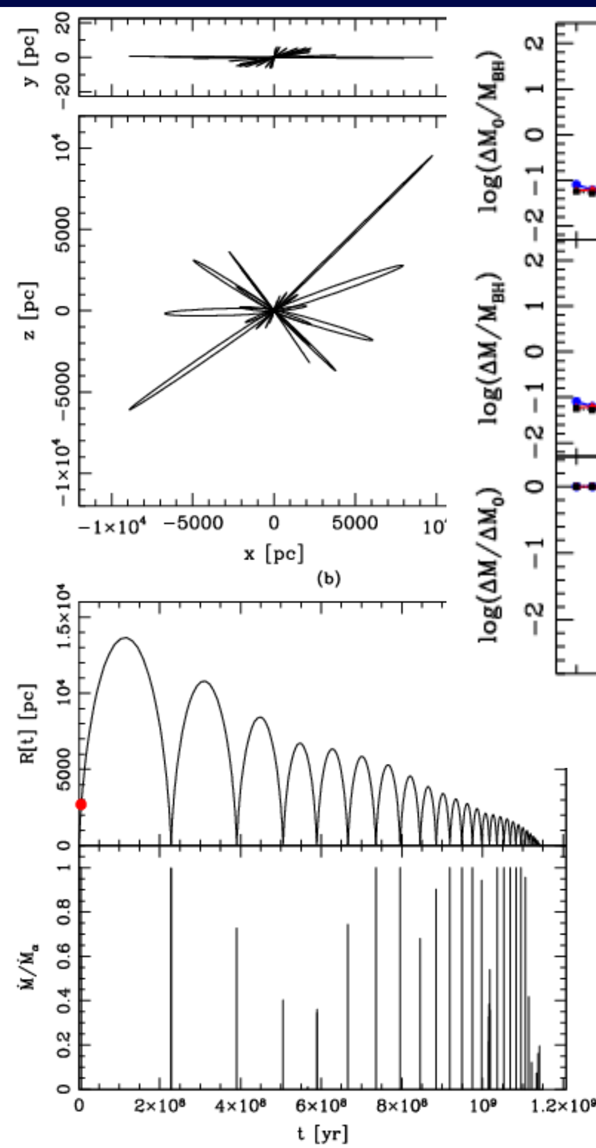

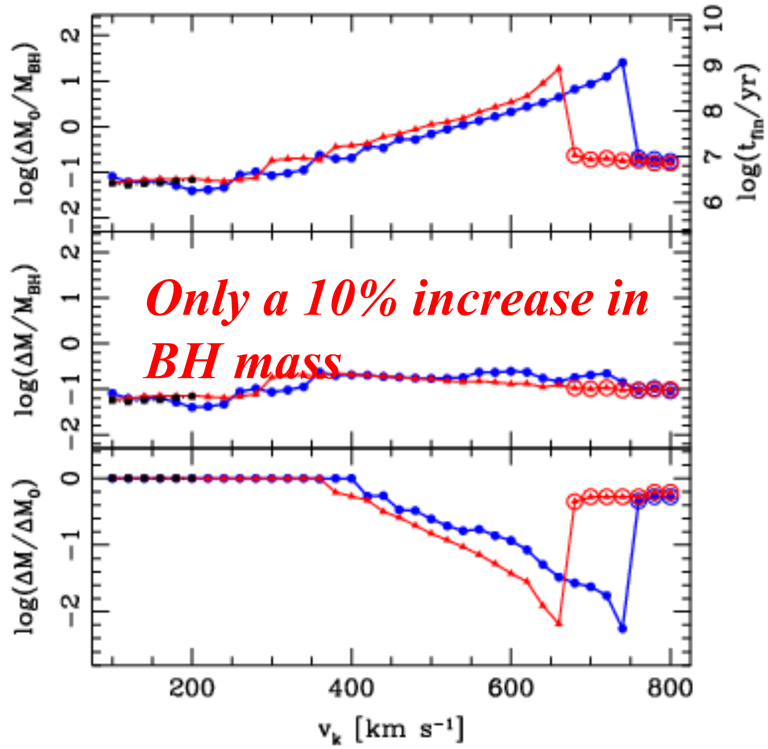

Only a 10% increase in BH mass

Blecha & Loeb
arXiv:0805.1420

Virial Temperature of Halos

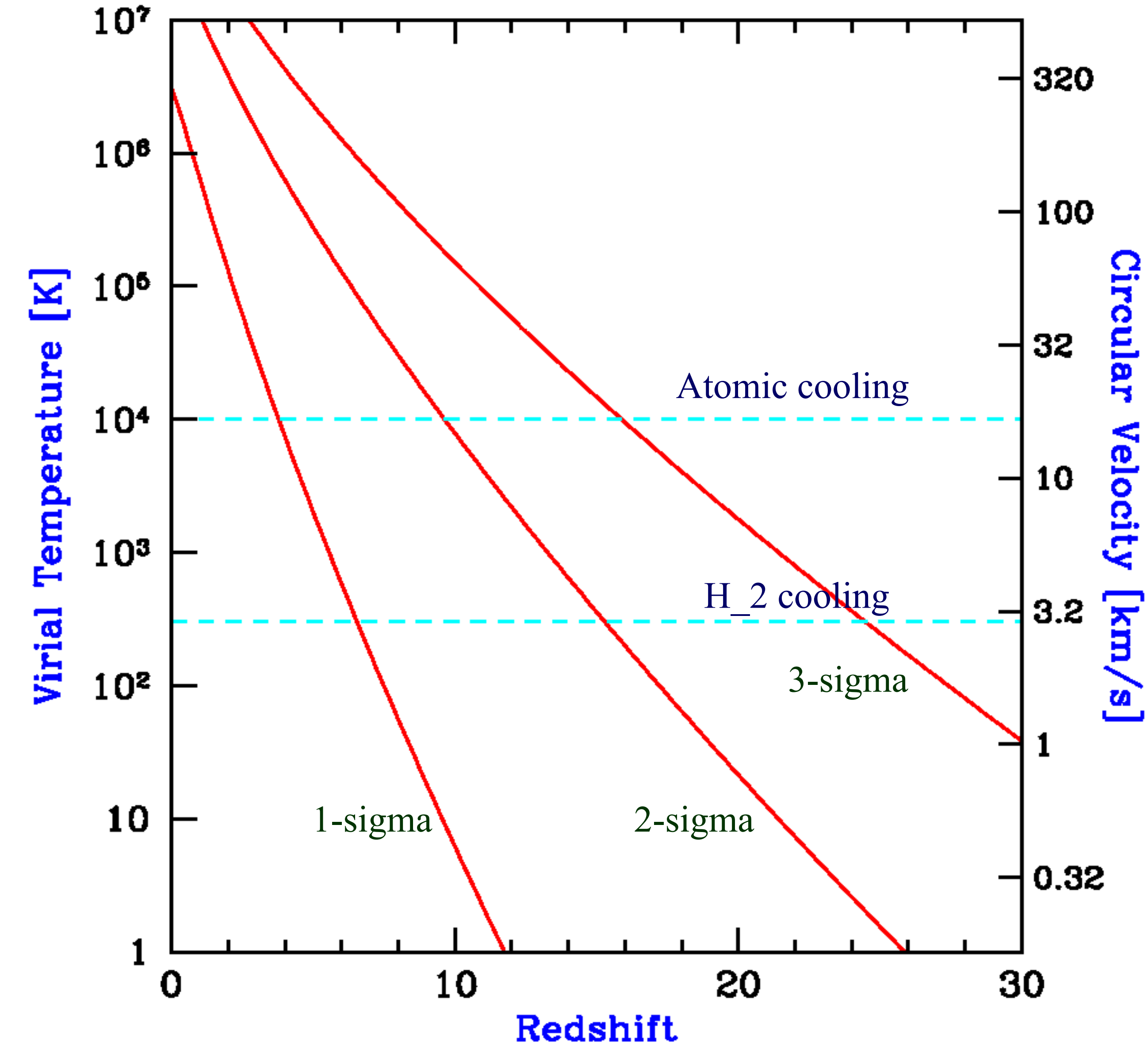

Line-of-Sight Anisotropy of 21cm Flux Fluctuations

$$T_b = ü \left(\frac{T_s à T_í}{1+z} \right)$$

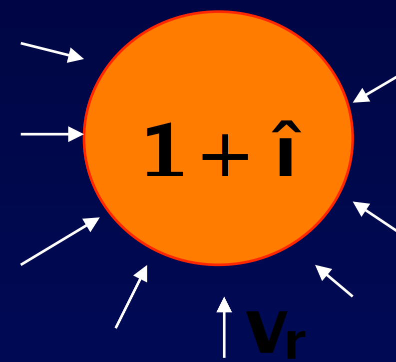

Peculiar velocity changes $ü \,/\, \frac{n_{HI}}{dv_r = dr} \; \begin{matrix} = \bar{ü}(1+î) \\ ø \; \bar{H}(1 à \frac{1}{3} î) \end{matrix}$

→ *Power spectrum is not isotropic   ("Kaiser effect")*

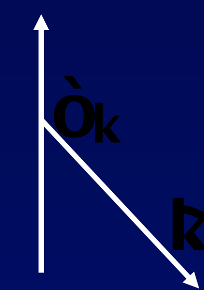

$$\frac{dv_r}{dr} \; ! \qquad î_v(k) = à \cos^2 ò_k \, â \, î(k)$$

$$P_{T_b} = [\cos^2 ò_k î(k) + î_{iso}(k)]^2$$

$$î_{iso} = ì \, î + î_{x_{HI}} + î_T + :::$$

$\cos^4 ò_k; \cos^2 ò_k; \cos^0 ò_k$ ***terms allow separation of powers***

Barkana & Loeb, astro-ph/0409572; see also Bharadwaj & Ali, astro-ph/0401206

Primary challenge: foregrounds

- Terrestrial: radio broadcasting
- Galactic synchrotron emission
- Extragalactic: radio sources

Although the sky brightness (>10K) is much larger than the 21cm signal (<10mK), the foregrounds have a smooth frequency dependence while the signal fluctuates rapidly across small shifts in frequency (=redshift). Theoretical estimates indicate that the 21cm signal is detectable with the forthcoming generation of low-frequency arrays
(Zaldarriaga et al. astro-ph/0311514; Morales & Hewitt astro-ph/0312437)

21cm Cosmology After Reionization?

Damped Lya absorbers: $\Omega_{DLA} \approx 10^{-3}$

$$f_{HI} = (\Omega_{DLA}/\Omega_b) \sim 3\%; \text{ at } z < 6$$

$$\sigma_8 \approx 0.2; \text{ at } z \approx 4 \rightarrow (\Delta T)_{signal} \approx 0.1 mK$$ on 10cMpc

$$(\Delta T)_{noise} \propto (1+z)^{2.6}$$

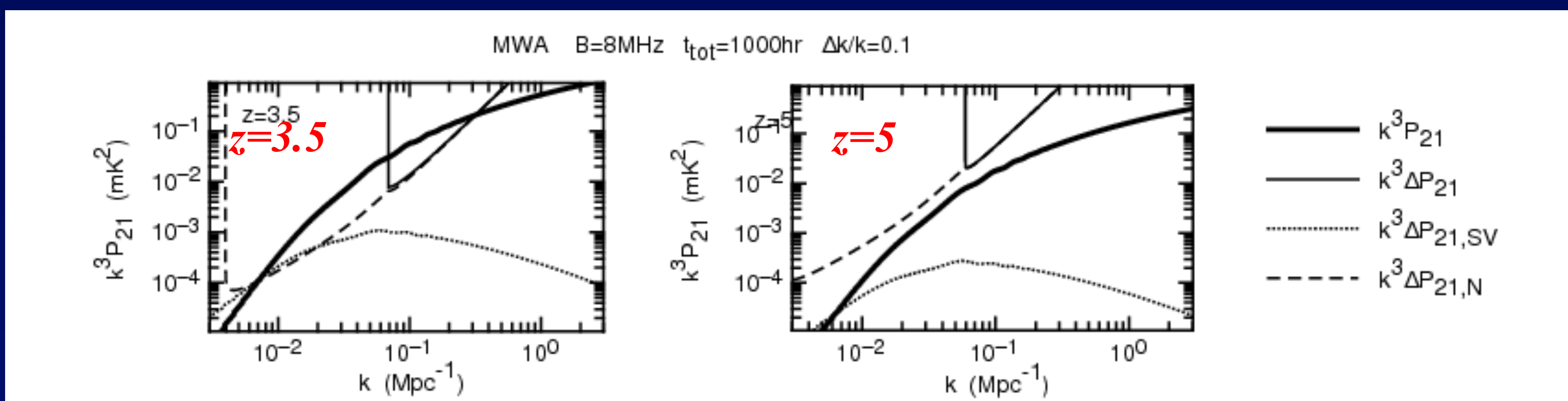

Acoustic peak: constrain dark energy at 0<z<15

Wyithe & Loeb 2007

Acoustic Oscillations

Wyithe, Loeb & Geil

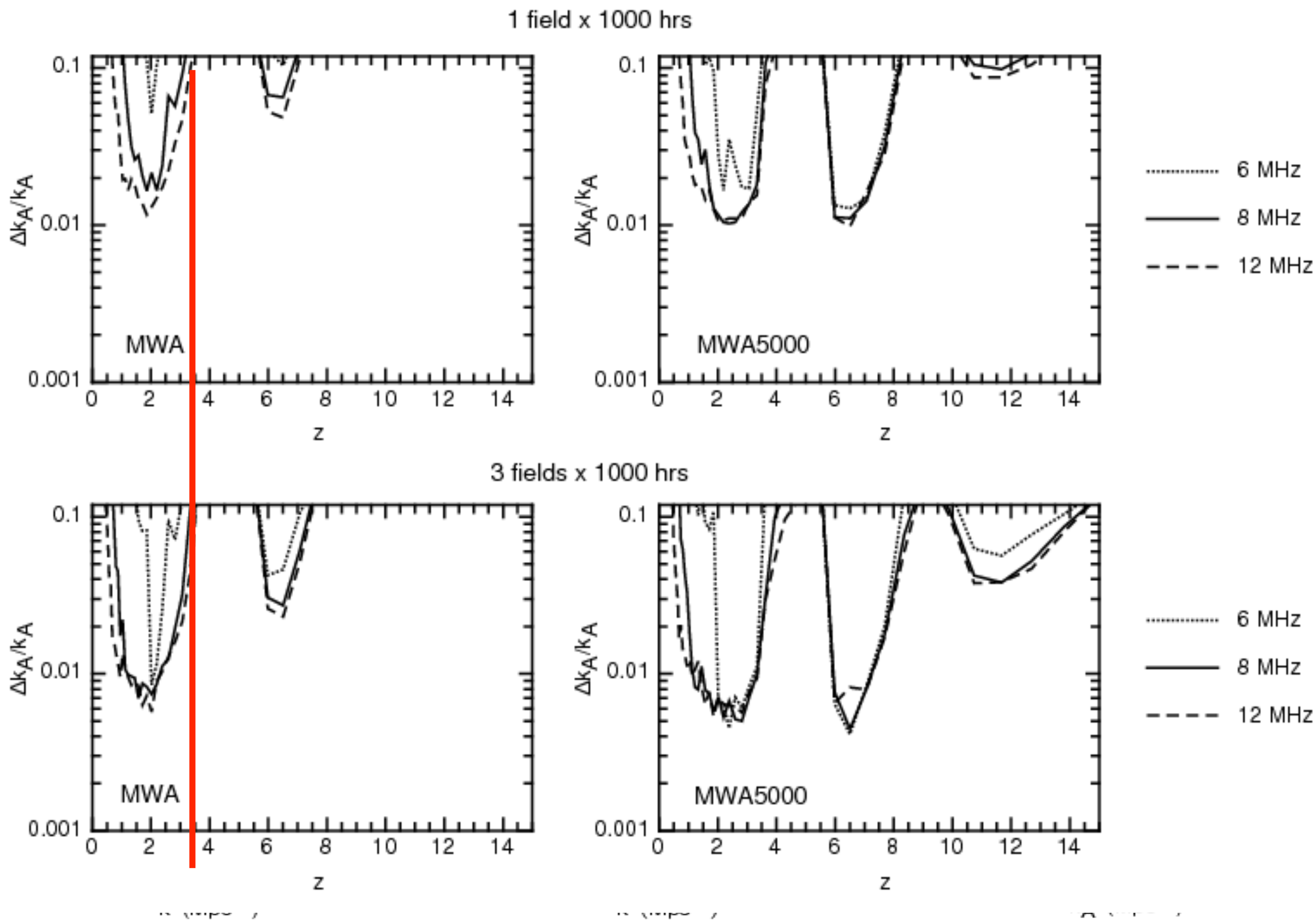

Weighting Neutrinos with a 21cm Survey at z<6

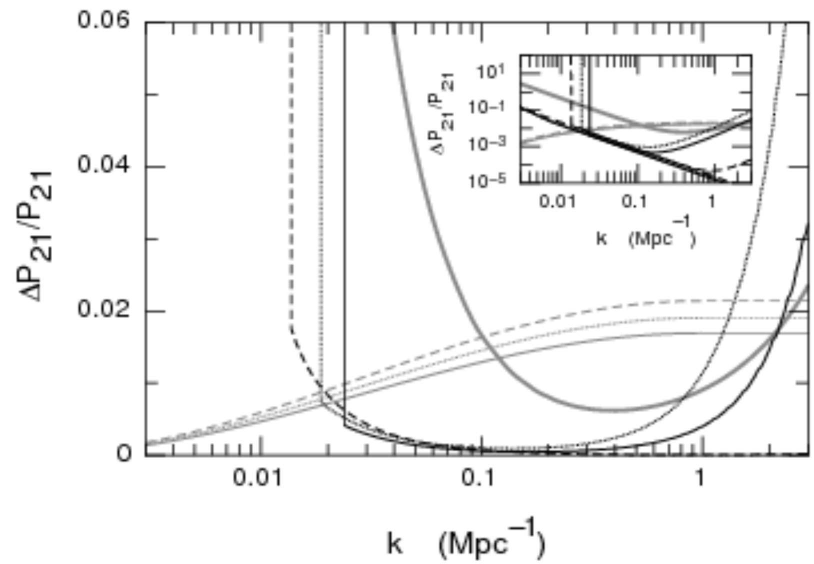

: The fractional change in the amplitude of the power-spectrum owing to the presence of a massive neutrino (horizontal grey lines, asymptoting towards a constant at high k values). The case shown, $f_\nu = 0.004$, corresponds to $m_\nu = 0.05$eV. For comparison, the limits imposed by cosmic variance on the *SDSS*-LRG measurements of the power-spectrum are marked by the thick grey line. The *U*-shaped error curves correspond to an all-sky 21cm survey [$f_{\rm sky} = 0.65$ over a redshift range spanning a factor of 3 in $(1+z)$] with MWA5000 and a 10^3 hour integration per field (line styles for $z = 1.5, 3.5, 6.5$ as in Figure 2). The inset shows these results on logarithmic axes that span a larger dynamic range of achievable precision. The straight thin lines in the inset show the cosmic-variance uncertainty in the power-spectrum measurement owing only to the number of available modes.

Loeb & Wyithe

arXiv:0801.1677

From the Subaru Deep Field at z=6.6

$x_i^n < 0.5$ at 2 à û

But subject to uncertianties due to detailed radiative transfer effects: see Dijkstra et al, arXiv:astro-ph/0701667

14 *M. McQuinn et al.*

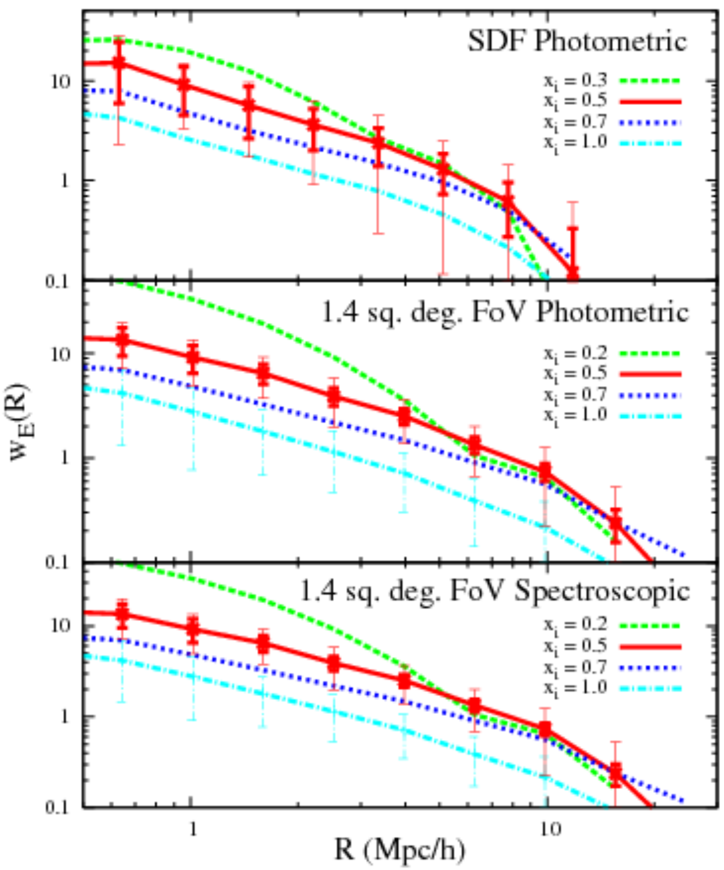

Figure 10. Angular correlation function of emitters at $z = 6.6$, assuming that observed emitters reside in halos with $m\ \exp(-\tau_\alpha(\nu_0)) > 7 \times 10^{10}\ M_\odot$. The curves in the top panel are calculated in the same volume and with the same number of emitters, 58, as the SDF photometric sample. The bottom two panels are in a volume a slightly larger volume than the upcoming 1 sq. deg. Subaru/XMM-Newton Deep Survey (SXDS), with 250 emitters in the middle panel and with 190 in the bottom one. The thick error bars owe to shot noise, and the thin owe to shot noise plus cosmic variance. To calculate these errors, we conservatively assume $F_c = 0.25$ in the top two panels ($F_c = 0$ in the bottom panel). Current surveys can potentially distinguish an ionized universe (the curves labeled "intrinsic") from a universe with $\bar{x}_i \lesssim 0.5$.

The Impact of The IGM on High-Redshift Lyα Emission Lines 7

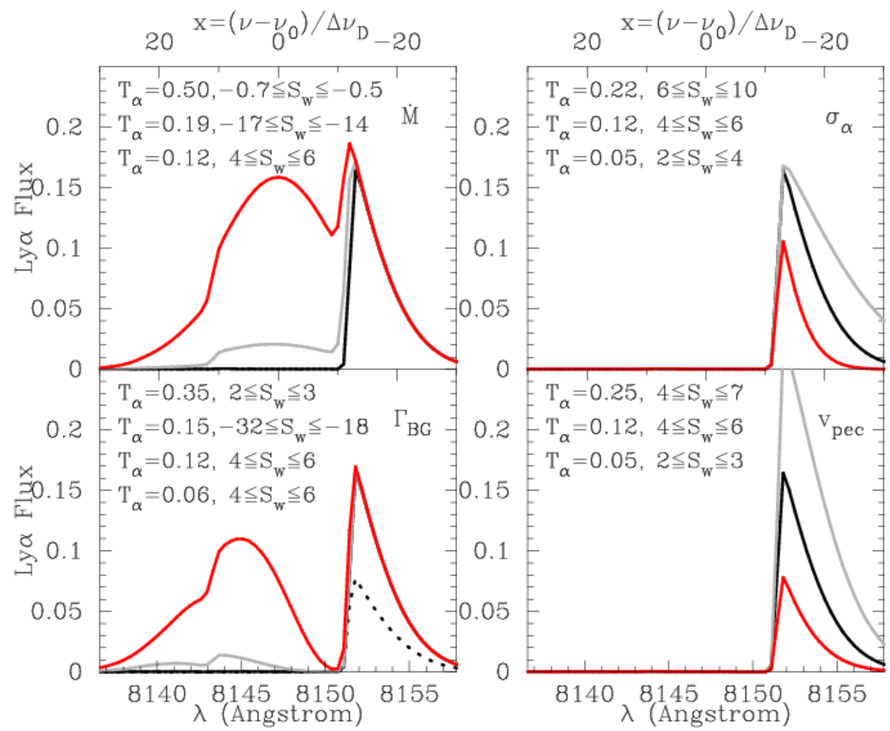

Figure 4. The observed Lyα line from $z = 5.7$ galaxies in a reionised IGM for a range of different models. The upper right corner of each panel shows the model-parameter that is varied. *Top Left:* $\dot{M}_* = 10 M_\odot$/yr (*black*), $\dot{M}_* = 10^2 M_\odot$/yr (*grey*) and $\dot{M}_* = 10^3 M_\odot$/yr (*red*). *Top Right:* $\sigma_\alpha = 1.0 v_{\rm circ}$ (*black*), $\sigma_\alpha = 0.7 v_{\rm circ}$ (*red*) and $\sigma_\alpha = 1.5 v_{\rm circ}$ (*grey*). *Lower Left*: Variation of the ionising background: no ionising background (*dotted*), $\Gamma_{\rm BG}$(*black*), $10\Gamma_{\rm BG}$ (*grey*) and $100\Gamma_{\rm BG}$ (*red*). *Lower Right*: Impact of galaxies peculiar velocity: $v_{\rm pec} = 0$ (*black*), $v_{\rm pec} = -0.5\sigma_\alpha$ (*red*) and $v_{\rm pec} = 0.5\sigma_\alpha$ (*grey*). For each model the total transmission, T_α and the skewness of the line, S_W, are shown.

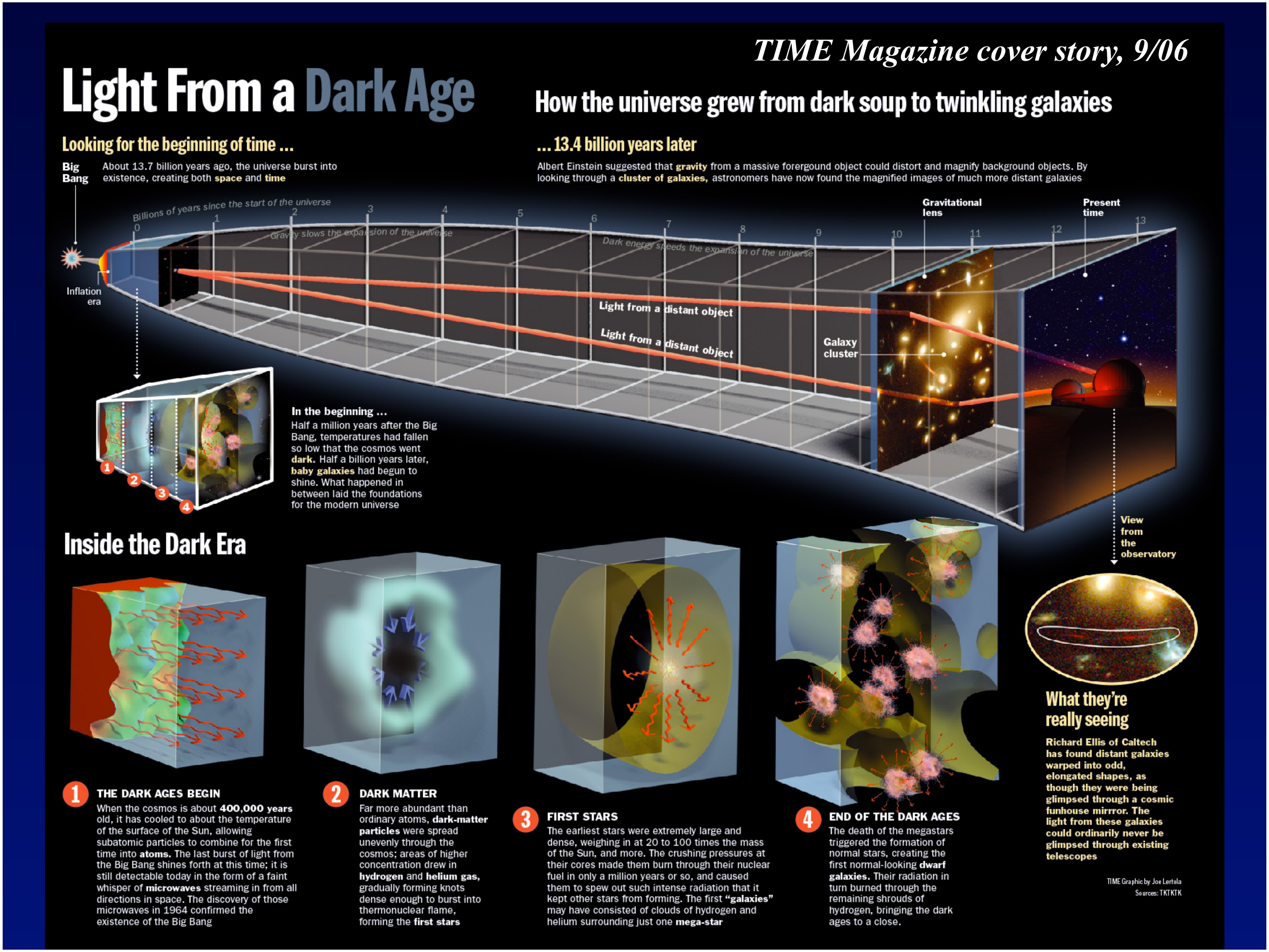

TIME Magazine cover story, 9/06
Light From a Dark Age
How the universe grew from dark soup to twinkling galaxies
Looking for the beginning of time ...
Big Bang
About 13.7 billion years ago, the universe burst into existence, creating both space and time
... 13.4 billion years later
Albert Einstein suggested that gravity from a massive foregergound object could distort and magnify background objects. By looking through a cluster of galaxies, astronomers have now found the magnified images of much more distant galaxies
Billions of years since the start of the universe
0
1
2
3
4
5
6
7
8
9
10
11
12
13
Gravity slows the expansion of the universe
Dark energy speeds the expansion of the universe
Inflation era
Light from a distant object
Light from a distant object
Gravitational lens
Present time
Galaxy cluster
View from the observatory
In the beginning ...
Half a million years after the Big Bang, temperatures had fallen so low that the cosmos went dark. Half a billion years later, baby galaxies had begun to shine. What happened in between laid the foundations for the modern universe
1
2
3
4
Inside the Dark Era
1 THE DARK AGES BEGIN
When the cosmos is about 400,000 years old, it has cooled to about the temperature of the surface of the Sun, allowing subatomic particles to combine for the first time into atoms. The last burst of light from the Big Bang shines forth at this time; it is still detectable today in the form of a faint whisper of microwaves streaming in from all directions in space. The discovery of those microwaves in 1964 confirmed the existence of the Big Bang
2 DARK MATTER
Far more abundant than ordinary atoms, dark-matter particles were spread unevenly through the cosmos; areas of higher concentration drew in hydrogen and helium gas, gradually forming knots dense enough to burst into thermonuclear flame, forming the first stars
3 FIRST STARS
The earliest stars were extremely large and dense, weighing in at 20 to 100 times the mass of the Sun, and more. The crushing pressures at their cores made them burn through their nuclear fuel in only a million years or so, and caused them to spew out such intense radiation that it kept other stars from forming. The first "galaxies" may have consisted of clouds of hydrogen and helium surrounding just one mega-star
4 END OF THE DARK AGES
The death of the megastars triggered the formation of normal stars, creating the first normal-looking dwarf galaxies. Their radiation in turn burned through the remaining shrouds of hydrogen, bringing the dark ages to a close.
What they're really seeing
Richard Ellis of Caltech has found distant galaxies warped into odd, elongated shapes, as though they were being glimpsed through a cosmic funhouse mirrror. The light from these galaxies could ordinarily never be glimpsed through existing telescopes
TIME Graphic by Joe Lertola
Sources: TKTKTK

HOW TO SEE IN THE DARK

Despite the lack of stars, the Dark Ages were not completely dark. A rare process caused hydrogen gas to glow dimly.

For hydrogen to glow, there had to be a source of energy. The only available ones were the atoms' own kinetic energy (released by collisions between atoms) and the photons of the cosmic background radiation. A smattering of unattached electrons was available to help transfer energy between the atoms and the photons.

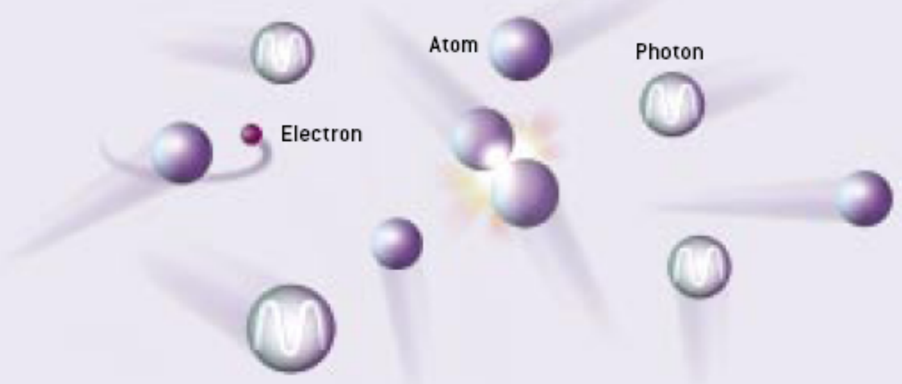

The collisions and photons did, however, pack just enough punch to flip an electron so that its spin pointed the same way as the proton's. When the electron flipped back, it released a photon with a wavelength of 21 centimeters.

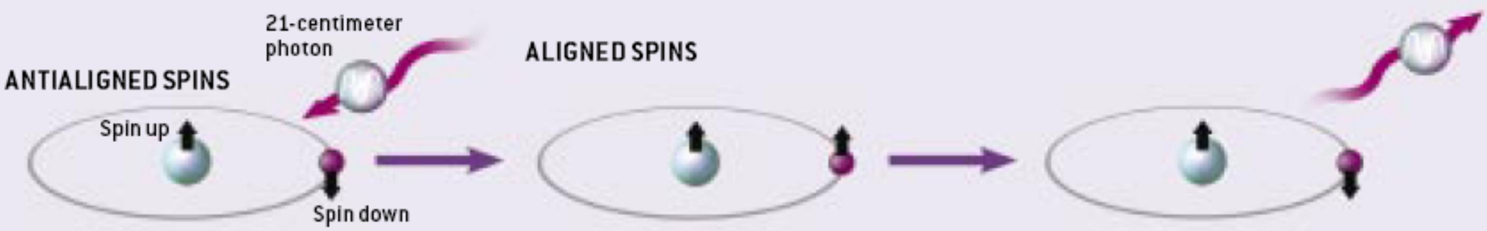

The kinetic energy, photon energy and spin energy were three reservoirs that interchanged energy by various means.

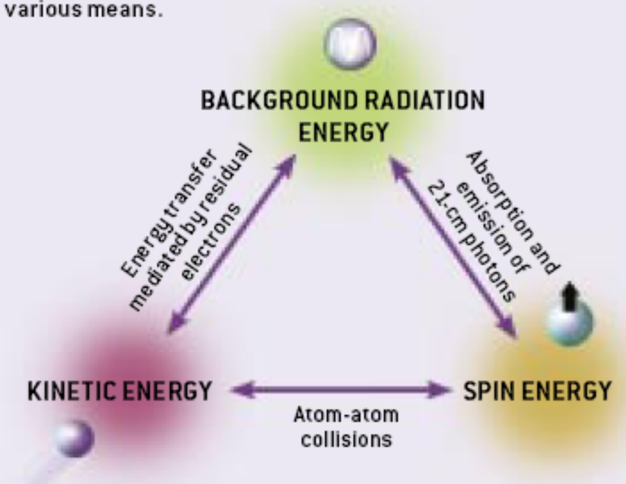

The amount of energy in each reservoir can be represented in terms of temperature: the higher the temperature, the greater the energy. At the start of the Dark Ages, all three temperatures were the same (*a*). Then the kinetic and spin temperature began to fall faster than the photon energy (*b*). After a while, the spin temperature returned to equilibrium with the photon temperature (*c*). Finally, stars and quasars warmed the gas, pumping up the kinetic and spin temperatures (*d*). The relative temperatures determine how (and whether) the hydrogen can be observed.

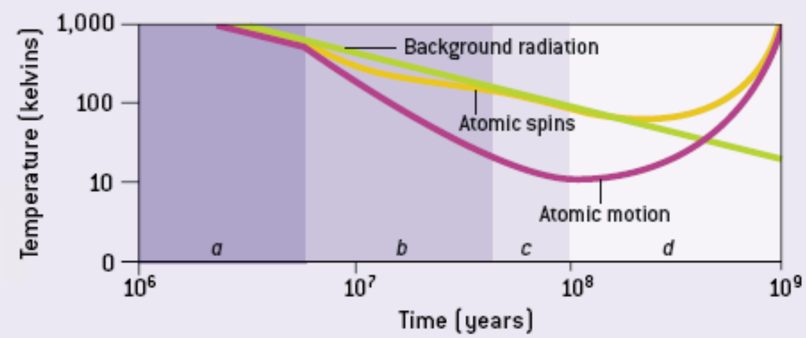

Largest Data Set on the Sky

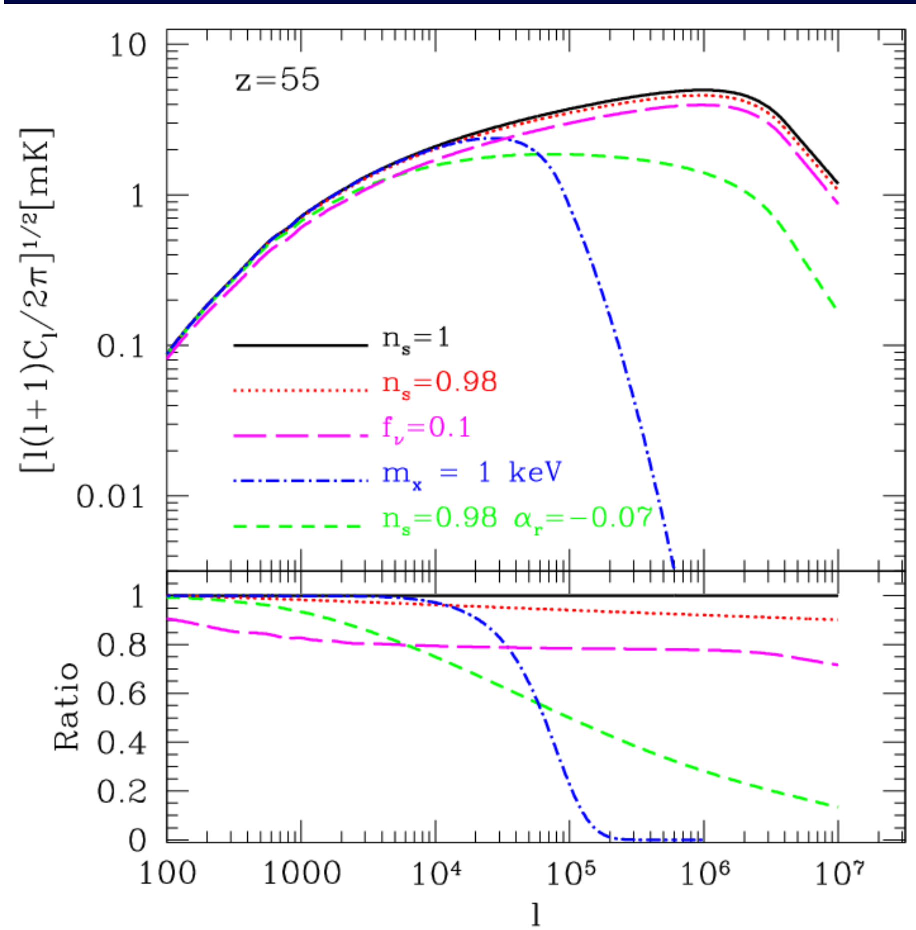

Number of independent patches:

$$\sim 10^{16}\left(\frac{l_{max}}{10^6}\right)^3$$

while Silk damping limits the primary CMB anisotropies to only $\sim 10^7$

Noise due to foreground sky brightness:

$$N_\nu \sim 0.4\ \mathrm{mK}\left(\frac{I_\nu}{5\times 10^5\ \mathrm{Jy\ sr^{-1}}}\right)\left(\frac{l_{min}}{35}\right)\left(\frac{5000}{l_{max}}\right)\left(\frac{0.016}{f_{cover}}\right) \times\left(\frac{1\ \mathrm{year}}{t_0}\right)^{1/2}\left(\frac{\Delta\nu}{\nu}\right)^{-1/2}\left(\frac{50\ \mathrm{MHz}}{\nu}\right)^{5/2},$$

Loeb & Zaldarriaga, Phys. Rev. Lett., 2004; astro-ph/0312134

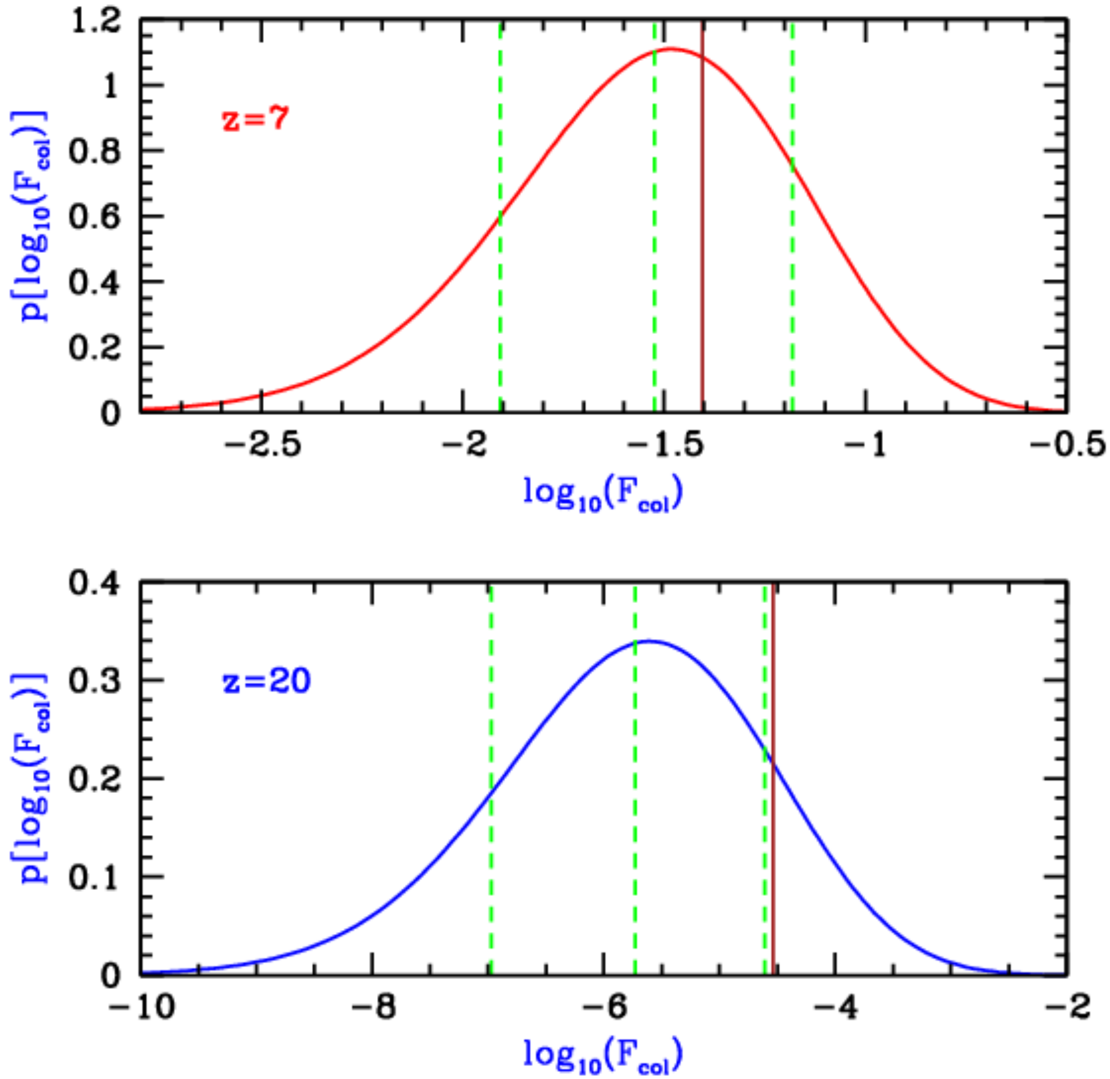

Figure 2: Probability distribution within a small volume of the total mass fraction in galactic halos. The normalized distribution of $\log_{10}$ of this fraction $F_{\rm col}(M_{\rm min})$ is shown for two cases: $z = 20$, $l_{\rm box} = 1$ Mpc, $M_{\rm min} = 7 \times 10^5 M_{\odot}$ (bottom panel), and $z = 7$, $l_{\rm box} = 6$ Mpc, $M_{\rm min} = 10^8 M_{\odot}$ (upper panel). In each case, the value in a periodic box ($\bar{\delta}_R = 0$) is shown along with the value that would be expected given a plus or minus $1 - \sigma$ fluctuation in the mean density of the box (dashed vertical lines). Also shown in each case is the mean value of $F_{\rm col}(M_{\rm min})$ averaged over large cosmological volumes (solid vertical line).

Computational Challenge for Simulations: *Unusually Large Fluctuations in the Statistics of Galaxy Formation at High Redshifts*

Bias in numerical simulations:

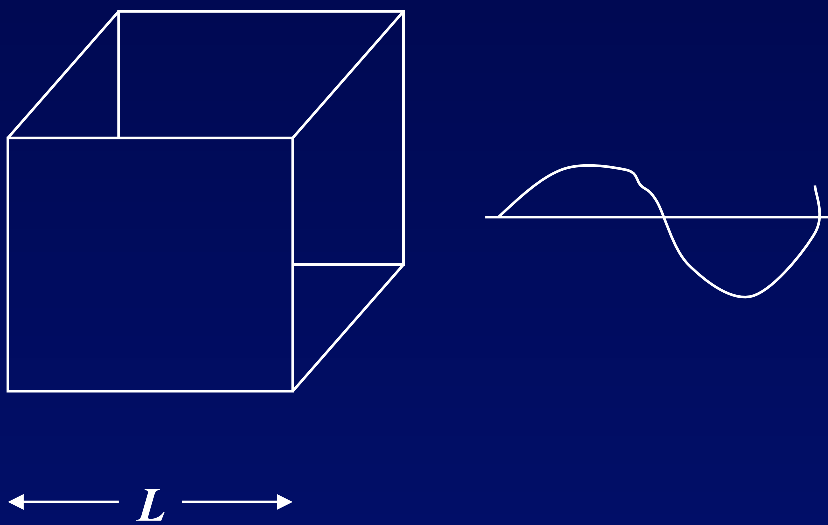

Assumption : $\hat{\imath}_L = 0$

Barkana & Loeb, ApJ, 2003

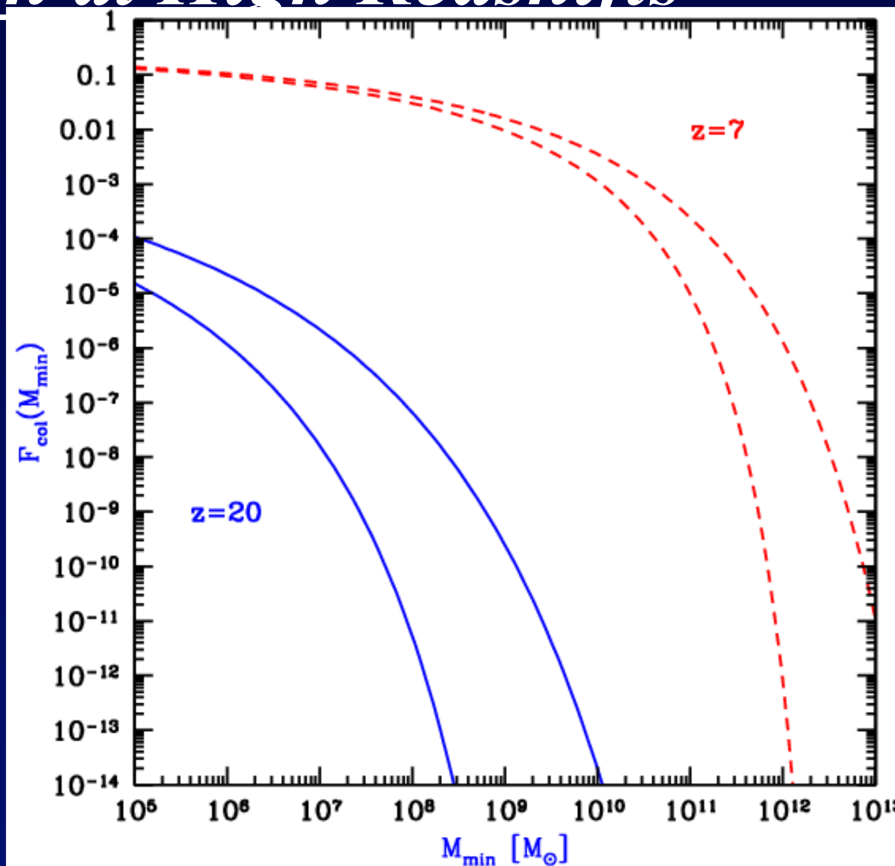

Figure 1: Bias in the halo mass distribution in simulations. We consider the total amount of mass contained in all halos of individual mass $M_{\rm min}$ or greater, expressed as a fraction of the total mass in a given volume. This cumulative fraction $F_{\rm col}(M_{\rm min})$ is shown as a function of the minimum halo mass $M_{\rm min}$. We consider $z = 20$, $l_{\rm box} = 1$ Mpc (solid curves), and $z = 7$, $l_{\rm box} = 6$ Mpc (dashed curves). At each redshift, we compare the true average distribution in the universe (upper curve) to the biased distribution that would be measured in a simulation box with periodic boundary conditions (for which $\bar{\delta}_R$ is artificially set to zero).

Self-Regulated Star Formation

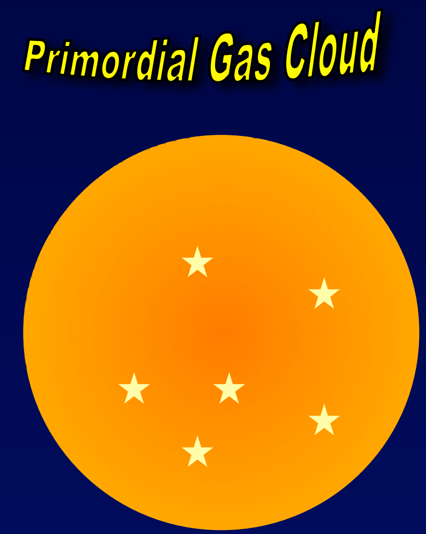

Virial temperature < 10,000K

H_2 *destruction by starlight (10.2<E<13.6 eV)*

Evaporation of gas cloud by photo-ionization heating to >10,000K

Virial temperature > 10,000K

$$M_\star \propto E_{SN} \approx \tfrac{3}{2} M_{gas} v^2$$

$$f_\star = \frac{M_\star}{M_{gas}} \propto v^2 \propto M_{halo}^{2/3}$$

As observed for local dwarf galaxies $(M_\star < 3 \times 10^{10} M_\odot)$

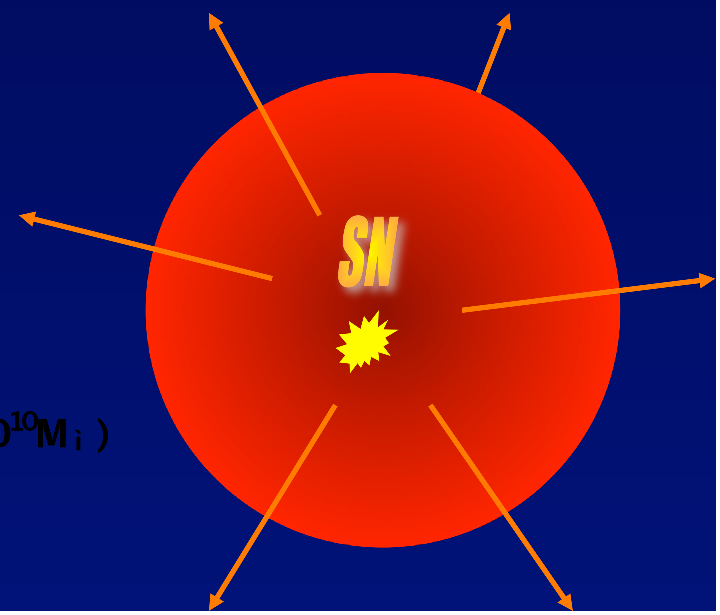

Binding Energy of Dark Matter Halos

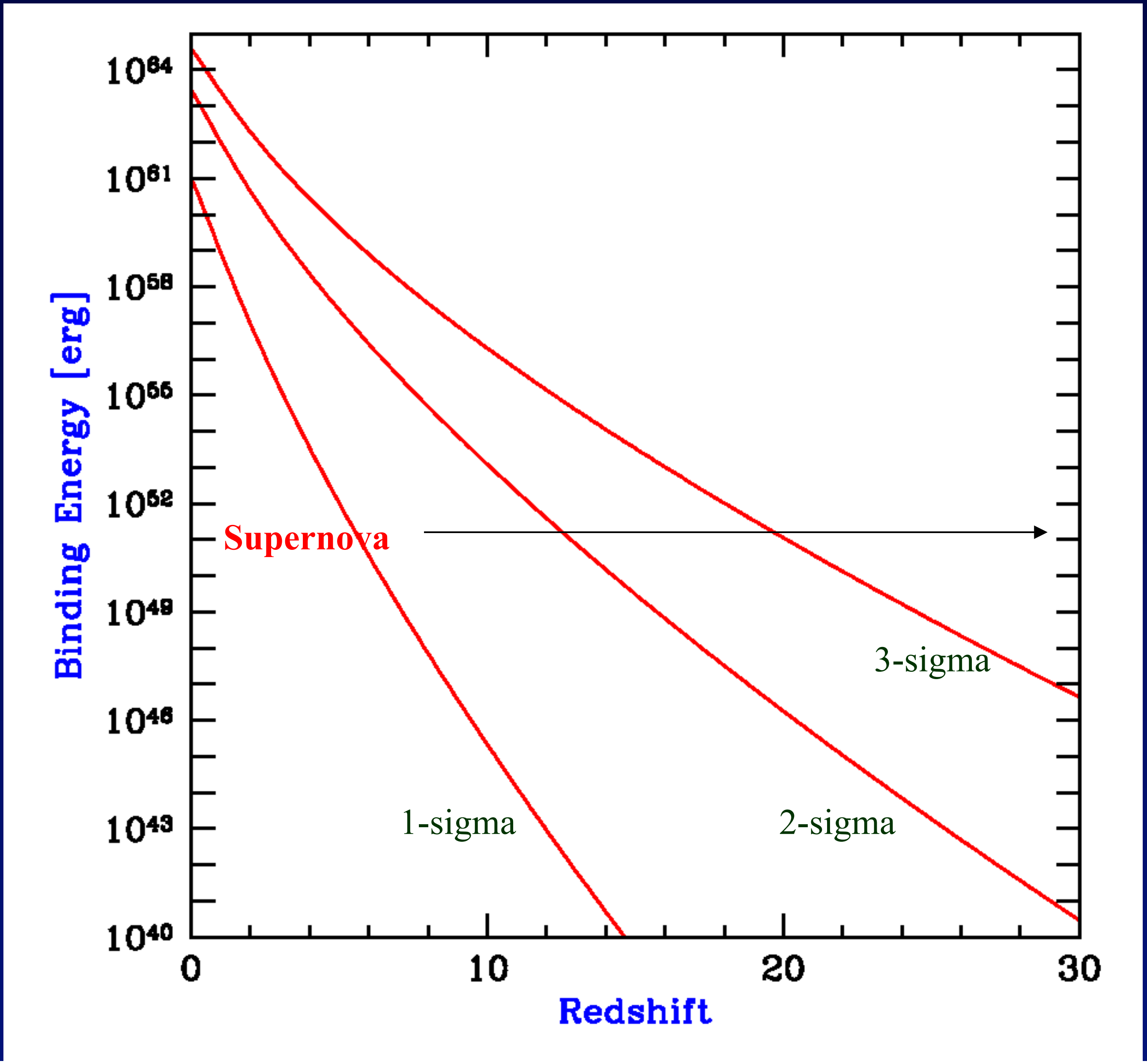

Cross-correlation between 21cm brightness and galaxy density

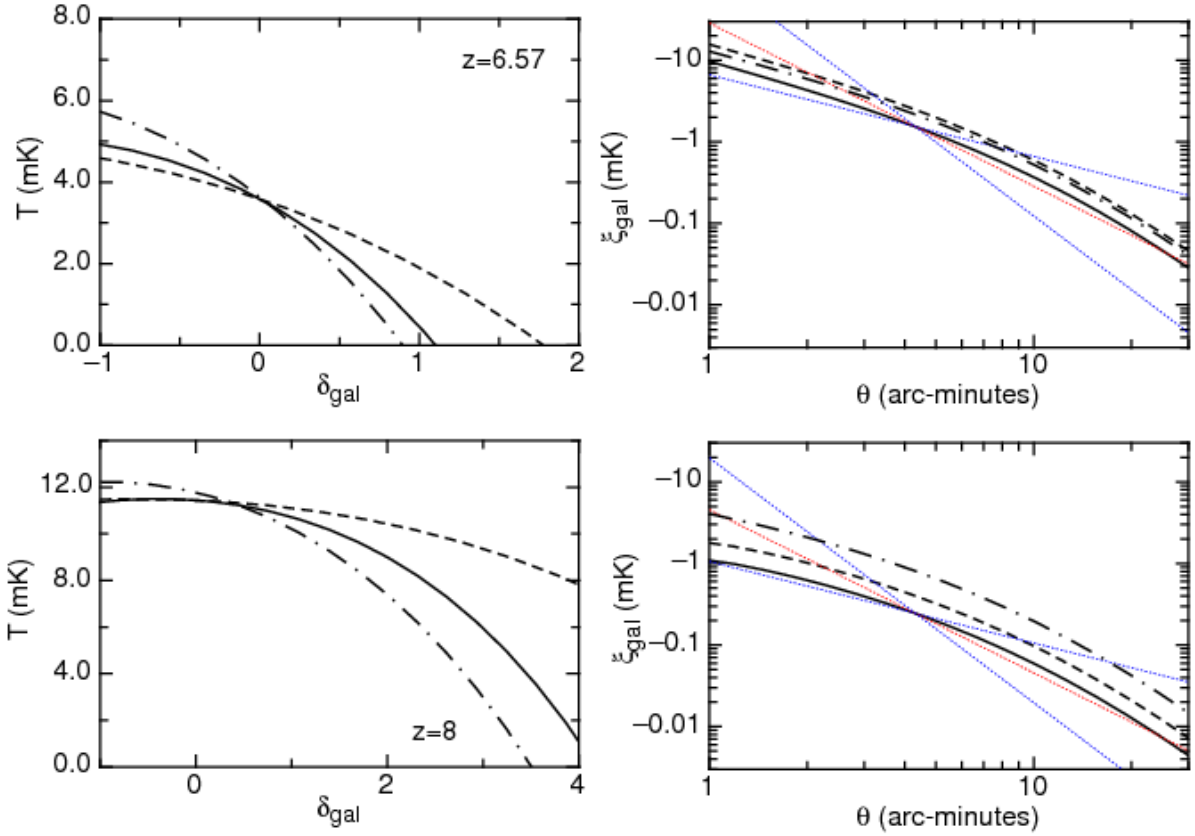

Figure 4. *Left*: 21cm brightness temperature as a function of $\delta_{\rm gal}$. Two values of galaxy mass are assumed for a clumping of $C = 10$, $M = 10^{10}M_\odot$ (solid line) and $M = 10^{11}M_\odot$ (dashed line). The dot-dashed line shows $C = 2$ with $M = 10^{10}M_\odot$. *Right*: The cross-correlation function $\xi_{\rm gal} = \langle\delta_{\rm gal}(T - \langle T\rangle)\rangle$ for the IGM smoothed on various angular scales (θ). The function is presented assuming $C = 10$ for masses of $M = 10^{10}M_\odot$ (solid line) and $M = 10^{11}M_\odot$ (dashed line). The dot-dashed line represents $C = 2$ with $M = 10^{10}M_\odot$. The lines show power-laws of slope $d(\log\xi_{\rm gal})/d(\log\theta) = -1$, -2 and -3. The upper and lower rows correspond to observations at $z = 6.57$ and $z = 8$ respectively.

Infrared imaging

21cm mapping

Wyithe & Loeb (2006)

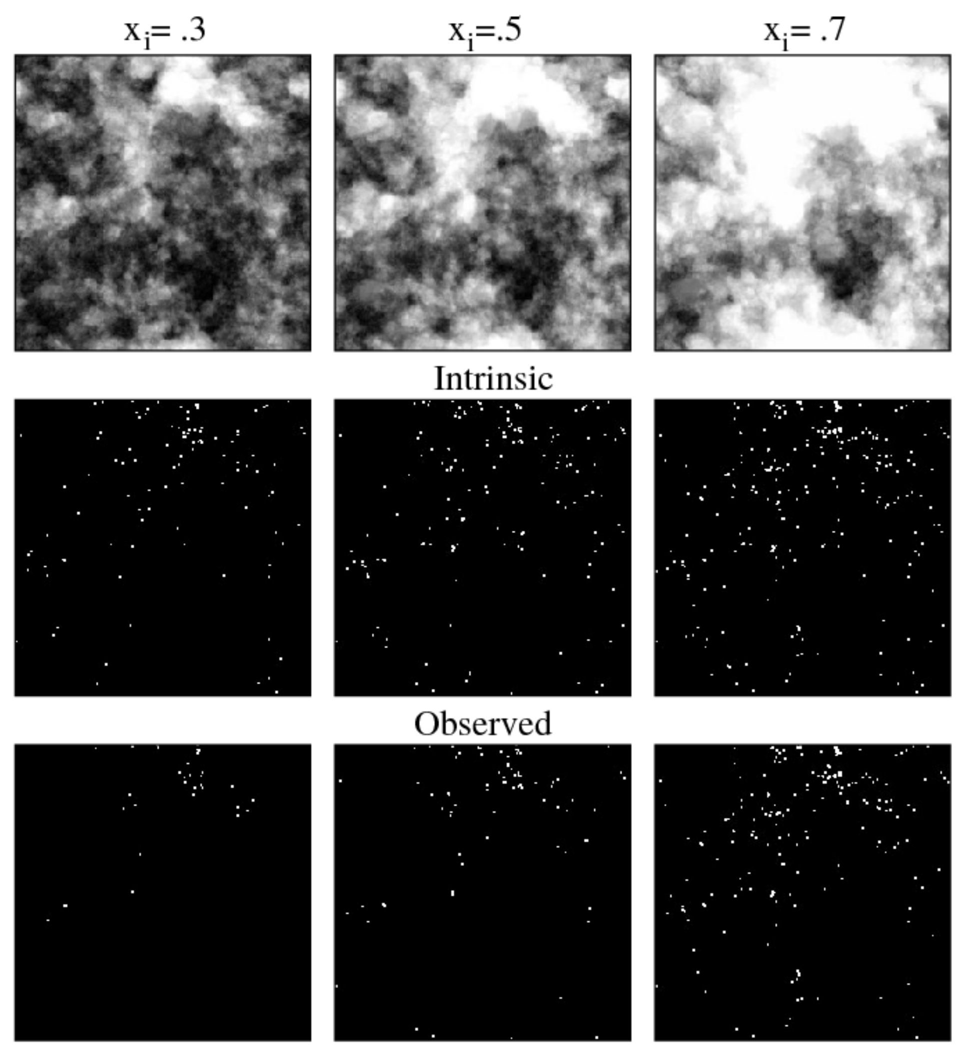

Figure 2. Top panels show the projection of $\bar{x}_i$ in the survey volume. In the white regions the projection is fully ionized and in black it is neutral. The left, middle, and right panels are for $z = 8.2$ ($\bar{x}_i = 0.3$), $z = 7.7$ ($\bar{x}_i = 0.5$), and $z = 7.3$ ($\bar{x}_i = 0.7$). The middle and bottom rows are the intrinsic and observed Lyα emitters maps, respectively, for $f_{\rm E} = 0.25$ and assuming that we can observe unobscured emitters with $m \exp(-\tau_\alpha(\nu_0)) > 7 \times 10^{10} M_\odot$. (Note that $L_{\rm int,E} \propto m$.) The observed distribution of emitters is modulated by the location of the HII regions (compare bottom panels with corresponding top panels). Each panel is 94 Mpc across (or 0.6 degrees on the sky), roughly the area of the current Subaru Deep Field (SDF) at $z = 6.6$ (Kashikawa et al. 2006). The depth of each panel is $\Delta\lambda = 130$ Å, which matches the FWHM of the Subaru 9210 Å narrow band filter. The number densities of Lyα emitters for the panels in the middle row are few times larger than the number density in the SDF photometric sample of $z = 6.6$ LAEs.

Clustering of Lya Emitters

McQuinn et al.

arXiv:0704.2239

The Imprint of Reionization on Galaxy Clustering

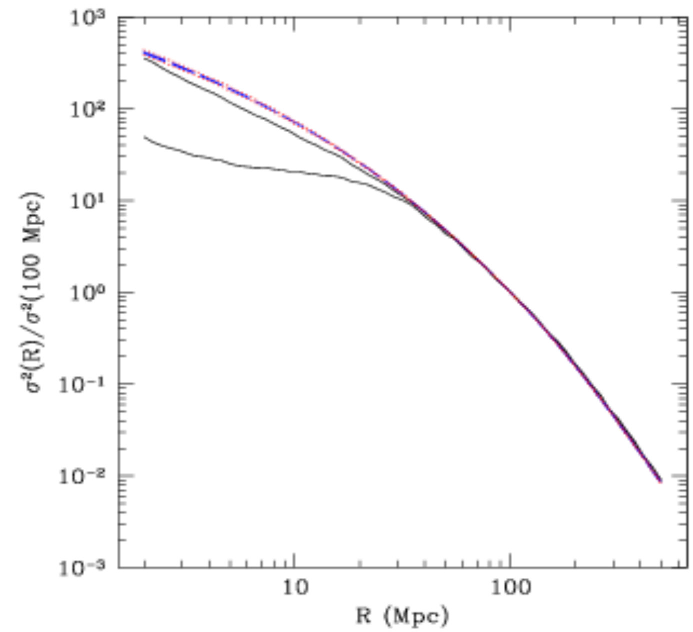

FIG. 5.— The normalized $\sigma^2(R)$ for $z_R = 15$ and $z_R = 6$ (upper and lower solid black curves, respectively); the limiting cases of the best current constraints of n (red, dotted curves) and α (blue, dashed curves).

Inhomogeneous photo-ionization heating to ø 10^4K *modulates the minimum mass of galaxies on scales of tens of comoving Mpc*

Babich & Loeb 2006, ApJ, 640, 1

21 cm Absorption During the Dark Ages

$$T_b = ü \left(\frac{T_s à T_í}{1+z}\right) \qquad T_b = 28\mathrm{mK}\left(\frac{1+z}{10}\right)^{1=2}\left(\frac{T_s à T_í}{T_s}\right)$$

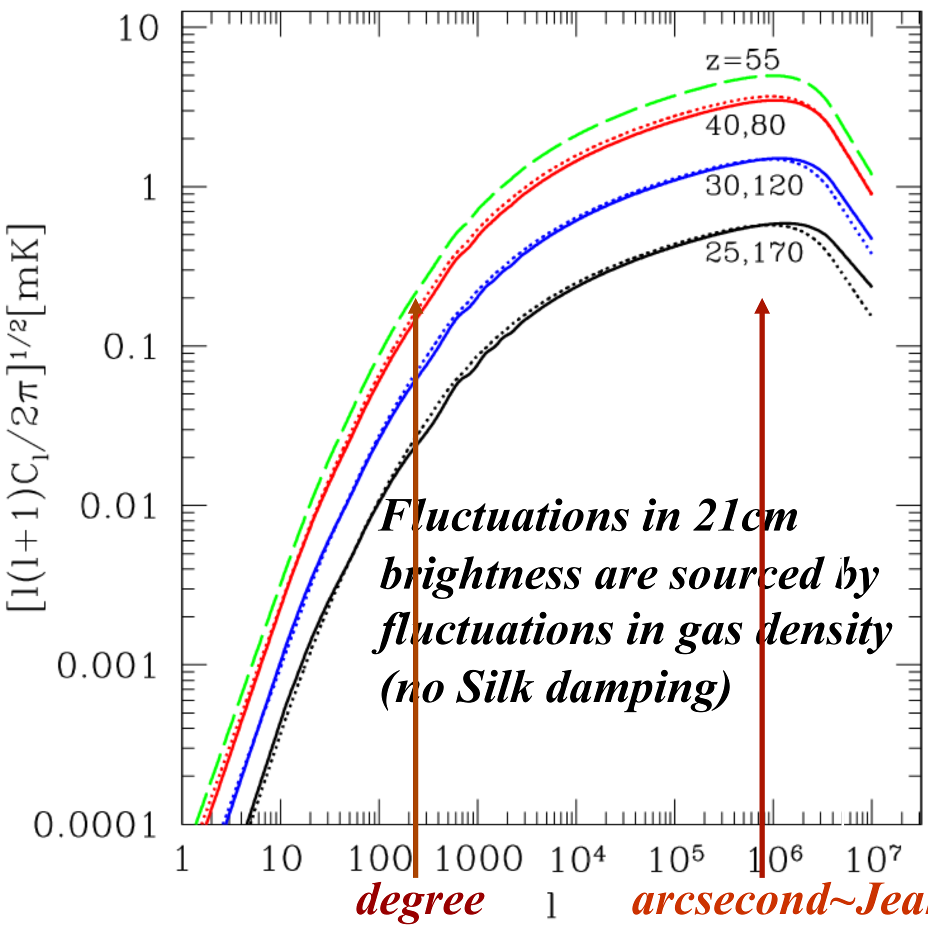

degree *arcsecond~Jeans scale*

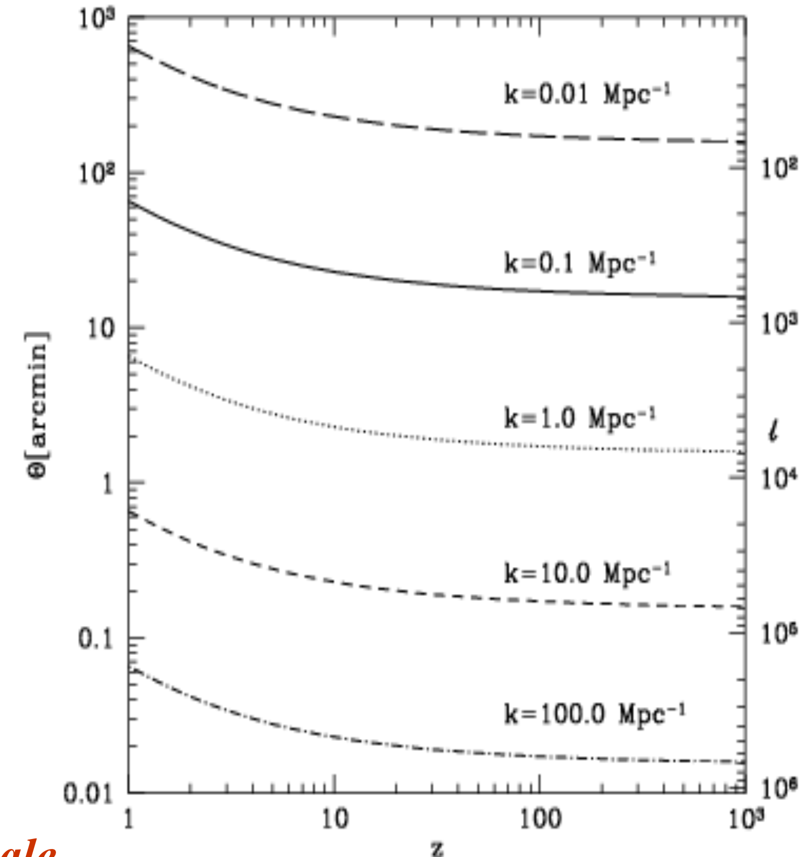

Loeb & Zaldarriaga, Phys. Rev. Lett., 2004

So far, the hydrogen was only probed by quasars

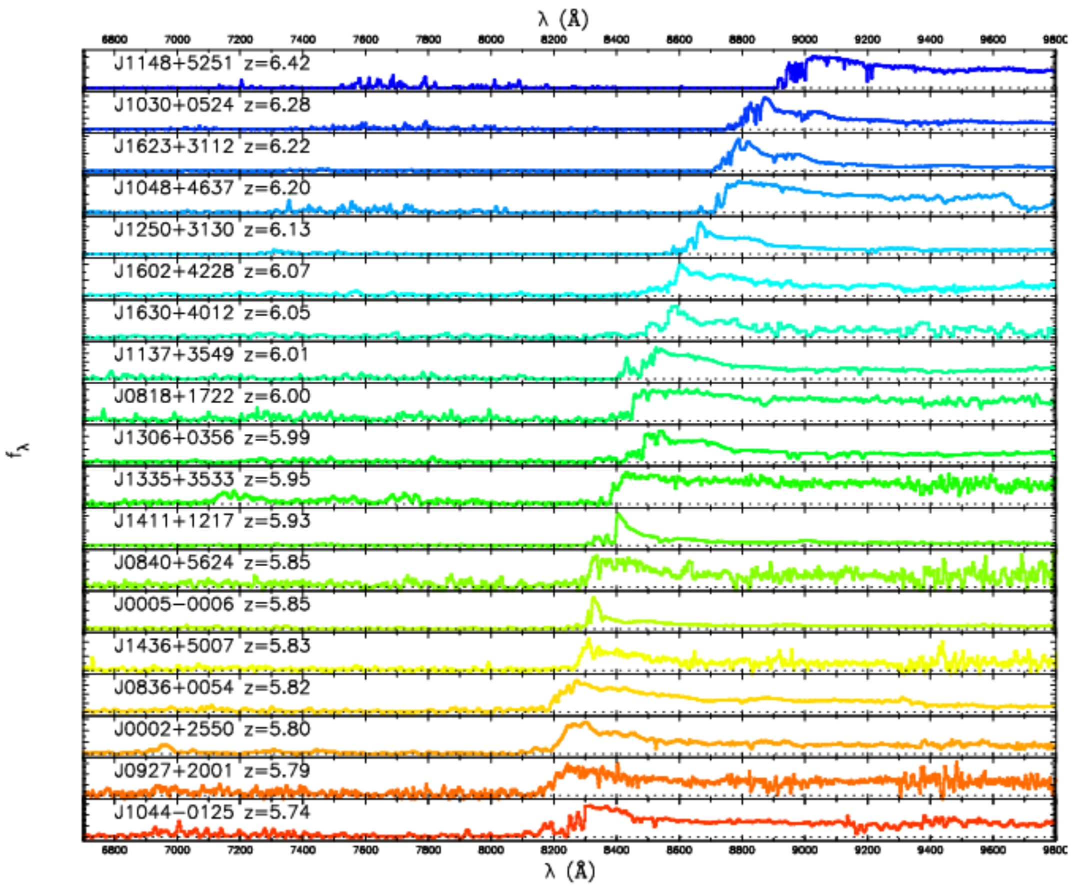

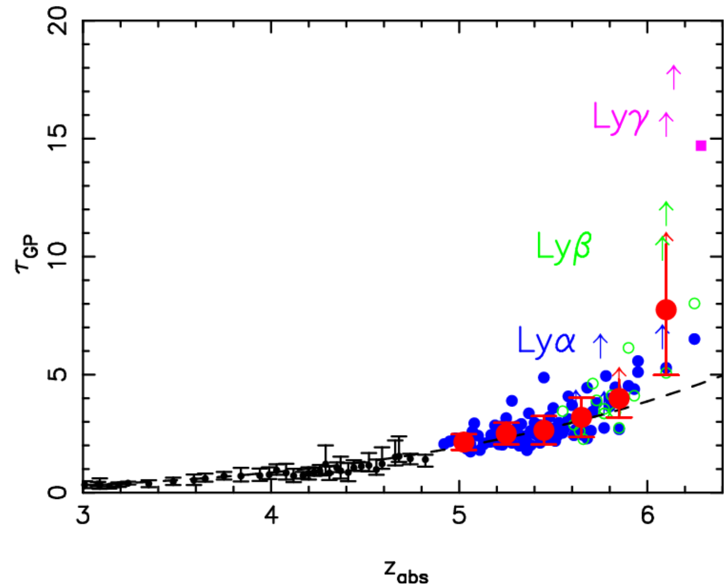

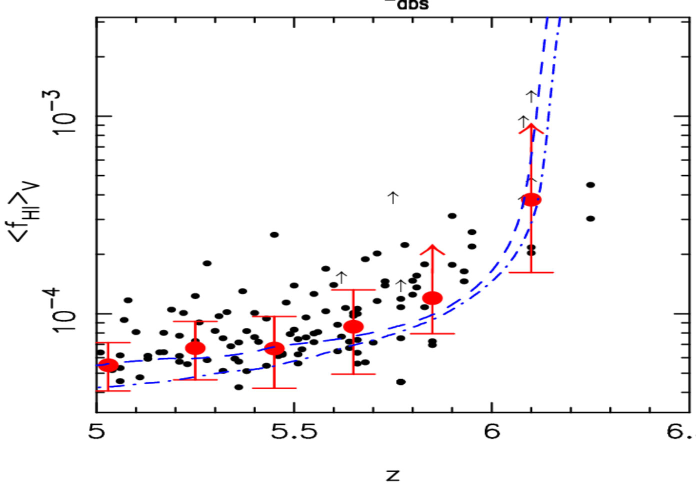

Spectra of our sample of nineteen SDSS quasars at $5.74 < z < 6.42$. Twelve of the spectra were taken with Keck/ESI, while the others were observed with the MMT/Red Channel and Kitt Peak 4-meter/MARS spectrographs. See Table 1 for detailed information.

Fan et al. 2005

GRB080319B at higher redshifts

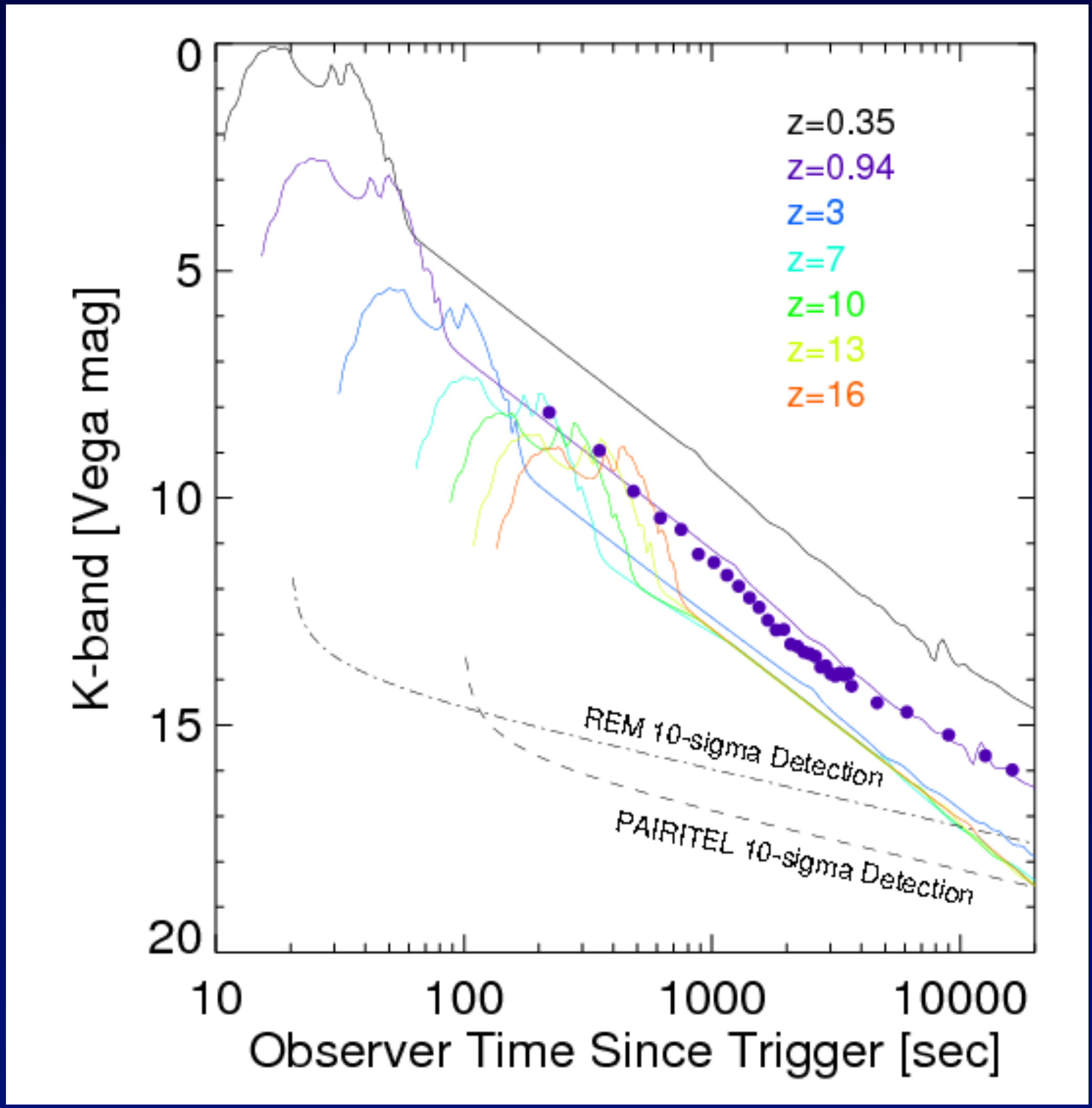

Bloom et al. arXiv:0803.3215

Cosmic Microwave Background *(WMAP5)*

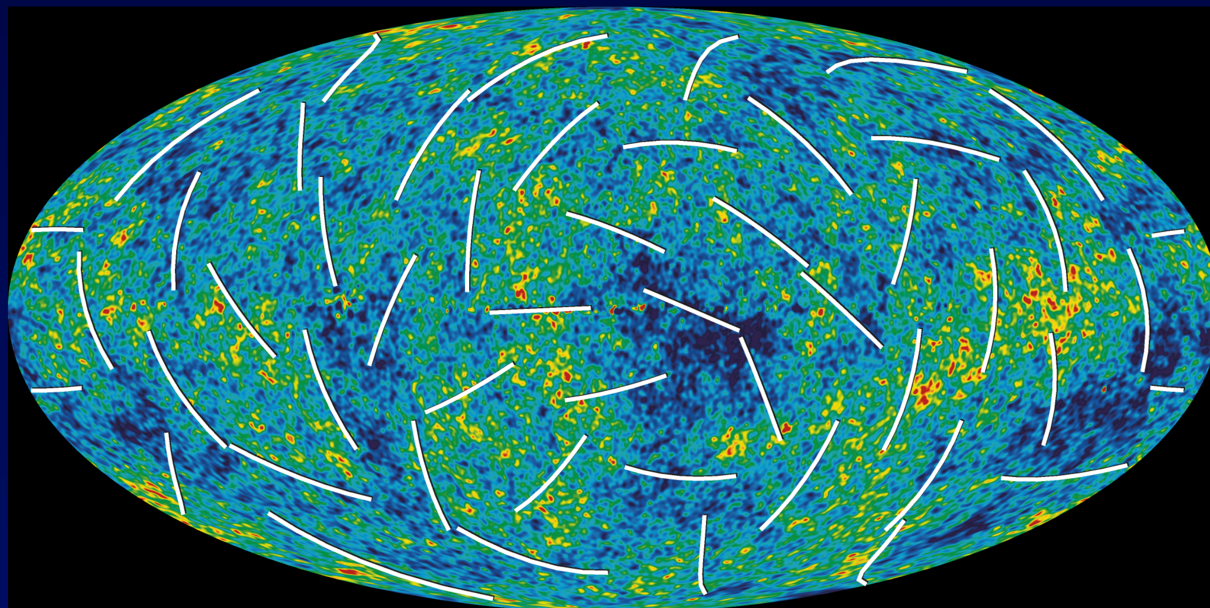

ü = 0:09 æ 0:02

The polarization data indicates that the first stars must have formed 400 million years after the big bang, when the universe was only a few percent of its current age!

Dunkley et al. 2008

How do massive stars end their life?

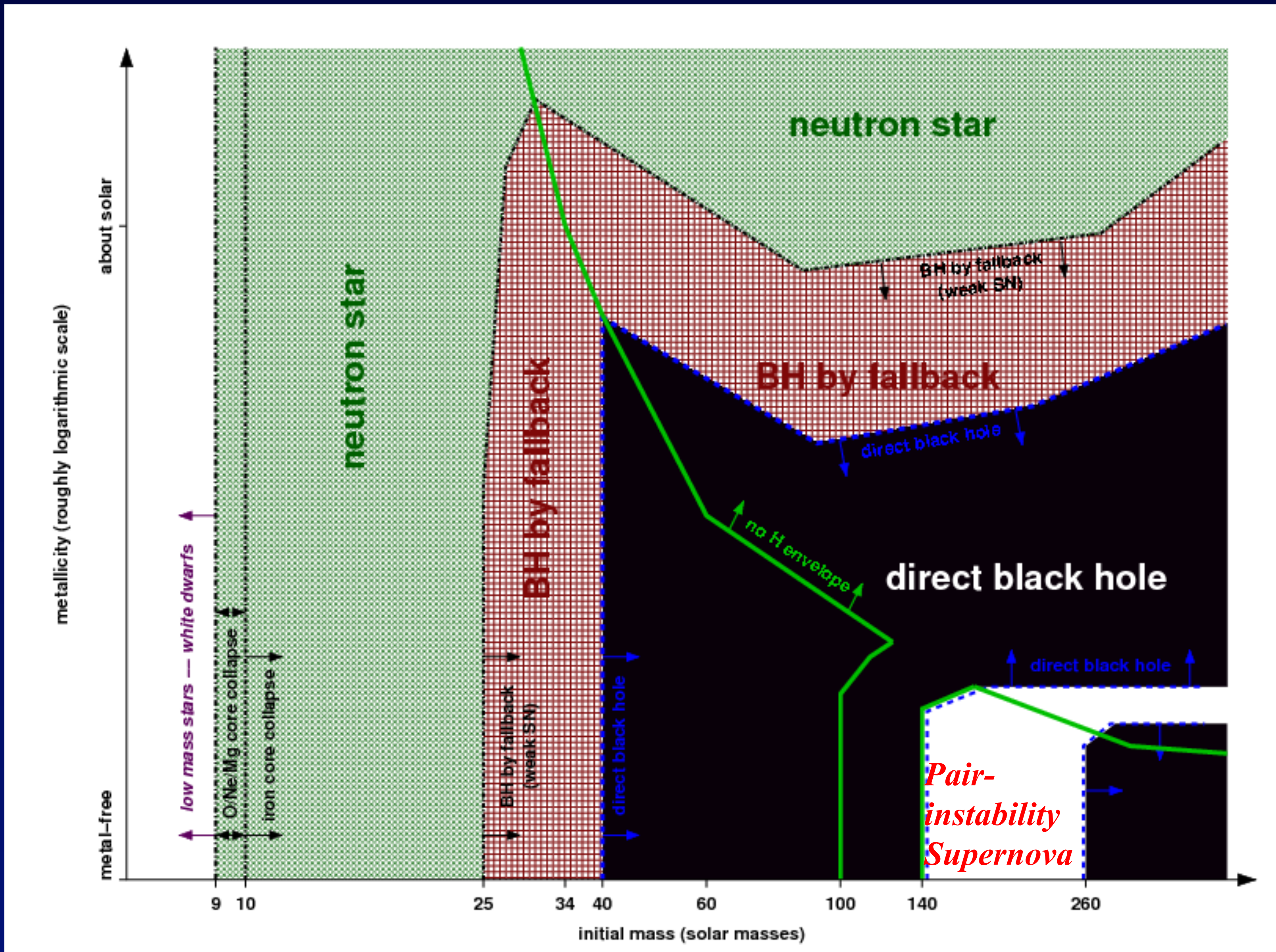

Heger et al. 2003

Early Galaxies: *Parametrizing Our Ignorance*

Star Formation

- Mass function of dark matter halos: *N-body simulations*.
- Minimum halo mass for star formation:

  200K – H_2 cooling

  10^4 K -- atomic H cooling

  10^5 K -- assembly of gas from a photo-ionized IGM
- Star formation efficiency: $f_{?}$ ø 10%
- # of ionizing photons/baryon in stars:

~4000 – Pop I/II; ~ 10^5 -- Pop III (metal free)

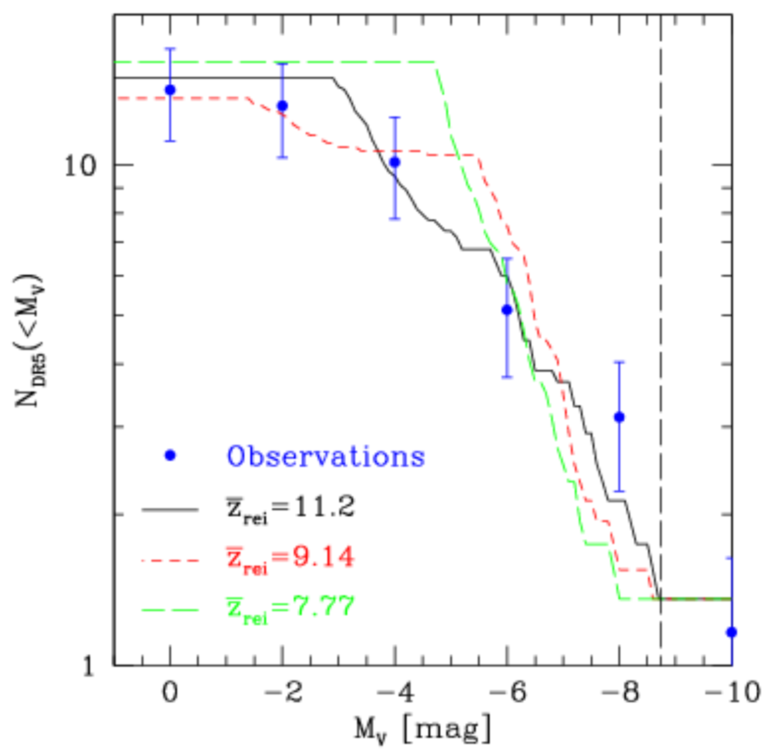

Figure 2. The faint end of the luminosity function of MW satellites in the SDSS footprint with the DR5 selection threshold. The observed function is shown by the blue points with the non-SDSS objects each contributing a fractional amount $f_{DR5} = 0.194$ to the total. The curves show the theoretical predictions for different values of $\bar{z}_{rei}$ with $z_{H_2} = 23.1$ and other model parameters optimized to produce the best agreement with luminosity function data. The solid, black; short-dashed, red; and long-dashed, green curves have $\bar{z}_{rei} = 11.2$, 9.14, and 7.77, respectively. The long-dashed vertical line demarcates the luminosities at which pre- vs. post-SDSS satellites are observed.

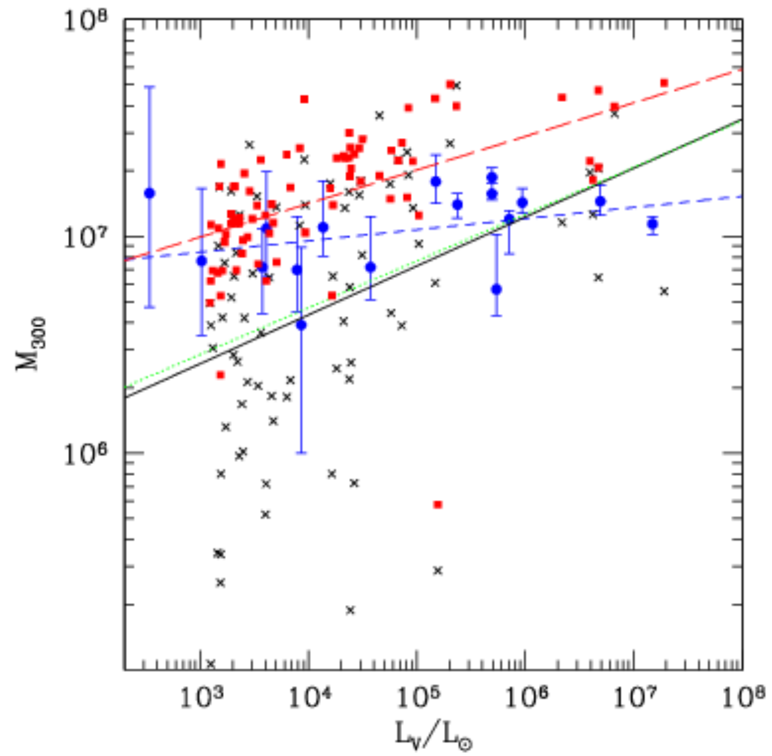

Figure 5. Scatter plot of M_{300}, the mass within 300 pc of the satellite center, versus satellite visual luminosity, L_V. Known MW satellites are represented by blue circles, while black x's denote illuminated subhalos from our $(\bar{z}_{rei}, z_{H_2}) = (11.2, 23.1)$ model with M_{300} measured directly from the simulation. Red squares show values of M_{300} measured, for each subhalo, at the time when the evolution in its maximum circular velocity has reached its peak and assuming an NFW profile. The short-dashed blue, solid black, dotted green, and long-dashed lines represent power-law fits of the $M_{300} - L_V$ relation respectively from observations, directly from the simulation, assuming NFW profiles for simulated subhalos today, and assuming NFW profiles for the subhalos when their maximum circular velocities peak.